ICR

ANNUAL REPORT 2000

Kyoto University

Institute for Chemical Research

Volume 7

***ICR* ANNUAL REPORT 2000 (Volume 7)**
For the calendar year 1 January 2000 to 31 December 2000

Editors:
Professor Toshinobu YOKO (Editor in chief)
Professor Nobuyosi ESAKI
Professor Kazuyoshi YAMADA

Managing editor:
Tatsuo OHYAMA

Published and distributed by:
Institute for Chemical Research (*ICR*), Kyoto University

Note: *ICR* Annual Report available from the *ICR* Office,
Institute for Chemical Research, Kyoto University,
Uji, Kyoto 611-0011, Japan.
Tel: +81-(0)774-38-3344
Fax: +81-(0)774-38-3014
E-mail: jimu-icr@uji.kyoto-u.ac.jp

ISSN 1342-0321

Printed by
Nakanishi Printing Co. Ltd.
Shimotachiuri-dori Ogawa Higashi-iru, Kamigyo-ku, Kyoto 602-8048, Japan.
TEL:+81-(0)75-441-3155. FAX:+81-(0)75-417-2050;441-3159.
E-mail: info@nacos.com
HP URL http://www.nacos.com/

31 March 2001

Front cover

The figures shown on the front cover represent a relativistic effect on the inelastic partial cross-section of electron beam for carbon K-shell excitation in a thin graphite film.

The upper figures show energy-filtered diffraction patterns obtained at the incident electron energy of 1000keV (a) and 400keV (b), respectively. The intensity of the 1000keV pattern is distributed in a smaller scattering angular region than that of the 400keV pattern. It should be noticed that the intensity maximum is observed in both cases.

The lower figures show the corresponding intensity profiles along the radial direction of the energy-filtered diffraction patterns of (a) and (b). The solid line illustrates the theoretical profiles including the relativistic term and the dashed line represents the non-relativistic Lorentzian profile. The experimental intensity profiles indicated by the dots agree well with the relativistic ones. When the scattering angle increases, the intensity distribution approaches the non-relativistic Lorentzian distribution. The deviation from the non-relativistic profile is remarkable at higher incident energy and also at smaller scattering angle. These results prove directly the validity of the prediction of relativistic inelastic scattering theory.

The values of partial cross-section for carbon K-edge at 1000keV are concluded to be larger than those at low energy electrons, which suggests that high sensitivity for detecting an element is expected for high voltage electron energy-loss spectroscopy and energy-filtered imaging.

CONTENTS

Preface

At the dawn of the long-awaited 21st century, we chemists are looking to the future with ambition. In the final decades of the last century, chemists have been claiming that chemistry should play a key role as the central science in the new century in every area including life science, information technology, nano-technology, the environment, and the graying society. We are now in the 21st century and are ready to put our best foot forward.

In this context, our Institute for Chemical Research, ICR, has entered into the new century with ideal situations. The proposal for our new attached research center, the Bioinformatics Center, was approved at the end of December as the fiscal 2001 draft budget. Thus, from April 2001, two new laboratories will join our Institute, making 29 laboratories in total. The bioinformatics research in this center will be led by Prof. KANEHISA Minoru who was awarded a special budget for the so-called Millennium Project in April 2000. Also, from April 2000, the Kyoto University Center of Excellence (COE) Project entitled "Elements Science" started as a five-year research project; Eight of the total ten research members, including the project leader TAMAO, have joined this project from ICR, representing the core of the project. In addition, many research staff members have received a variety of special grants. Thus our ICR is now growing steadily not only in quantity but also in quality, and thus keeping the vitality necessary for overcoming the forthcoming inevitable turning points of national universities, such as transformation into agencies, the evaluation of research and education by an independent assessment body, and policy changes in the budget distribution.

There was also a significant change in the ICR administration office last year. The previous six individual offices belonging to the five institutes and one center located on the Uji campus were combined into a single office. On January 6, 2001, the reform of the Japanese Government was carried out to regroup the government ministries and agencies into 13 from the previous 23. The previous Monbusho and Kagaku-Gijutsu-cho were combined into the Monbu-Kagaku-sho, the Ministry of Education, Culture, Sports, Science and Technology. It is hoped that these reforms were carried out in an effort to increase efficiency and flexibility. Therefore, we expect an increase in their services.

The ICR Annual Report continues to strive to provide timely and important information on the scientific activities of the ICR. At the end of March, 2000, Prof. MUKOYAMA Takeshi of the Laboratory of

Atomic and Molecular Physics retired from our institute and was appointed to a Professorship at Kansai Gaidai University. The former Director, Prof. MIYAMOTO Takeaki of the Laboratory of Polymeric Materials retired a year early from our institute and became the President of the Matsue National College of Technology. At the end of March 2001, Prof. KOBAYASHI Takashi of the Laboratory of Crystal Information Analysis will also retire from the ICR. Sadly, Technician Ms. SUZUKI Mitsuko suddenly passed away in December; May she rest in peace.

We have appointed two new young professors in 2000. In April, Prof. TOKITOH Norihiro moved from Kyushu University to the Laboratory of Organoelement Chemistry. In May, Prof. SORIN Yoshiki returned from Kanazawa University to chair the professorship of the Laboratory of Hydrospheric Environment Analysis at ICR. At the present stage, 23 full professors, 27 associate professors, and 41 instructors work in the ICR, and about 220 graduate students and 23 foreign researchers study at the ICR.

Finally, I would like to congratulate Prof. SHINJO Teruya for being awarded a Purple Ribbon Medal (Shijuhosho) and Prof. SUGIURA Yukio for the Pharmaceutical Society of Japan Award.

January, 2001

TAMAO Kohei
DIRECTOR

TOPICS AND INTRODUCTORY COLUMNS OF LABORATORIES

Key to headline in the columns

RESEARCH DIVISION — Laboratory (Subdivision)*

*** See also "Organization and Staff" on pages 84 and 85.**

Abbreviations used in the columns

Prof Em	Professor Emeritus
Prof	Professor
Vis Prof	Visiting Professor
Assoc Prof	Associate Professor
Lect	Lecturer
Lect(pt)	Lecturer
Instr	Instructor
Assoc Instr	Associate Instructor
Techn	Technician
Guest Scholar	Guest Scholar
Guest Res Assoc	Guest Research Associate
Univ	University

GS	Graduate Student
DC	Doctor's Course (Program)
MC	Master's Course (Program)
UG	Undergraduate Student
RF	Research Fellow
RS	Research Student

D Sc	Doctor of Science
D Eng	Doctor of Engineering
D Agr	Doctor of Agricultural Science
D Pharm Sc	Doctor of Pharmaceutial Science
D Med Sc	Doctor of Medical science

The Effect of Crystal Dispersion on the X-ray Emission Spectrum Observed using a Double Crystal Spectrometer

Tatsunori Tochio, Yoshiaki Ito and Kazuhiko Omote

The effect of the rocking curve on the x-ray emission spectrum observed using a double-crystal spectrometer was discussed. The results for Si (220) crystal at 1.54056Å (Cu $K\alpha_1$) show that the x-ray of wavelength λ_0-$\Delta\lambda$ ($\Delta\lambda$=0.00007Å) is much more reflected by the double crystal put in the (++) position of θ_B than the x-ray of wavelength λ_0 which exactly satisfies the Bragg condition. In the last we mentioned what we observe in our measurement with a double-crystal spectrometer.

Keywords: double-crystal spectrometer/ rocking curve/ x-ray emission spectrum

X-ray emission spectroscopy is known as a valuable tool for estimating the level width and the probabilities of various multi-electron transitions. In spite of its usefulness the instrumental function which is specific for the spectrometer used makes a precise analysis difficult. The instrumental function for a double-crystal spectrometer is relatively small compared with that for a single crystal spectrometer because the first crystal plays the same role as a narrow slit. But even for a double crystal spectrometer the instrumental function cannot be neglected. The aim of our work is to evaluate the effect of the crystal dispersion on the x-ray emission spectrum observed by means of a double-crystal spectrometer and to establish the way to analyze it. The crystal dispersion is considered to be a main component of the instrumental function in a double-crystal spectrometer and we may assume that the contributions from other components are almost negligible.

First we consider the monochromatic x-ray which has the wavelength λ_0 satisfying the Bragg condition with the Bragg angle θ_B determined by the positions of two crystals. As can be seen from the Figure1, the beam reflected on the first crystal by the angle of $\theta=\theta_B+d\theta$ makes an incidence angle of $\theta'=\theta_B-d\theta$ with the surface of the second crystal. This gives us the expression for the rocking curve for double crystal ($R_D(\theta_B;\lambda_0;\theta')=R_D(\theta_B;\lambda_0;2\theta_B-\theta)$) as follows.

$$R_D(\theta_B;\lambda_0;\theta')=R_S(\theta_B;\lambda_0;\theta')\times R_S(\theta_B;\lambda_0;2\theta_B-\theta'). \quad (1)$$

Here, $R_S(\theta)$ expresses the rocking curve for single crys-

STATES AND STRUCTURES — Atomic and Molecular Physics —

Scope of Research

In order to obtain fundamental information on the property and structure of materials, the electronic states of atoms and molecules are investigated in detail using X-ray, SR, ion beam from accelerator and nuclear radiation from radioisotopes. Theoretical analysis of the electronic states and development of new radiation detectors are also performed.

Assoc. Prof
ITO,
Yoshiaki
(D Sc)

Instructor
KATANO,
Rintaro
(D Eng)

Instructor
NAKAMATSU,
Hirohide
(D Sc)

students:
SHIGEMI, Akio (DC)
TOCHIO, Tatsunori (DC)
MASAOKA, Sei (DC)
SHIGEOKA, Nobuyuki (DC)
MUTAGUCHI, Kohei (MC)
OHASHI, Hirofumi (MC)
NAKANISHI, Yoshikazu (RF)

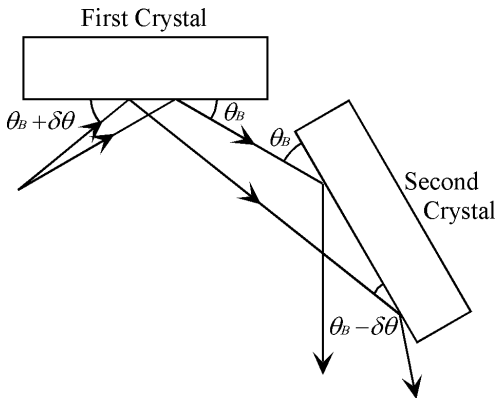

Figure1. Schematic diagram of the reflections by double-crystal with (++) position

tal which we define as the average of the rocking curve for the normal polarization and that for the parallel polarization. In the normal polarization the electric vector ***E***, at the moment when the x-ray is reflected, is normal to the plane containing the wave vector for the incident beam $\boldsymbol{k_0}$ and that for the diffracted beam $\boldsymbol{k_H}$, while in the parallel polarization the electric vector ***E*** lies in that plane. The curves of $R_D(\theta')= R_D(2\theta_B-\theta)$ for Si(220) at Cu Kα_1 energy are shown in the Figure 2- (a).

Now we consider the beam having the wavelength λ' which is very close to λ_0. The Bragg angle for this beam θ_B' is given by

$$\theta_B' \cong \theta_B + \left(\frac{d\theta}{d\lambda}\right)_{\lambda=\lambda_0}(\lambda'-\lambda_0) = \theta_B + \frac{\lambda'-\lambda_0}{\lambda_0}\tan\theta_B \qquad (2)$$

This leads to the expression for the rocking curve in a double-crystal (The attention should be paid to the fact that the positions of the two crystals are not for θ_B' but for θ_B.) at the wavelength of λ' as follows.

$$\begin{aligned} R_D(\theta_B;\lambda';\theta') &= R_S(\theta_B;\lambda';\theta')\times R_S(\theta_B;\lambda';2\theta_B-\theta') \\ &\cong R_S\left(\theta_B;\lambda_0;\theta'-\frac{\lambda'-\lambda_0}{\lambda_0}\tan\theta_B\right) \\ &\quad\times R_S\left(\theta_B;\lambda_0;2\theta_B-\theta'+\frac{\lambda'-\lambda_0}{\lambda_0}\tan\theta_B\right). \qquad (3) \end{aligned}$$

We can easily check that $R_D(\theta_B;\lambda';\theta)$ corresponds to equation (1) when λ' is equal to λ_0. For $\lambda'=\lambda_0-\Delta\lambda$, $\lambda_0+\Delta\lambda$ ($\Delta\lambda$=0.00007 Å), the curve of $R_D(x;\theta)$ is shown in the Figure 2-(b),(c) respectively. Figure 2- (a),(b),(c) show that the x-ray of wavelength $\lambda_0-\Delta\lambda$ is reflected most strongly compared with the others. In fact *S(a)* : *S(b)* : *S(c)*, the ratio of the area under the curve, is approximately 4 : 67 : 1. When the intensity distribution of the incident beam on the wavelength λ is $I_{in}(\lambda)$, the intensity distribution of the diffracted beam becomes

$$I_{out}(\theta_B;\lambda) = \int I_{in}(\lambda)R_D(\theta_B;\lambda;\theta')d\theta' . \qquad (4)$$

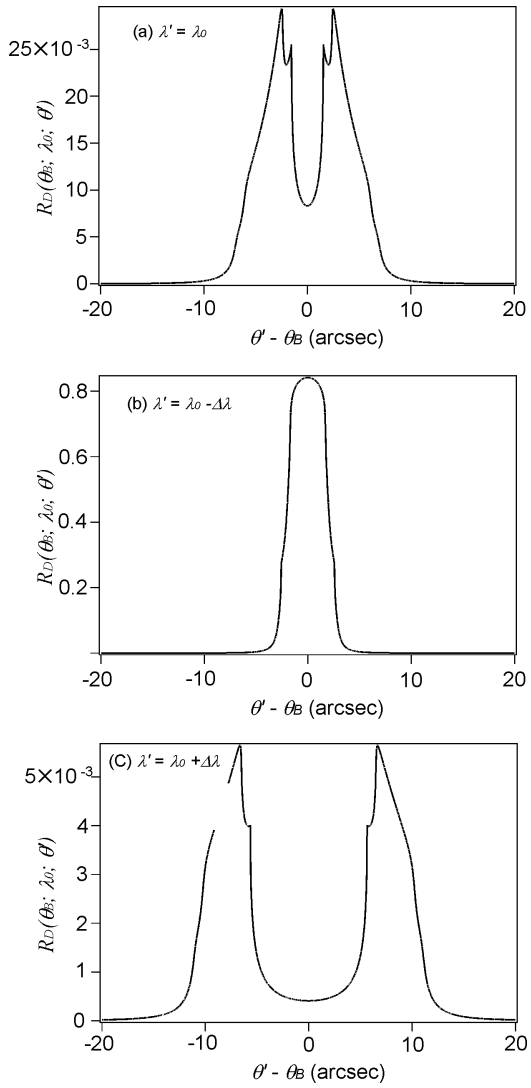

Figure 2. $R_D(\theta_B;\lambda';\theta')$ for Si (220) at (a) $\lambda'=\lambda_0$ (λ_0 =1.54056**Å**), (b) $\lambda'=\lambda_0-\Delta\lambda$ ($\Delta\lambda$=0.00007 **Å**), (c) $\lambda'=\lambda_0+\Delta\lambda$ ($\Delta\lambda$=0.00007 **Å**)

Inversely, the the intensity distribution of the diffracted beam in the direction θ' is expressed as follows .

$$I_{out}(\theta_B;\theta') = \int I_{in}(\lambda)R_D(\theta_B;\lambda;\theta')d\lambda . \qquad (5)$$

The range of angle or wavelength having a significant intensity is so small that the detector can count all the photons in this range. Then the expression for what we observe is written as

$$I_{out}(\theta_B) = \iint I_{in}(\lambda)\,R_D(\theta_B;\lambda;\theta')\,d\lambda\,d\theta' \qquad (6)$$

The observed spectrum is considered to be the trace of $I_{out}(\theta_B)$ at each point of θ_B which we change during the scan.

Branching Ratio and L_2+L_3 Intensities of 3d-Transition Metals in Phthalocyanines and the Amine Complexes

Masanori Koshino, Hideki Kurata, Seiji Isoda and Takashi Kobayashi

$L_{2,3}$ inner-shell excitation spectra were obtained by electron energy-loss spectroscopy (EELS) for the divalent first transition series metals in phthalocyanine complexes. It was found that the value of normalized total intensity of I(L_2+L_3) was nearly proportional to the formal electron vacancies of each 3d-state, and the values of the branching ratio, I(L_3)/I((L_2+L_3), represented a high spin state rather than low spin state. EELS was also applied to charge-transfer complexes of FePc with amine. It was concluded that their I(L_2+L_3) intensity of Fe showed the decrease in vacancies of 3d-states on the formation of the charge transfer complex, which suggests some electron transfer from the amine to Fe in phthalocyanine.

Keywords: Electron energy-loss spectroscopy/ Transition metals/ Phthalocyanines/ Charge transfer

For the 3d-transition metal atoms with open shell structures, characteristics of such metal compound predominately depend on its d-electronic states which contribute to the chemical bonding and also are affected easily by surrounding atoms. Electron energy-loss spectroscopy (EELS) can be used to get information on the d-states even from a small region of a specimen. Like other optical analytical methods, the $L_{2,3}$ spectra which can be obtained as a result of an excitation, for example, from the initial states $2p^6 3d^n$ to the final states $2p^5 3d^{n+1}$ will be available to investigate d-occupancy and other d-electronic states. In the present study, we examined relation between 3d-occupancy and L-edge spectra of phthalocyanines (Pc) with various 3d-metals. We also examined the spectral changes in FePc due to complex formation with gas phase amines such as pyridine or γ-picoline, where the amines are expected to act as electron donors. The branching ratio I(L_3)/I(L_2+L_3), which depends on both the valence band spin-orbit coupling and the electrostatic interactions between core-hole and valence-electron, was also obtained in each complex and compared to the calculated values on metal oxides by Thole and Laan [1].

The normalized spectra of TiOPc, CrPc, MnPc, FePc, CoPc, NiPc and CuPc are shown in Fig.1. L_2+L_3 integral intensities were measured on each spectrum in Fig.1 and plotted against the number of formal 3d-electrons as shown in Fig.2. The result reveals that the increases in d-electrons causes the decrease of L_2+L_3 intensities; that is, the metal phthalocyanines with larger number of 3d-electrons show lower L_2+L_3 intensities. It is due to the decrease in the number of vacancies in 3d-orbitals.

Relative L_3 intensities in the excitation, the branching

STATES AND STRUCTURES — Crystal Information Analysis —

Scope of research

Structures of materials and their structural transition associated with chemical reactions are studied through the direct observation of atomic or molecular imaging by high resolution spectro-microscopy. It aims to explore new methods for imaging with high resolution and for obtaining more detailed chemical information. The following subjects are studied: direct structure analysis of ultrafine crystallites and ultrathin films, crystal growth and adsorption states of organic materials, and development on high resolution energy filtered imaging as well as electron energy-loss spectroscopy.

Prof
KOBAYASHI, Takashi
(D Sc)

Assoc Prof
ISODA, Seiji
(D Sc)

Instr
OGAWA, Tetsuya
(D Sc)

Instr
NEMOTO, Takashi
(D Sc)

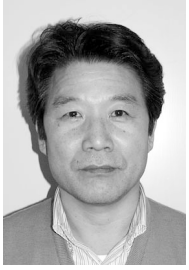

Assoc Instr
MORIGUCHI, Sakumi

Students:
SUGA, Takeo (RF, D Sc)
KUWAMOTO, Kiyoshi (DC)
KOSHINO, Masanori (DC)
YAJI, Toyonari (DC)
FUJIWARA, Eiichi (DC)
TSUJIMOTO, Masahiko (DC)
YOSHIDA, Kaname (DC)
FURUKAWA, Chieko (DC)
HASEGAWA, Yuko(MC)
TAKAJYO, Daisuke(MC)
TAKANO, Hiroki(MC)
HAYASHI, Masayuki(MC)

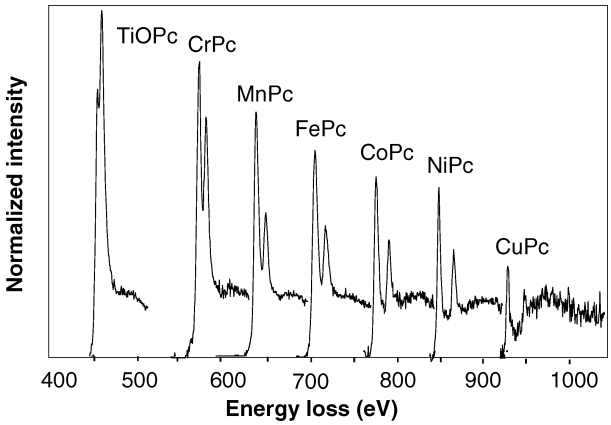

Figure 1. Series EELS spectra of MPc.

ratio $I(L_3)/I(L_2+L_3)$ is sensitive to the spin-states of 3d-electrons and shows large value for high spin-state and vice versa [2-4]. The correlation between formal 3d-occupancy and the branching ratio is shown in Fig.3 with the open circles of the line (a). These values are gradually increasing to reach the highest one of 0.72 for MnPc which has d^5 electrons and then decreasing slightly with increasing further the number of 3d-electrons. In the absence of both the electrostatic interactions between core-hole and 3d-electron and the spin-orbit coupling in the valence electrons, the branching ratio is 2/3. Actually, however, the branching ratio varies depending on spin-orbital and electrostatic interactions as well as on ligand field. Laan *et. al*. have calculated the branching ratio relating to the transition from the initial state $2p^63d^n$ to the final state $2p^53d^{n+1}$ in the series of 3d-metal ions [2]. In the figure, the calculated branching ratios for high- and low-spin states were obtained for the case when all spin-orbital split levels of

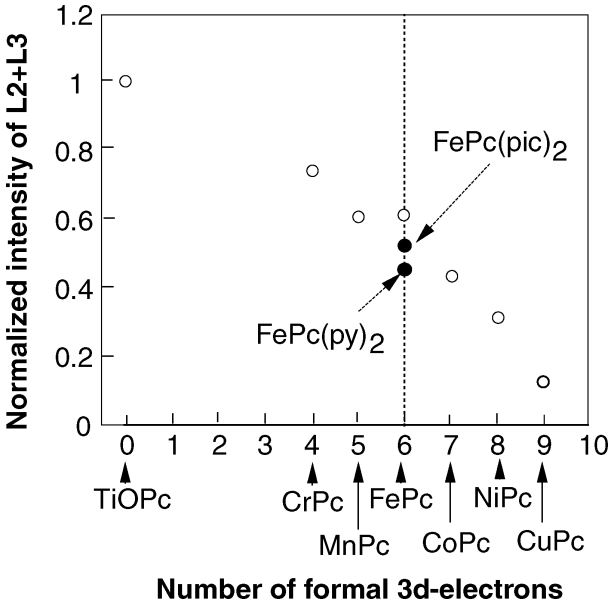

Figure 2. Normalized total intensities of L_2+L_3 as a function of the number of formal 3d-electrons.

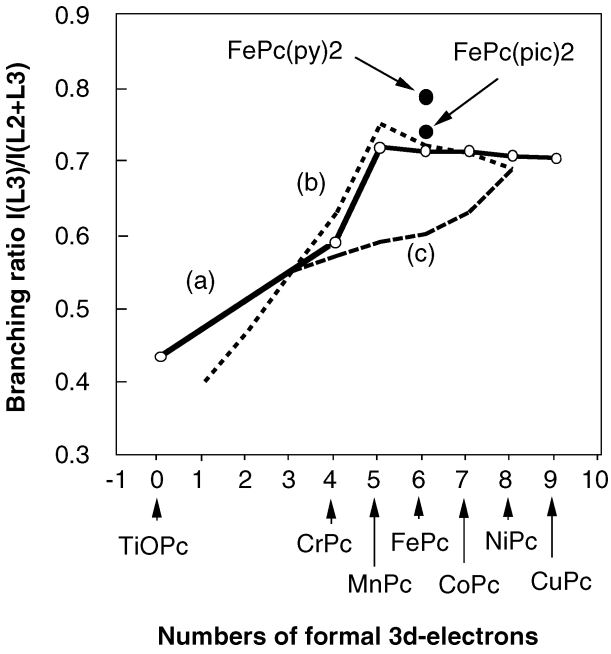

Figure 3. Branching ratio against number of formal 3d-electrons; (a) measured branching ratios of metal phthalocyanines, (b) calculated for high spin-state and (c) for low spin-state

the ground state term are equally populated (z=0, in their notation), which are represented by the curves (b) and (c) in Fig.3, respectively. The present results on MnPc, FePc and CoPc, agree well with those of the calculated ones for high-spin state. This indicates that the metal phthalocyanines from MnPc to CoPc has high spin state.

FePc-amine complexes show smaller intensity of L_2+L_3 compared to that of pristine FePc as already summarized in Fig.2, which suggests that the addition of amine ligands leads to the decrease in vacancy of 3d-states of Fe atom; that is, the amines donate some amount of electrons to Fe in FePc. In the normalized intensities of L_2+L_3 in Fig.2, the pyridine seems to donate more electrons to FePc than γ-picoline. As for the branching ratio, the amine complexes have larger values than that of FePc (Fig.3), which suggests that the spin-orbit coupling may be changed by addition of amine ligands. Here we can conclude that the amines affect not only the population of electrons, but also on the electronic interaction in FePc.

References

1. Thole, B T and van der Laan, G :Phys.Rev. **B38**, 3158-3171 (1988).
2. van der Laan, G and Thole, B T: Phys. Rev. **B43**, 13401-13410 (1991).
3. Kurata, H and Colliex, C: Phys. Rev. **B48**, 2102-2108 (1993).
4. Kurata, H, Hojou, K and Uozumi, T: J.Electron Microscopy **47**, 293-299 (1998).

High-Resolution Observation of Crystal Transformation in Isotactic Polybutene-1 Single Crystals

Masatoshi Tosaka, Takashi Kamijo, Masaki Tsuji and Shinzo Kohjiya

The crystal transformation in lamellar crystals of polybutene-1 grown from an amyl acetate solution was studied by cryogenic high-resolution transmission electron microscopy. The shape of the transformed trigonal (form-1) crystal domains in the surrounding tetragonal (form-2) crystal was successfully revealed. Along with the nucleation of "untwinned" form-1, the existence of another nucleation mechanism which creates "twinned" form-1 was suspected. The growth of form-1 crystal was thought to progress not stem by stem but by pulling in the molecular chains from the surrounding form-2, creating new stems of form-1. The shape of the form-1 domain was irregular, and no specific crystallographic direction along which the form-1 domain tends to grow was found.

Keywords : Transmission electron microscopy/ Lattice fringes/ Image processing/ Nucleation/ Molecular mechanism

Three major crystalline forms have been reported for isotactic polybutene-1 (PB1) so far. Form-1 is characterized by the trigonal unit cell (space group $R3c$ or $R\bar{3}c$; a = 1.77 nm, c (chain axis) = 0.65 nm) and 3/1 helical conformation of backbone chains. Form-2 has the tetragonal unit cell ($P\bar{4}$; a = 1.542 nm, c (chain axis) = 2.105 nm) in which four molecular chain stems with 11/3 helical conformation are packed. In form-3, molecular chains with 4/1 helical conformation are packed in the orthorhombic unit cell ($P2_12_12_1$; a = 1.238 nm, b = 0.888 nm and c (chain axis) = 0.756 nm). Form-2 gradually transforms into form-1 on aging at room temperature [1]. It is still unclear, in terms of the molecular movements, how form-2 transforms into form-1 without changing the original shape. In this paper, solution-grown lamellar crystals of PB1 are studied by high-resolution transmission electron microscopy (HREM). The shape of each crystal domain is discussed on the basis of the distribution of corresponding lattice fringes in the HREM image.

The as-received PB1 was dissolved in amyl acetate to be an 0.01 or 0.02 wt% solution. Isothermal crystallization was performed by putting a test tube containing the solution into an oil bath thermostated at the prefixed crystallization temperature. For HREM, a cryogenic transmission electron microscope (JEOL JEM-4000SFX; 400kV) was used. In this case, the built-in MDS was utilized and the specimen was cooled down to the liquid helium temperature (4.2K) to suppress electron irradiation damage [2,3]. The HREM images were processed with a computer for detection of the domains in which certain lattice fringes appear [4]. First, by applying a Fourier-filtering technique, an intermediate image was created from the original image using a pair of intensity maxima in the reciprocal space (viz., $hk0$ and $\overline{hk}0$; the origin, 000, was not included in processing). This intermediate image showed the corresponding lattice fringes on the whole area; the strength (contrast) of the lattice fringes was different from place to place. The intermediate image was

STATES AND STRUCTURES — Polymer Condensed States —

Scope of research

Attempts have been made to elucidate the molecular arrangement and the mechanism of structural formation/change in crystalline polymer solids, polymer gels and elastomers, polymer liquid crystals, and polymer composites, mainly by electron microscopy and/or X-ray diffraction/scattering. The major subjects are: synthesis and structural analysis of polymer composite materials, preparation and characterization of polymer gels and elastomeric materials, structural analysis of crystalline polymer solids by direct observation at molecular level resolution, and *in situ* studies on structural formation/change in crystalline polymer solids.

Prof KOHJIYA, Shinzo (D Eng)

Assoc Prof TSUJI, Masaki (D Eng)

Instr URAYAMA, Kenji (D Eng)

Instr TOSAKA, Masatoshi (D Eng)

Instr MURAKAMI, Syozo (D Eng)

Students
BEDIA, Elinor L.(DC)
FUJITA, Masahiro (DC)
KAWAMURA, Takanobu (DC)
NAKAO, Toshio (DC)
KOJIMA, Masaaki (DC)
KITADE, Taku (MC)
ENDO, Yoshiyuki (MC)
UEDA, Kazuhiro (MC)
OKUNO, Yuko (MC)
TOGAMI, Tadahiro (UG)
KITAMURA, Kenji (UG)

Research Fellow
MURAKAMI, Takeshi
SENOO, Kazunobu
ASAEDA, Eitaro
OHARA, Masayoshi

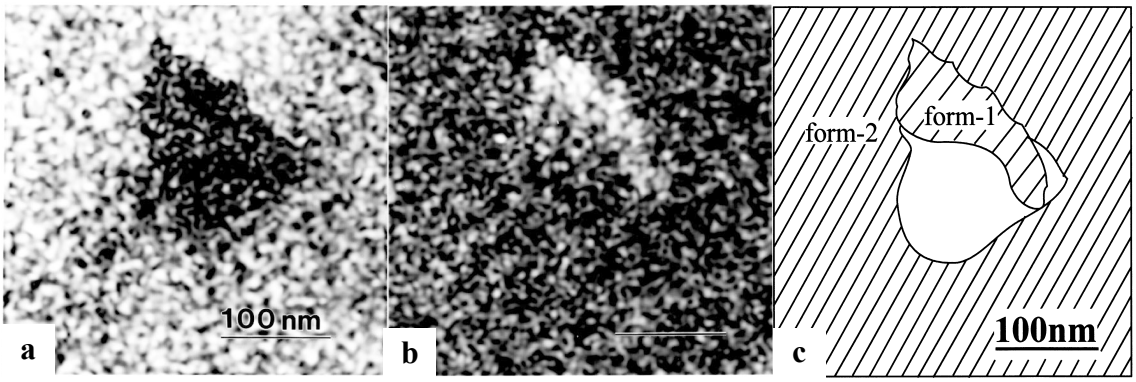

Figure 1. Partly transformed PB1 lamellar crystal. The specimen was kept at room temperature for 4 days before taking the HREM image. The bright regions are (a) form-2 and (b) form-1. The corresponding area and the orientation are summarized in (c), in which the stripes are drawn parallel to the (110) plane.

further processed by calculating the "local standard deviation" (LSD) of several (typically 5×5) pixels surrounding and including every given pixel. The LSD filter is a kind of smooth-edge detector and returns a larger value leading to an increase in brightness over a certain domain with inherent lattice fringes, namely lattice fringes that existed in the original image. By the image processing applied here, only the regions with inherent lattice fringes having a high contrast ought to be highlighted.

Figure 1 shows a set of images processed from one of the HREM images. The bright regions in parts a and b of Figure 1 show the form-2 and form-1 domains, respectively. Since the small spots in the processed images should have come from the noise in the original micrograph, they were neglected. Figure 1c summarizes the arrangement of these form-2 and form-1 domains. The stripes in each domain are drawn as to be parallel to the (110) plane. Because there is only one form-1 domain of single orientation, form-1 seems to have nucleated in a manner which does not include twinning.

Figure 2 summarizes the results from another set of processed images. It should be noted that four form-1 domains meet at one "point" indicated by the arrow in Figure 2. The convergence of separately-nucleated four domains at one "point" should be statistically rare. Furthermore, each pair of the two domains opposed at the "point" has the same crystallographic orientation. Therefore, it is strongly believed that the four form-1 domains nucleated at the point indicated by the arrow as a twin crystal. Figure 2 suggests that there is another nucleating mechanism which starts from a certain peculiar "point", creating the "twinned" form-1 crystallites.

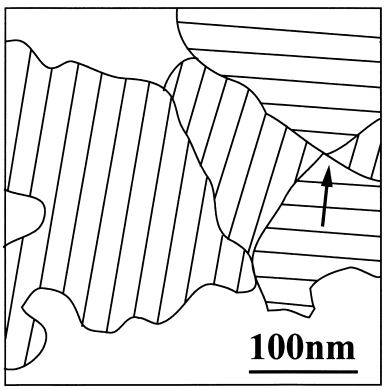

Figure 2. Arrangement of transformed form-1 crystallites in a lamella. The specimen was kept at room temperature for 4 days before taking the original HREM image. The stripes are drawn parallel to the (110) plane.

Because of the conformational change, the transformation from form-2 to form-1 accompanies the increase in length (by ca. 13%) of a molecular stem which is composed of a given number of monomer units. At the same time, the density of the crystallites increases and the area for a given number of stems decreases (by ca. 24% on the *ab*-plane). However, we observed neither the variation of lamellar thickness nor the generation of vacancies in the lamellae. Therefore, a considerable part of the increment of the stem length on the transformation should be consumed to fill the vacancy which results from the density change. The form-1 domain may grow by reeling in the molecular chains from the surrounding form-2 domain, uncoiling the form-2 crystallites and creating new stems of form-1. This hypothesis is supported by the fact that we found a region of several hundreds of nanometers of square, where three crystallites of the form-1 are closely packed without discernible vacancy. If the transformation were to progress stem by stem without changing the number of stems, then some of the stems would have to travel several tens of nanometers of distance (much more larger than the stem length) to form such a large crystallite.

References

1. Holland V F, Miller R L, *J. Appl. Phys.,* **35**, 3241 (1964).
2. Tsuji M, Kohjiya S, *Prog. Polym. Sci.*, **20**, 259 (1995).
3. Tosaka M, Tsuji M, Kohjiya S, *Mat. Sci. Res. Int.*, **4**, 79 (1998).
4. Tosaka M, Tsuji M, Cartier L, Lotz B, Kohjiya S, Ogawa T, Isoda S, Kobayashi T, *Polymer*, **39**, 5273 (1998).

Dynamics of supercritical water

Nobuyuki Matubayasi, Naoko Nakao and Masaru Nakahara

The rotational dynamics of water in super- and subcritical conditions is investigated by measuring the spin-lattice relaxation time T_1 of heavy water (D_2O). The experimentally determined T_1 is shown to be governed by the quadrupolar relaxation mechanism even in the supercritical conditions and to provide the second-order reorientational correlation time τ_{2R} of the O-D axis of a single water molecule. It is then found that while τ_{2R} decreases rapidly with the temperature on the liquid branch of the saturation curve, it remains on the order of several tens of femtoseconds when the density is varied up to twice the critical at a fixed supercritical temperature of 400 ºC. The comparison of τ_{2R} with the angular momentum correlation time shows that the rotational dynamics is not diffusive in supercritical water. The dependence of τ_{2R} on the hydrogen bonding state is also examined in combination with molecular dynamics simulations, and the effect of the hydrogen bonding on the rotational dynamics in supercritical water is found to be weaker than but to be on the same order of magnitude as that in ambient water on the relative scale.

Keywords : supercritical water / rotational dynamics / NMR / inertial effect / hydrogen bonding

Supercritical water receives much attention recently as a novel and clean medium for chemical processes of environmental and industrial importance. The rate of a chemical process in a fluid medium is determined by the thermodynamics and dynamics of hydration of the chemical species involved in the process. Although the overall behavior of a chemical reaction is governed by the free energy profile along the reaction coordinate, the dynamics of hydration often plays an important role in determining the reaction rate constant and is indispensable for a molecular description of the rate constant. The dynamics of supercritical hydration is inseparably related to the dynamical structure of pure solvent water at the supercritical state. Thus, in order to establish the molecular picture of the hydration dynamics in supercritical water, it is essential to characterize the dynamics of supercritical water as a pure solvent. In this work, we determine the reorientational correlation time of a single water molecule in supercritical heavy water (D_2O) by measuring the deuteron NMR spin-lattice relaxation time. We show that the deuteron spin-lattice relaxation time of supercritical heavy water is governed by the quadrupolar mechanism and provides information about the motion of a single water molecule in the configuration space.

In order to realize a supercritical state of heavy water (D_2O), the capillary method was employed. In this method, water is confined in a sealed capillary made of quartz and the capillary is placed in an NMR sample tube. The content of water in the capillary uniquely determines the density at supercritical conditions. The density of supercritical heavy water can be conveniently expressed by the packing fraction, which is defined as the ratio of the (liquid) water volume in the capillary to the total volume of the capillary at room temperature. When the packing frac-

INTERFACE SCIENCE — Solutions and Interfaces —

Scope of research

Structure and dynamics of a variety of ionic and nonionic solutions of physical, chemical, and biological interests are systematically studied by NMR under extreme conditions. High pressures and high temperatures are employed to shed light on microscopic controlling factors for the structure and dynamics of solutions. Vibrational spectroscopic studies are carried out to elucidate structure and orientations of organic and water molecules in ultra-thin films. Crystallization of protein monolayers, advanced dispersion systems at liquid-liquid interfaces, and biomembranes are also investigated.

Prof
NAKAHARA, Masaru
(D Sc)

Assoc Prof
UMEMURA, Junzo
(D Sc)

Instr
MATSUMOTO, Mutsuo
(D Sc)

Instr
MATUBAYASI, Nobuyuki
(Ph D)

Assoc Instr
OKAMURA, Emiko
(D Pharm Sci)

Assoc Instr
WAKAI, Chihiro
(D Sc)

Lecturer(part-time)
BOSSEV, Dobrin (D Sc)
Students
YAMAGUCHI, Tsuyoshi (DC)
KONISHI, Hirofumi (DC)
KIMURA, Tomohiro (DC)
MCNAMEE, Cathy (DC)
TSUJINO, Yasuo (DC)
TOYA, Hiroshi (MC)
KAKITSUBO, Ryou (MC)
NAKAO, Naoko (MC)
NAGAI, Yasuharu (MC)
MURAKAMI, Takashi (MC)
IWASA, Masaki (MC)
TAKIZAWA, Takeyuki (MC)

tion is ρ, the density of heavy water at a supercritical temperature is 1.1ρ g/cm^3, provided that the liquid density is 1.1 g/cm^3 at room temperature. The packing fractions examined in the present work are ρ = +0.0, 0.1, 0.2, 0.3, 0.4, 0.5, and 0.6 with errors of less than 0.03. The expression ρ = +0.0 means that the packing fraction is smaller than 0.02, though water is definitely present in the capillary. We adopt this expression for the lowest packing fraction since it is not possible in our capillary apparatus to identify ρ precisely when $\rho < 0.02$. Actually, it is sufficient for the following discussion simply to specify that the lowest ρ examined is certainly smaller than 0.1.

The T_1 was determined by the inversion recovery method, and it is related to the reorientational correlation time τ_{2R} of a single water molecule through

$$\frac{1}{T_1} = \frac{3\pi^2}{2}\left(\frac{e^2Qq}{h}\right)^2 \tau_{2R} \qquad (1)$$

where e^2Qq/h is the quadrupolar coupling constant (QCC) which represents the interaction between the quadrupole moment of the D nucleus (eQ) and the electric field gradient at the nucleus (eq). In Fig. 1, we show τ_{2R} as a function of the density ρ over the thermodynamic states examined in the present work. In this figure, the QCC value adopted in Eq. (1) is the ambient liquid phase value of 256 kHz when $\rho > 0.6$ and the system is on the liquid branch of the saturation curve. At the supercritical states with $\rho \le 0.6$, τ_{2R} shown in Fig. 1 is determined through Eq. (1) by assuming that the deviation of the QCC value at a given thermodynamic state from that at the dilute gas state is proportional to the corresponding deviation of the average dipole moment of a water molecule calculated from computer simulations of the TIP4P-FQ model. It is seen that τ_{2R} decreases rapidly with the temperature on the liquid branch of the saturation curve. While the reorientational relaxation proceeds on the order of picosecond in ambient water, it is on the order of several tens of femtoseconds when a supercritical state is realized. At a fixed supercritical temperature of 400 ºC, τ_{2R} is between 45 and 80 fs at the densities from ρ = 0.1 to 0.6. When the chemical shift δ is concerned in the supercritical conditions, it was found that the strength of the density dependence expressed as $\rho\partial\delta/\partial\rho$ is comparable to δ itself.

For the reorientational correlation time τ_{2R}, in contrast, Fig. 1 shows that τ_{2R} changes only by ~30% in response to the density variation from ρ = 0.1 to 0.6 at a fixed temperature of 400 ºC. This shows that the rotational dynamics reflects only partially the change in the state of the hydrogen bonding caused by the density variation. When the intermolecular interaction is absent, τ_{2R} is to diverge due to the conservation of angular momentum. Figure 1 then shows that the intermolecular interaction is effective when the density is above ~1/3 of the critical.

In order to closely see the effect of the hydrogen bonding state on the rotational dynamics, we examine the dependence of τ_{2R} on the number N_{HB} of hydrogen bonds by using the molecular dynamics simulations. It was then observed that the absolute change in τ_{2R} against the variation of N_{HB} is larger by orders of magnitude at the ambient state than at the supercritical states. On the other hand, the relative change at the supercritical states is on the average ~2/3 of that at the ambient state. When seen on the relative scale, therefore, the dependence of the rotational dynamics on the hydrogen bonding state in supercritical water is weaker than but is on the same order of magnitude as that in ambient water. According to Fig. 1 and the number N_{HB} of hydrogen bonds determined from the chemical shift, the experimental τ_{2R} increases by ~20% per hydrogen bond when the density is varied at a constant supercritical temperature.

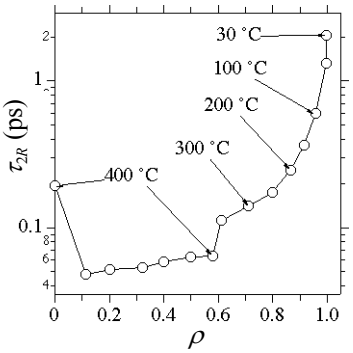

Figure 1. The reorientational correlation time τ_{2R} of heavy water as a function of density ρ.

The angular momentum correlation time τ_J can also be determined from T_1 of light water (H_2O). It is then found that τ_{2R} is comparable to or smaller than τ_J over the entire range of the supercritical conditions examined. In this case, the reorientational relaxation is not diffusive and that the inertial effect is operative. Furthermore, the ratios of τ_{2R} and t_J of D_2O to those of H_2O in the supercritical conditions are ~1.3 and are close to the square root of the ratio of the moment of inertia. Since the viscosity is experimentally coincident within ~5% between H_2O and D_2O in the supercritical conditions, the τ_{2R} difference between H_2O and D_2O reflects the inertial effects in the reorientational relaxation. At the ambient condition of ρ = 1.0 and 30 ºC, on the other hand, since the angular momentum relaxation was found to be faster than the reorientational relaxation by orders of magnitude, the rotational diffusion limit is realized.

In order to obtain quantitative insights into a reaction dynamics in supercritical water, it is often necessary to estimate the lifetime of the hydration structure around the reactive species. According to the previously accumulated data concerning the rotational dynamics of solutions at ambient conditions, it is natural to consider for both ionic and nonpolar solutes that when a super- or subcritical condition is realized, the reorientational relaxation of a water molecule around the solute deviates from that in the pure solvent by a factor of less than ~2. Thus, τ_{2R} determined in the present work serves as the characteristic time for the orientational part of a dynamical process in super- and subcritical water.

Electron Injection to Unoccupied Electronic States in Organic Semiconductor Thin Films Studied by Inverse Photoemission Spectroscopy

Hiroyuki Yoshida, Kiyohiko Tsutsumi and Naoki Sato

Inverse photoemission spectroscopy (IPES) in the vacuum ultraviolet region was applied to directly observe behaviors of electron injection into unoccupied electronic states in perylene-3,4,9,10-tetracarboxylic dianhydride (PTCDA) thin films due to alkali metal. By the analysis of the observed results the amount of injected electrons per PTCDA molecule was evaluated with relation to the dopant concentration. The derived relationship has been explained with the aid of DV-Xα calculations of energy levels concerned.

Keywords: *Inverse photoemission/ Unoccupied electronic state/ Organic semiconductor/ Alkali metal doping /Electron injection*

As electronic properties of organic semiconductors are predominated by their electronic structures around the energy gap, examining those of unoccupied states as well as valence states is essentially important; Photoemission spectroscopy (PES), particularly ultraviolet photoemission spectroscopy (UPS), has widely been applied to observe valence electronic structures, however, the direct observation of unoccupied electronic structures using inverse photoemission spectroscopy (IPES) has so far been carried out only for a few organic materials because of difficulties in the experimental method chiefly caused by a very low efficiency of the inverse photoemission process.

Recently we designed and installed an apparatus of IPES in the mode of Bremsstrahlung Isochromat Spectroscopy (BIS), with aiming at the measurements of organic samples in particular [1]. In this work we have studied the charge carrier injection into an organic semiconductor by direct examination of electron transfer into unoccupied electronic states in perylene-3,4,9,10-tetracarboxylic dianhydride (PTCDA) thin films by alkali metal doping which is usually employed. Observed results with different dopant concentrations will be discussed in terms of electron-transfer equilibrium reaction from alkali metals to a PTCDA molecule [2].

PTCDA purchased from BASF were purified by repeated sublimation. Its thin films in the thickness of 6 nm were vacuum-deposited onto gold substrates under the pressure lower than 5×10^{-8} Pa. IPES measurements of these specimen films were carried out in situ as follows: mono-energetic electrons in the range of 4-12 eV were irradiated onto a sample film and vacuum ultraviolet light emitted from the film was detected by a band-pass detector with sensitivity maximum at 9.8 eV (1 eV ≈ 0.1602 aJ) and the full width at half maximum (FWHM) of 0.65 eV. The detected photocurrent normalized by the

INTERFACE SCIENCE — Molecular Aggregates —

Scope of research

The research at this subdivision is devoted to correlation studies on structures and properties of both natural and artificial molecular aggregates from two main standpoints: photoelectric and dielectric properties. The electronic structure of organic thin films is studied using photoemission and inverse photoemission spectroscopies in connection with the former, and its results are applied to create novel molecular systems with characteristic electronic functions. The latter is concerned with heterogeneous structures in microcapsules, biopolymers, biological membranes and biological cells, and the nonlinearity in their dielectric properties is also studied in relation to molecular motions.

Professor
SATO, Naoki
(D Sc)

Associate Professor
ASAMI, Koji
(D Sc)

Instructor
KITA, Yasuo
(D Sc)

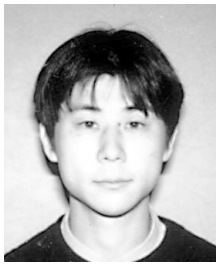

Instructor
YOSHIDA, Hiroyuki
(D Sc)

Students
TSUTSUMI, Kiyohiko (DC)
OKAZAKI, Takashi (MC)
KITA, Hiroki (MC)
SAKOU, Machiko (MC)
YAMAMOTO, Daisuke (MC)

incident electron-beam current was recorded to give an IPE spectrum, with the overall energy resolution of about 0.80 eV. Alkali metal doping into a PTCDA film was carried out using a SAES Getters alkali metal dispenser, followed by aging. The dopant concentration was determined by a quartz oscillator monitor and also by X-ray photoemission spectroscopy in C1s and K2p regions. All the experiments were performed at room temperature.

Fig. 1 depicts IPE spectra (drawn in dotted lines) observed for potassium doped PTCDA thin films, *i.e.* K_nPTCDA, where n is potassium concentration defined as the mole fraction of potassium atoms against PTCDA molecules. The abscissa is energy of the state relative to the Fermi level. The decrease in intensity of the first or lowest-energy feature among three ones with increasing n is most notable. To make a close study of this phenomenon we tried to deconvolute each spectrum using three Gaussians; the spectrum fitted by these Gaussians indicated by a solid line reproduces the observed one well. By such a procedure it is demonstrated that the intensity of the first feature decreases with increasing n while those of the second and third ones almost unchanged. This can be explained by a decrease in density of the lowest unoccupied states in PTCDA caused by electron injection from potassium atoms.

The first feature of IPE spectrum is derived only from LUMO of PTCDA which can accommodate maximal two electrons and a decrease of its intensity is proportional to the amount of electrons transferred to LUMO, so that the number δ of electrons injected to a PTCDA molecule in the film can be expressed as follows:

$$\delta = 2\,(1 - I / I_0) \qquad (1)$$

where I_0 and I are intensities of the first feature before and after potassium doping, respectively. In order to explain the obtained result that δ values calculated from I using eq (1) are much less than the corresponding n especially at large n values, the following simple electron-transfer equilibrium is considered:

$$\mathrm{PTCDA} + n\,\mathrm{K} = \mathrm{PTCDA}^{-\delta} + n\,\mathrm{K}^{+\delta/n} \qquad (2)$$

At the initial stage the highest occupied atomic orbital (HOAO) of a potassium atom is located energetically higher than LUMO of PTCDA. On the one hand, the increase of electron density on an atom or a molecule will raise its one-electron levels. With taking this into account, electrons pre-distributed at HOAOs of n potassium atoms to be interacted with a PTCDA molecule are possible to transfer to LUMO of the PTCDA molecule so far as the energies between LUMO of PTCDA, $E_P(-\delta)$, and HOAO of the potassium, $E_K(+\delta/n)$, coincide with each other.

To consider this, orbital energies of LUMO in a PTCDA molecule and HOAO in a potassium atom, *i.e.* $E_P(q)$ and $E_K(q)$, respectively, were calculated as functions of nominal charge qe by the DV-Xα method, where q is a real number not restricted to the integer and e is the elementary charge. From the results of such density functional calculations it is clarified that both $E_P(q)$ and $E_K(q)$ are expressed by linear functions of q as follows: $E_P(q) = A_P + qB_P$ and $E_K(q) = A_K + qB_K$, where A_P and B_P are constants determined for PTCDA and A_K and B_K are for potassium. With bearing in mind eq (2), the electron transfer reaction will reach equilibrium when the energy-level matching, $E_P(-\delta) = E_K(+\delta/n)$, is established. By combining this relation with the linear functions above, the number δ of electrons injected from n potassium atoms to a PTCDA molecule can therefore be evaluated by the following equation:

$$\delta = \delta(n) = (A_P - A_K) / (B_P + B_K/n) \qquad (3)$$

Thus-obtained result of $\delta(n)$ turned out to be in good agreement with the experimental one for δ *vs.* n. This conformity leads us to conclude that the number of electrons transferred from potassium atoms to a PTCDA molecule in the thin film is predominantly regulated by the electronic reciprocation between LUMO of the molecule and HOAO of a potassium atom with electron correlations involving Coulombic screening and repulsion in those atoms and molecules.

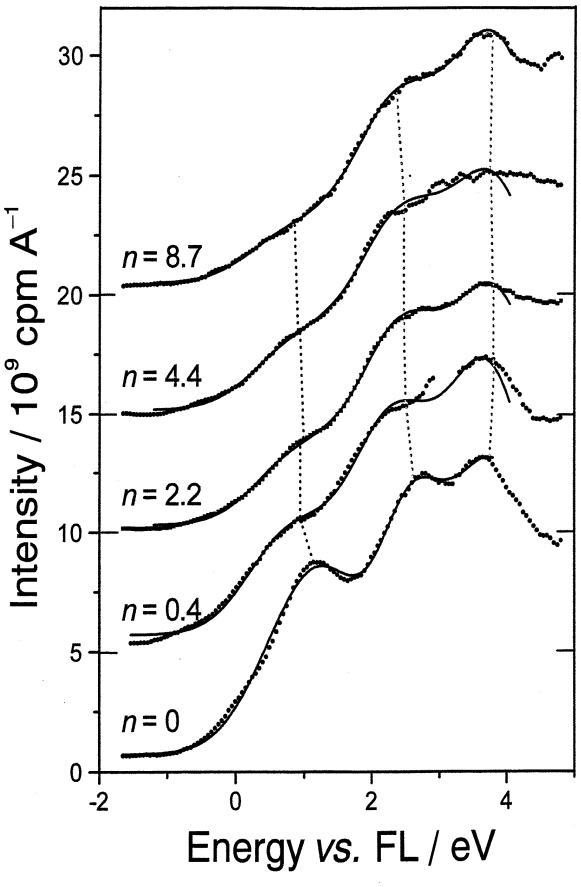

Figure 1 IPE spectra of a PTCDA evaporated thin film at different levels of potassium doping, K_nPTCDA.

References

1. Sato N, Yoshida Y and Tsutsumi K, *J. Elect. Spectrosc. Relat. Phenom.*, **88-91**, 861 (1998).
2. Sato N, Yoshida Y and Tsutsumi K, *J. Mater. Chem.*, **10**, 85 (2000).

Dissolved Trace Elements in Lake Biwa

Saeko Mito, Masakazu Matsui, Yoshiki Sohrin, Hiroshi Hasegawa, and Munetsugu Kawashima

A clean technique for analysis of freshwater has been developed. Lake water was collected from the northern basin of Lake Biwa, an oxic and monomictic lake, from 21 May 1994 to 4 December 1998. Dissolved trace elements (Al, P, V, Cr, Mn, Fe, Ni, Zn, As, Y, W and U) were measured by high-resolution inductively coupled plasma mass spectrometry (HR-ICP-MS). Their spatial and temporal distributions were strongly affected by the cycle of Fe and Mn.

Keywords: dissolved trace elements / freshwater / Lake Biwa /clean technique / HR-ICP-MS

Trace elements in freshwater have been studied with a view to understanding biogeochemical cycles of elements and protecting the environment from pollution. It has become clear that concentrations of dissolved trace elements in freshwater are lower than those previously reported (e.g., Pb and Cd in the Grate Lakes [1]). Contamination with trace elements through sampling, filtration, preconcentration and determination has been a serious problem. Investigation of trace elements in oxic lakes has been difficult, because many elements are present at a low concentration under well-oxygenated conditions. The northern basin of Lake Biwa (Northern Lake) is both a mesotrophic and monomictic lake, of which the water column is enough deep (average 44 m) to develop a summer thermocline but oxic throughout the year. We have developed a clean technique for the determination of trace elements in fresh water and observed their spatial and temporal distributions in Northern Lake. This is one of the largest set of data collected on dissolved trace elements in an oxic lake.

The lake water samples were collected by a Niskin sampling bottle or a Niskin-X sampling bottle, of which inner spring and latex tubing were replaced with silicon tubing. The interior of the samplers was precleaned with a standard procedure, which contains cleaning with detergent and 4 M HCl followed by rinsing with ultra pure water (MQW) produced with a Milli-Q water system. Immediately after sampling, lake water was transferred to a low-density polyethylene (LDPE) bottle using a silicon tubing and bell in order to prevent contamination with airborne particles. The LDPE bottle was precleaned with the standard procedure and with hot 4 M HCl, hot 0.5 M

INTERFACE SCIENCE — Hydrospheric Environment Analysis —

Scope of research

Research activities are concerned with geochemistry, oceanography, limnology and analytical chemistry, which are important basic sciences in order to realize the sustainable society. Major research subjects are as follows: (i) Biogeochemistry of trace elements in the hydrosphere. (ii) Hydrothermal activity and deep biosphere. (iii) Fe-uptake mechanism of phytoplankton. (iv) Ion recognition. (v) Non-linear chemical reaction.

Prof
SOHRIN, Yoshiki
(D Sc)

Assoc Prof
UMETANI, Shigeo
(D Sc)

Instr
SASAKI, Yoshihiro
(D Sc)

Instr
OKAMURA, Kei
(D Sc)

Techn
SUZUKI, Mitsuko
(D Sc)
She passed away on December 2, 2000.

Students

MITO, Saeko (DC)
NAITO, Kanako (DC)
NORISUYE, Kazuhiro (DC)
ITO, Makoto (MC)
SHIMOJO, Shinichiro (MC)
SHINOURA, Misato (MC)
KISHIDA, Koichi (MC)
KINUGASA, Masatoshi (MC)
YOSHIMOTO, Shinichi (MC)

HNO_3 and hot MQW. The samples were filtered on board with a closed filtering system constructed in a clean box. The closed filtering system was assembled with LDPE bottles, PFA tubing and a PFA filter holder. PFA materials were precleaned by heating in a mixture of H_2SO_4, HNO_3 and $HClO_4$. The interior of the filtering system was cleaned with hot 0.5 M HNO_3 and hot MQW before use. Polycarbonate membrane filters (0.2 μm of pore size) were precleaned by heating in a mixture of acids (1 M HCl, 0.5 M HNO_3 and 0.5 M HF) and in MQW. Using clean N_2 gas pressure, the sample solution was passed through the filter and collected in another LDPE bottle. The sample was acidified to pH 1 with ultra pure HNO_3 for preservation.

Simplifying the analytical procedure is the best way to reduce the risk of contamination. High-resolution inductively coupled plasma mass spectrometry (HR-ICP-MS) has the highest sensitivity to analyze simultaneously multi-elements in solution [2]. The method allows one to determine the total concentration of dissolved trace elements in freshwater directly. Dissolved concentrations for Al, P, V, Cr, Mn, Fe, Ni, Zn, As, Y, W and U were determined by a calibration curve method. The accuracy of the HR-ICP-MS measurement was ascertained for Al, V, Cr, Mn, Fe, Ni, Zn, As and U by analysis of a certified riverine water reference material (SLRS-3; National Research Council, Canada). Our results corresponded to the certified values within 10%. The interference from matrices for the 12 elements was studied by analyzing a Lake Biwa water sample with and without spiked elements. The recovery was quantitative for all the elements (93-104%).

In order to estimate a blank value throughout the procedure, MQW was filtrated and acidified on board the ship. The blank represented as the field blank and the detection limit throughout the procedure defined as three times the standard deviation of the field blank are listed in Table 1. The field blank values for Cr, Mn, Fe, Ni and Zn are on the same order of magnitude as with that obtained in the Great Lakes using a portable clean laboratory [1]. The field blank and detection limit values are low enough to allow determination of the 12 elements in the lake water.

The concentration ranges of the trace elements at N1, off Ohmi-maiko (75 m of water depth), are shown in Table 1. The medians of Mn, Fe, Ni, Zn and U found in this study are lower than the minimum concentrations reported previously (7.5, 18, 4.8, 11 and 0.084 nM, respectively [3]). The difference between our data and the previous data may originate from a difference in size fractionation. The previous workers used a filter of 0.4-0.45 μm of pore size. Another possibility is that the data of the previous workers may have been influenced by contamination.

Table 1. Field blank (pM), detection limit (pM) and concentrations at N1 (nM).

Element	Field blank (pM)	Detection limit (pM)	Concentration at N1 (nM)		
			Min.	Max.	Median
Al	687 ± 8	23	1.1	672	29
P	2050 ± 79	236	26	586	82
V	15 ± 3	11	0.79	5.7	2
Cr	15 ± 1	3.6	0.38	5.1	0.83
Mn	146 ± 1	3.6	0.36	311	5.1
Fe	525 ± 9	26	< 0.026	611	12
Ni	29 ± 1	4	1.6	25	3.5
Zn	429 ± 18	54	0.35	68	3.1
As	54 ± 4	12	5.2	25	11
Y	0.57 ± 0.04	0.13	0.049	0.27	0.11
W	0.73 ± 0.01	0.022	0.013	0.13	0.045
U	0.21 ± 0.03	0.076	0.027	0.2	0.061

The feathers of distribution of the dissolved trace elements are following. The residence time of Al, Fe and Mn was the shortest (0.03-0.12 yr) and the particulate/dissolved ratio was as high as 26-45. While the dissolved concentrations of Al, Fe, Mn and Y were uniformly low throughout the water column at N1, maximums occurred occasionally at the surface, thermocline and bottom. These maximums were caused by precipitation, resuspension of sediments and reductive dissolution of Fe and Mn oxides in the anoxic sediments. The concentrations of Cr, Ni and Zn were almost uniform throughout the water column but increases at the surface were sometimes observed. These distributions suggest that the effects of strong scavenging by Fe and Mn oxides prevail over the effects of the biogeochemical cycle and that atmospheric flux is significant for these metals. The concentrations of As and P increased with depth during the stagnation period. Their distribution was controlled by the biological cycle and scavenging of Fe and Mn oxides. The oxyacid species, such as V, W and U, accumulated in the epilimnion and were removed from the bottom during the stagnation period. This behavior may be attributed to the pH dependent interaction of these elements with Fe and Mn oxides.

References

1. Nriagu J O, Lawson G, Wong H K T and Cheam V, *Environ. Sci. Technol.*, **30**, 178-187 (1996).
2. Moens L and Jakubowski N, *Anal. Chem.,* **70**, 251A-256A (1998).
3. Haraguchi H, Itoh A, Kimata C and Miwa H, *Analyst,* **123**, 773-778 (1998).

Magnetic Vortex Core Observation in Circular Dots of Permalloy

Takuya Okuno, Ralf Hassdorf, Kunji Shigeto, Teruo Ono and Teruya Shinjo

Spin structures of nanoscale magnetic dots are the subject of increasing scientific effort, as the confinement of spins imposed by the geometrical restrictions makes these structures comparable to some internal characteristic length scales of the magnet. For a vortex (a ferromagnetic dot with a curling magnetic structure), a spot of perpendicular magnetization has been theoretically predicted to exist at the center of the vortex. Experimental evidence for this magnetization spot is provided by magnetic force microscopy imaging of circular dots of permalloy ($Ni_{80}Fe_{20}$) 0.3 to 1 micrometer in diameter and 50 nanometers thick.

Keyword: Magnetic vortex / MFM / Submicron magnetic dot / Turned-up magnetization core

Ferromagnetic materials generally form domain structures to reduce their magnetostatic energy. In very small ferromagnetic systems, however, the formation of domain walls is not energetically favored. Specifically, in a dot of ferromagnetic material of micrometer or submicrometer size, a curling spin configuration (that is, a magnetization vortex) has been proposed to occur in place of domains. When the dot thickness becomes much smaller than the dot diameter, usually all spins tend to align in-plane. In the curling configuration, the spin directions change gradually in-plane so as not to lose too much exchange energy, but to cancel the total dipole energy. In the vicinity of the dot center, the angle between adjacent spins then becomes increasingly larger when the spin directions remain confined in-plane. Therefore, at the core of the vortex structure, the magnetization within a small spot will turn out-of-plane and parallel to the plane normal. Although the concept of such a magnetic vortex with a turned-up magnetization core has been introduced in many textbooks [1], direct experimental evidence for this phenomenon has been lacking. That is because, as suggested by theoretical calculations, the size of the perpendicular magnetization spot at the vortex core should be fairly small. So, it is impossible to distinguish a fraction of perpendicular magnetization from the surrounding vortex magnetic structure with conventional magnetization measurements.

We have reported magnetic force microscopy (MFM) measurements on circular dots of permalloy ($Ni_{80}Fe_{20}$) and given clear evidence for the existence of a vortex spin structure with perpendicular magnetization core [2]. In MFM, a low-moment ferromagnetic tip of CoCr was used to minimize the effect of stray fields. Sample scans were taken in air at ambient temperature. An MFM image of an array of 3 × 3 dots of permalloy 1 μm in diam-

SOLID STATE CHEMISTRY — Artificial Lattice Alloys —

Scope of research

By using vaccum deposition method, artificial multilayers have been prepared by combining various metallic elements. The recent major subject is an interplay of magnetism and electric transport phenomena such as the giant magnetoresistance effect. Fundamental magnetic properties of metallic multilayers have been studied by various techniques including Mössbauer spectroscopy using Fe-57, Sn-119, Eu-151 and Au-197 as microprobes, and neutron diffration. Microstructured films such as wires and dots were successfully prepared by electron-beam lithography and novel magnetic and transport properties are investigated.

Prof
SHINJO, Teruya
(D Sc)

Assoc Prof
HOSOITO, Nobuyoshi
(D Sc)

Instr
FUJITA, Masaki
(D Sc)

Techn
KUSUDA, Toshiyuki
(D Sc)

Guest Research Associate:
SUN, Huiyuan(D Sc)
Students:
ALMOKHTAR, A. M. M. (DC)
MIYAKE, Kousaku(DC)
ISHII, Takahiro(MC)
OKUNO, Takuya(MC)
SHINGAKI, Yukihiro(MC)
Research Fellow:
HAMADA, Sunao(D Sc)
SHIGETO, Kunji (D Sc)

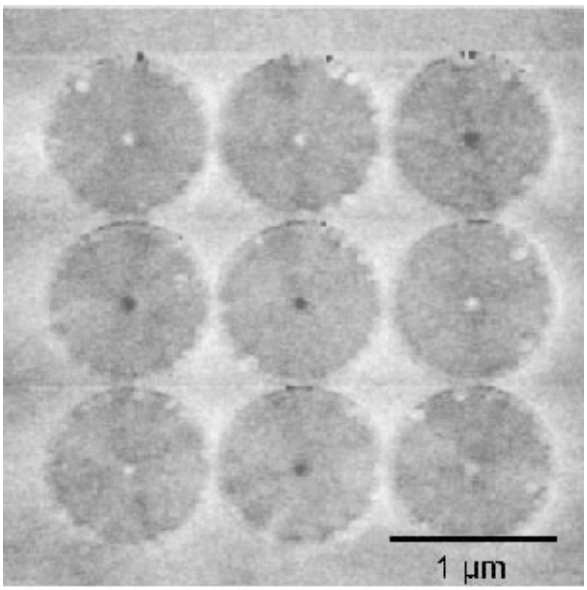

Figure 1. MFM image of an array of permalloy dots 1 μm in diameter and 50nm thick.

eter and 50 nm thick is shown in Fig. 1. For a thin film of permalloy, the magnetic easy axis typically has an in-plane orientation. If a permalloy dot has a single domain structure or shows a domain pattern, in MFM a pair of magnetic poles reflected by a dark and white contrast should be observed in either case. In fact, the image shows a clearly contrasted spot at the center of each dot. It is suggested that each dot has a curling magnetic structure and the spots observed at the center of the dots correspond to the area where the magnetization is aligned parallel to the plane normal. However, the direction of the magnetization at the center seems to turn randomly, either up or down, as reflected by the different contrast of the center spots. This seems to be reasonable, as up- and down-magnetizations are energetically equivalent without an externally applied field. The image shows simultaneously that the dot structures are of high quality and that the anisotropy effective in each dot is neg1igibly small, which is a necessary condition to realize a curling magnetic structure. (The spots in Fig. 1 around the circumference of each dot are artifacts caused by the surface roughness, mainly resulting from unremoved fractions of the resist layer.)

MFM scans were also taken for an ensemble of perma11oy 50nm thick dots with varying diameters, nominally from 0.1 to 1 μm (Fig.2). These images were taken after applying an external field of 1.5 T along an in-plane direction (Fig.2A) and parallel to the plane normal (Fig.2B). Again, the two types of vortex core with up- and down-magnetization are observed for dots larger than 0.3 μm in diameter (Fig.2A). In contrast, after applying an external field parallel to the plane normal, all center spots exhibit the same contrast (Fig. 2B), indicating that all the vortex core magnetizations have been oriented into the field direction.

From the above results, there is no doubt that the contrast spots observed at the center of each permalloy dot

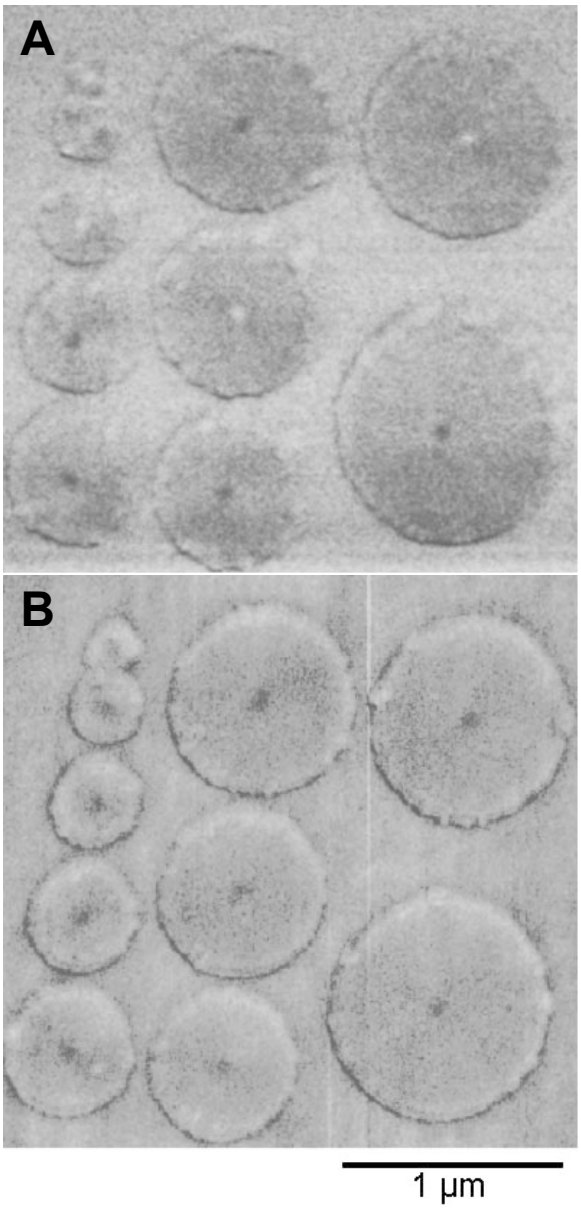

Figure 2. MFM image of an ensemble of 50-nm-thick permally dots with diameters varying from 0.1 to 1 μm after applying an external field of 1.5 T along an in-plane direction (A) and parallel to the normal(B).

correspond to the turned-up magnetization of a vortex core. To resolve a vortex core by MFM, it is necessary to pin the position of the core so that it is not affected by a stray field from the tip. In the experiments reported above, the vortex cores apparently have been so stable that a clear contrast appears in the MFM imaging process. Magnetic vortices are novel nanoscale magnetic systems, and it will be of great importance in the near future to study the dynamical behavior of turned-off magnetizations.

References

1. A. Hubert and R. Schafer, Magnetic Domains (Springer, Berlin, 1998)
2. T. Shinjo, T. Okuno, R. Hassdorf, K. Shigeto, T. Ono, Science 289(2000)930

(I) Crystal Transformation between Sheared and Layered Phases in Bi-2201

Y. Ikeda and T.Niinae

A detail study on the equilibrium phase diagram around $Bi_2Sr_2CuO_\delta$ in the Bi-Sr-Cu-O system newly found a crystal transformation between the sheared and layered phases in Bi-2201 by changing the oxygen stoichiometry. The transformation occurs in the finite composition area surrounded by $Bi_{43-y}Sr_{40+y}Cu_{17}O_z$ ($0 \leq y \leq 3$) and $Bi_{2+x}Sr_{2-x}CuO_{6+\delta}$ ($0 \leq x < 0.1$). The phase stability sensitively depends on the temperature as well as the oxygen partial pressure.

Keywords: equilibrium phase diagram/ bismuth cuprate/ high-Tc superconductor

It is now well known that in $Bi_{2+x}Sr_{2-x}CuO_{6+\delta}$ (Bi-2201) two distinct phases appear depending on the details of preparation process. One phase has the so-called sheared structure (S-2201), an insulator with a monoclinic symmetry, a ~ 2.45nm, b ~ 0.54nm, c ~ 2.2nm, β ~ 106º and the other is the so-called layered one (L-2201), a superconductor with a tetragonal a ~ 0.54nm,c ~ 2.45nm. However, the monophasic compositional region and the phase stability of both phases are one of the controversial issues due to the sensitivity of both phases to the heating temperature and the reaction process in addition to the difficulty in phase identification. In the present work, we firstly determined the location of both phases in the phase diagram of Bi-Sr-Cu-O system which will provides us invaluable information on the stable synthesis of both phases.

The solid-solution of S-2201, $Bi_{43-y}Sr_{40+y}Cu_{17}O_z$ ($0 \leq y \leq 3$), is newly found to exist in the $BiO_{1.5}$-SrO-CuO system at 830~860 ºC in air. In contrast, the solubility range of the S-2201 is found to extend toward the Cu-deficient region ($Bi_{2+x}Sr_{2-x}CuO_{6+\delta}$ $0 \leq x < 0.1$) by the heat treatment under Ar flow as shown in the figure. More interestingly, series of the S-2201 structure changes completely to the L-2201 upon annealing at 600ºC for 48h under high oxygen pressure (120atm) due to the change in the oxygen stoichiometry. The oxygen contents for cation stoichiometric $Bi_2Sr_2CuO_\delta$ is also determined to be δ=6 for the S-2201 and δ=6.2 for the L-2201. These results clearly demonstrate that the sheared phase has no excess oxygen. In the other word, the excess oxygen ions induce the layered structure to relaxing a mismatch between the Bi-double layer and the perovskite block accompanying with the incommensurable structural modulation.

This work was done in collaboration with Mie University (Y.Takeda), Okayama University (J.Takada, Y.Kusano)

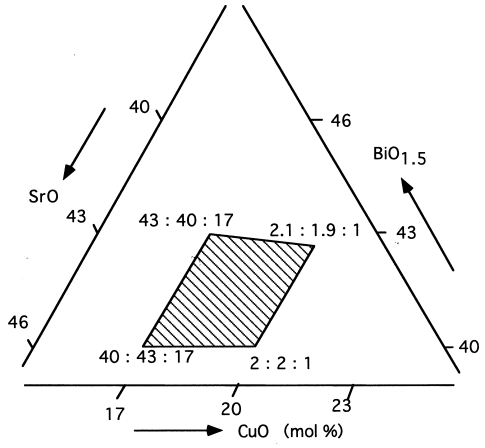

SOLID STATE CHEMISTRY — Quantum Spin Fluids —

Scope of research

Quantum spin oxide system such as high-T_c superconducting cuprates, $La_{2-x}Sr_xCuO_4$ and $Nd_{2-x}Ce_xCuO_4$ are synthesized in the form of single crystals using traveling-solvent-floating-zone method. Detailed equilibrium phase diagram of Bi cuprate systems is investigated. Main subjects and techniques are: mechanism of high-T_c superconductivity: origin of quantum phase separation in strongly correlated electron systems: spin excitations in quantum spin systems: interplay between spin and charge flow in doped spin system: neutron scattering by using triple-axis as well as time-of flight techniques.

Prof
YAMADA,
Kazuyoshi
(D Sc)

Assoc Prof
MIBU,
Ko
(D Sc)

Instr
IKEDA,
Yasunori

Students:

UEFUJI, Tetsushi (MC)
GOKA, Hideto (MC)
KAWASHIMA, Kazumasa (MC)
KUBO, Takuyu (MC)

(II) Effect of Crystal Structure on the Competitive Relation between the Magnetic Order and Superconductivity in $La_{1.875}Ba_{0.125-x}Sr_xCuO_4$

H. Goka, M. Fujita, T. Kubo and K. Yamada

We performed neutron scattering, μSR and magnetization measurements on $La_{1.875}Ba_{0.125-x}Sr_xCuO_4$ to investigate an interplay among the superconductivity, magnetic/charge order and crystal structure. The obtained phase diagram clearly demonstrates an intimate relation among these physical properties.

Keywords: 1/8-problem/crystal structure/magnetic order/stripe model/high-T_c superconductor

In $La_{2-x}Ba_xCuO_4$ the high-T_c superconductivity is strongly suppressed with x around 1/8[1]. This 1/8-problem is considered to be closely connected with the mechanism of high-T_c superconductivity, particularly with the role of magnetic order for the suppression of superconductivity. Inspite of a large number of experimental studies on the 1/8-problem, few systematic work has been done for the effect of crystal structure on both the magnetic order and superconductivity. Then we utilized neutron scattering, μSR and magnetic susceptibility measurements on $La_{1.875}Ba_{0.125-x}Sr_xCuO_4$(LBSCO) single crystals to elucidate the effect of crystal structure on the 1/8-problem. The LBSCO is one of the ideal system to study this problem since one can control the crystal structure with keeping the carrier concentration constant.

As shown in Fig. 1, we obtained a phase diagram of LBSCO which clearly demonstrates a role of crystal structure on the competitive relation between the superconducting transition and magnetic ordering. In the low temperature tetragonal(LTT) or *Pccn* orthorhombic phase in the region $x<0.07$, the superconductivity (magnetic ordering) is substantially suppressed (stabilized). While in the low temperature orthorhombic (LTO) phase the supeconductivity is more stable even with the 1/8-doping.

One of possible models to explain the present results is so-called stripe model [2]. In this model, the LTT structure is favorable for the pinning of dynamical hole stripes. In fact, as shown in Fig.2, we observed nonmagnetic superlattice peaks in the LTT/*Pccn* phase which reflects the stripe ordering of holes. Futher study on the spin/charge fluctuation will reveal the detailed nature of dynamical stripe correlations and the relation with the superconductivity.

This work was done in collaboration with I. Watanabe, K. Nagamine (RIKEN) and M. Matsuda(JAERI) and supported by a Grant-In-Aid for Scientific Research from Ministry of Education, Science, Culture and Sports of Japan and by the Core Research for Evolutional Science and Technology (CREST) Project sponsored by the Japan Science and Technology Cooperation.

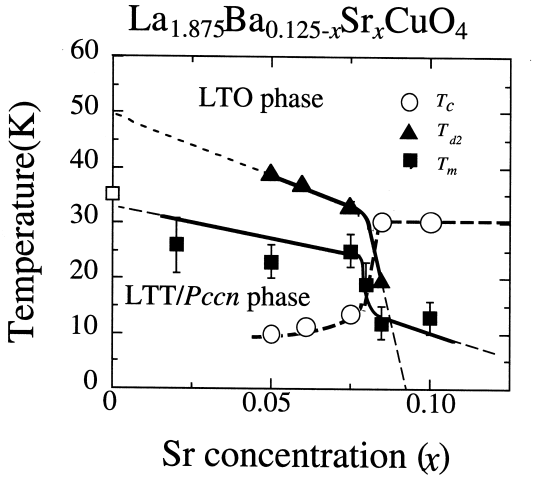

Figure 1. Phase diagram of LBSCO. Circles, triangles and squares denote the T_c, LTO-LTT(or *Pccn*) structural transition temperature T_{d2} by neutron scattering and the onset temperature for magnetic order T_m by μSR experiments, respectively. T_m for x=0 is quoted from [3]. Both solid and broken lines are guides to the eye.

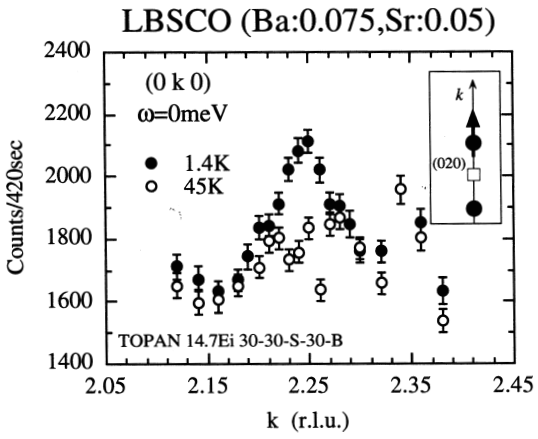

Figure 2. Superlattice peak at (0,2.25,0) observed by neutron scattering measurement. Inset shows the scan-trajectory.

References

[1] A. R. Moodenbaugh et al. Phys. Rev. B **38** 4596 (1988)
[2] J. M. Tranquada et al. Nature(London) **375** 561 (1995)
[3] K. Kumagai et al. J. Supercond. **7** 63 (1994)

Antiferromagnetism of S=1/2 triangles in $La_4Cu_3MoO_{12}$

Masaki Azuma, Shintaro Ishiwata and Mikio Takano

Magnetic properties of a cupric triangular cluster compound $La_4Cu_3MoO_{12}$ were investigated. Susceptibility data show that paramagnetic cupric spin (S=1/2) above room temperature form S=1/2 trimers at lower temperatures because of strong intra-trimer antiferromagnetic interactions. The cluster moments acquire antiferromagnetic order below 2.6 K. The trimers can be polarized in an external field of 20 T at 1.3 K. The magnetization remains nearly constant at 1 μ_B per trimer up to a magnetization plateau at 55 T.

Keywords: Spin trimer/ Magnetic susceptibility/ High field magnetization/ Neutron scattering

The spin quantum number (small, large, integer, half-integer) and the geometry of the magnetic sublattice affect the ground state of quantum antiferromagnets in various fashions. For examples, spin singlet ground states with finite gaps to magnetic excited states have been found in several 1D antiferromagnetic (AF) systems such as S=1/2 alternating bond chains, S=1/2 2-leg ladders and S=1 chains (Haldane systems). The discovery of inorganic model compounds such as $CuGeO_3$ (spin-Peierls), $(VO)_2P_2O_7$ (alternating chain) [1], Y_2BaNiO_5 (Haldane), $SrCu_2O_3$ [2] and $Sr_{14}Cu_{24}O_{41}$ (ladders) in the past decade has stimulated keen interest in such 1D systems. Their large AF interactions (J) and the thermal stability make it rather easy to finely tune the electronic properties of these materials by means of chemical doping.

In the gapped ground states of these compounds, two neighboring S=1/2 spins form a spin singlet. On the other hand, AF trimer compounds are rare in nature. $La_4Cu_3MoO_{12}$ is a layered compound with an average structure of the $YAlO_3$ type [3]. The Cu_3MoO_4 layer of this compound shown in Fig. 1 can be derived from a triangular CuO layer by replacing a quarter of the Cu^{2+} ions with nonmagnetic Mo^{6+} ions. One can consider the Cu_3MoO_4 layer as being made of Cu_3O triangular clusters as suggested from the bond lengths : The average Cu-O bond lengths within the triangle, 1.983Å, is much shorter than that between neighboring triangles of 2.690Å. The Cu_3MoO_4 layers are separated from each other by /O/La/O/ layers. The structure can be described as a quasi-2D orthorhombic lattice made of slightly distorted cupric (S=1/2) trimers [4].

Figure 2 shows the temperature dependences of magnetic susceptibility and its inverse measured on heating from 5 to 800 K in an external field of 1 T. The susceptibility above 400 K was fitted well to the Curie-Weiss law with μ_{eff} = 1.81 (g = 2.09) and a Weiss temperature (θ) of -558 K. On the other hand, the slope of the $1/\chi$-T plot below 250 K decreased to 0.39 times the high-temperature value. The small Curie constant (C) below 250 K indicates that each trimer has a total spin S_{total}=1/2. The large intra-trimer AF interactions give the large Weiss constant at high temperatures. The inter-trimer interactions seem to be weakly AF as suggested from the small Weiss constant of -16 K derived from the low temperature data.

In the data measured in a field of 0.1 T down to 1.8 K shown in the inset of Fig. 2, a maximum appeared at 5 K

SOLID STATE CHEMISTRY — Multicomponent Materials —

Scope of research

Novel 3d transition-metal oxides showing exotic electrical and magnetic properties are being searched for using different synthesizing techniques like high pressure syntesis (5 GPa and 1000°C, typically) and epitaxial film growth. Recent topics are:

- *High T_c superconductivity.*
- *Low-dimensional spin systems like ladders showing dramatic quantum effects.*
- *Oxides of late 3d transition metals like $SrFeO_3$ with strong oxygen-hole character.*

Prof
TAKANO, Mikio
(D Sc)

Assoc Prof
TERASHIMA, Takahito
(D Sc)

Instr
AZUMA, Masaki
(D Sc)

Students:
FURUBAYASHI, Yutaka (DC)
HAYASHI, Naoaki (DC)
SAITO, Takashi (DC)
ISHIWATA, Shintaro (MC)
MASUNO, Atsunobu (MC)
YAMAMOTO, Masamichi (MC)
YOSHIDA, Hirohumi (MC)
RIJSSENBEEK, Job T. (RS)
Ninjbadgar Tsedev (RS)

Research Fellow:
ICHIKAWA, Noriya
KAWASAKI, Shuji

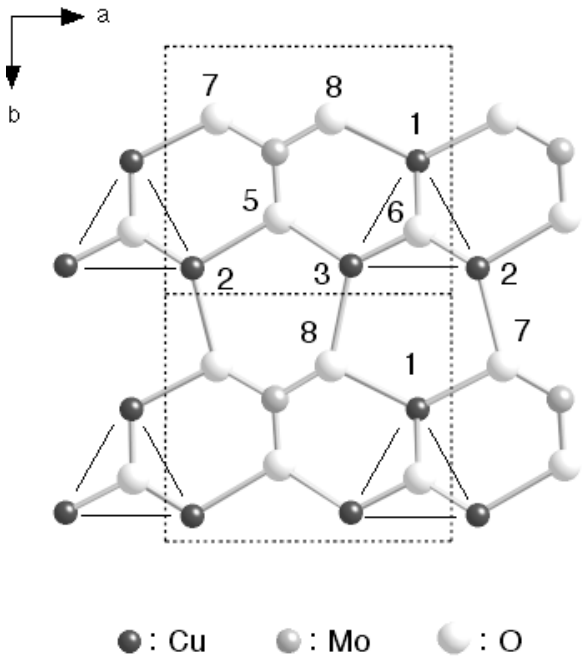

Figure 1. Cu_3MoO_4 plane of $La_4Cu_3MoO_{12}$. The numbers show the crystallographic sites. The solid line represent the triangle clusters.

and a kink at 2.6 K followed. The existence of the kink was clearly seen as a peak in the specific heat data. As can be seen in Fig. 1 there is no spin frustration among the S_{total}=1/2 spins, so it is reasonable to assume that the anomaly results from AF order of spin trimers. The susceptibility maximum at 5 K can be attributed to short range order in the two dimensional spin system. The elastic neutron scattering study confirmed the antiferromagnetic order with an ordered moment of 0.8 μ_B per trimer.

We propose the following picture for the present compound. Above 400 K, the susceptibility could be explained assuming S=1/2 spin localized on each Cu ion. The large AF interactions within the triangles led to a large Weiss temperature of -558 K. With decreasing the

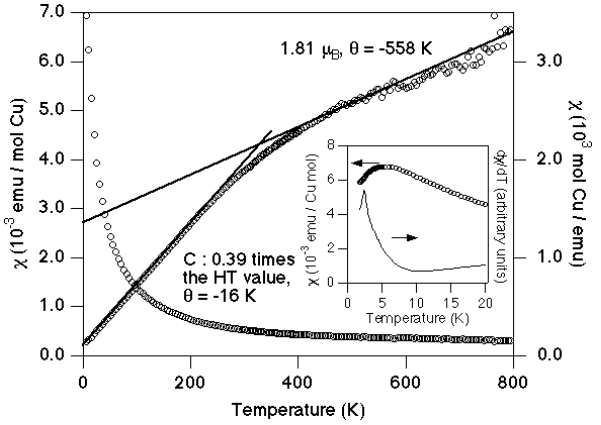

Figure 2. Temperature dependence of magnetic susceptibility of $La_4Cu_3MoO_{12}$ below 800 K. The solid lines correspond the fit to the Curie-Weiss law. The inset shows the data taken at 0.1 T.

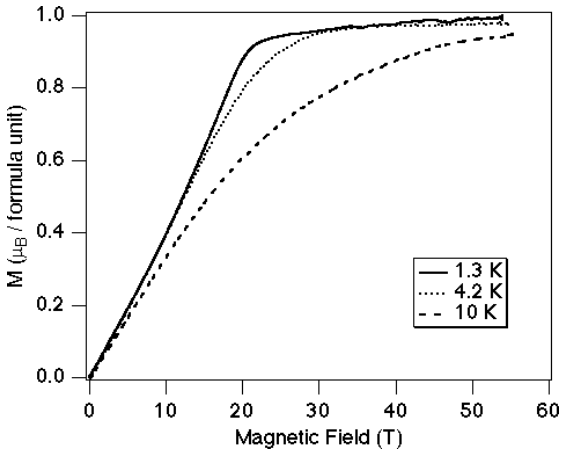

Figure 3. Magnetization curve of $La_4Cu_3MoO_{12}$ measured in pulsed magnetic field at 1.3, 4.2 and 10 K.

temperature, the Curie constant decreased to about 1/3 of the high-temperature value because only the ground state with S_{total}=1/2 per cluster was populated. Since the inter-triangle interactions are weak, the Weiss temperature is as small as -16 K. The S_{total}=1/2 spins localized on the trimers order antiferromagnetically at 2.6 K. If inter-triangle interactions are weak, it should be possible to align the ordered spins by applying magnetic field (spin flip). The results of the magnetization measurements at 1.3, 4.2 and 10 K are shown in Fig. 3. At 1.3 K, the data below 20 T were concave reflecting the AF ordering, whereas above 20 T the magnetization tended to saturate at 1 μ_B / formula unit, *i. e.*, 1 μ_B per trimer. This confirms that the system orders antiferromagnetically keeping the nature of the ground state with S_{total}=1/2. The full magnetization of this system should be 3 μ_B / formula unit, so the observed saturation-like behavior is actually an intermediate plateau. The excitation energy from S_{total} = 1/2 to S_{total} = 3/2 state is 3/2 J for an equilateral triangle. Applying J = 813 K estimated from the fitting of the susceptibility data, it is expected that another spin flip will be observed at 1500 T. Actually, inelastic neutron scattering data showed a well defined excitation at ΔE=133 meV (1542 K) which can be associated with an intratrimer doublet-quartet (S_{total}=1/2 to S_{total}=3/2) transition.

Reference

1. M. Azuma, T. Saito, Y. Fujishiro, Z. Hiroi, M. Takano, F. Izumi, T. Kamiyama, T. Ikeda, Y. Narumi and K. Kindo, Phsy. Rev. B **60**, 10145 (1999).

2. Z. Hiroi, M. Azuma, M. Takano and Y. Bando, J. Solid State Chem. 95, 230 (1991); M. Azuma, Z. Hiroi, M. Takano, K. Ishida and Y. Kitaoka, Phys. Rev. Lett. **73**, 3463 (1994).

3. D. A. Vander Griend, S. Boudin, V. Caignaert, K. R. Poeppelmerer, Y. Wang, V. P. Dravid, M. Azuma, M. Takano, Z. Hu and J. D. Jorgensen, J. Am. Chem. Soc **121**, 4787 (1999).

4. M. Azuma, T. Odaka, M. Takano, D. A. VanderGriend, K. R. Poeppelmeier, Y. Narumi, K. Kindo, Y. Mizuno and S. Maekawa, Phys. Rev. B **62**, R3588 (2000).

The Structure of Soda-Lime-Silicate Glass and Melt by X-ray Diffraction Method

Jisun Jin, Masahide Takahashi, Takashi Uchino and Toshinobu Yoko

The structure of soda-lime-silicate($16Na_2O{\cdot}10CaO{\cdot}74SiO_2$) glass and melt (~1500°C) was investigated by X-ray diffraction method in combination with molecular dynamics(MD) calculation. The short- and intermediate range structure of the glass was investigated as a function of temperature by using MD simulation. The experimental results clearly show that there is no distinct difference in structure between the present glass and melt. We also found from MD calculation that the linkage of Si-O network made of SiO_4 tetrahedra shows similarities between glass and melt. It is also found that the first sharp diffraction peak(FSDP) associated with intermediate range structure is contributed from the correlation between Na^+(or Ca^{2+}) and SiO_4 network.

Keywords : Silicate Glass / Melt/ Structure / X-ray diffraction / Molecular Dynamics Calculation

As well known, many commercial glasses are produced through melting process. Although enormous efforts have been made to investigate their physical and chemical properties in a melting state, such as viscosity, density and redox reaction etc., there are few works on the structure of oxide melts. On the other hand, MD calculation is regarded as one of the most powerful techniques to get insight into materials[1]. By a combination of high temperature X-ray radial distribution function(RDF) analysis and MD calculation, it is expected that we can get not only information about the average structure of specific elements but also structural parameters of short and medium range orders in glasses and melts.

In the present study, the technologically important soda-lime-silicate glass is chosen to investigate the local structure of glass and melts. The difference in structure between glass and melt is discussed with the result of MD calculation in order to explain the temperature dependence of macroscopic properties.

Figure 1 shows the interference functions of glass and melt obtained from X-ray diffraction together with the MD-derived ones. It is seen that the interference functions from MD calculation are in fairly well agreement with the experimental ones indicating that the MD simulation reproduces the characteristics of the real structures. It is also seen from Figure 1 that there are two peaks in the low-Q region at 15 and 21nm^{-1} which are hereafter referred to Q_1 and Q_2, respectively. It is clear that the Q_1 peak disappears at high temperature, while the Q_2 becomes more pronounced in a melting state. Our MD calculation also reproduced this result. By comparison between the total $Qi(Q)$ and pair $Qi(Q)_{ij}$, it is obvious that the peaks at ~15nm^{-1} and ~21nm^{-1} are assigned to Si-O(Si-Si) and Na(Ca)-Si correlations, respectively(see Figure 2).

SOLID STATE CHEMISTRY - Amorphous Materials -

Scope of Research

Inorganic amorphous materials with various functions are the targets of research in this laboratory. (1) To obtain a clear view of glass materials and the bases for designing functional glasses, we investigate the structure of glasses using X-ray and neutron diffraction analysis, high resolution MAS-NMR, and ab initio MO calculation. (2) To develop materials with high optical nonlinearity, we search heavy metal oxide-based glasses and transition metal oxide thin films, and evaluate the nonlinear optical properties by Z-scan methods. (3) Photosensitivity of glasses for optical fibers and waveguides is investigated to design efficient fiber gratings and optical nonlinear materials. (4)Using sol-gel method, synthesis and microstructure control are carried out on various functional oxide thin films.

Prof
YOKO, Toshinobu
(D Eng)

Assoc Prof
UCHINO, Takashi
(D Eng)

Instr
TAKAHASHI, Masahide
(D Sc)

Assoc. Instr
JIN, Jisun
(D Eng)

Students:

TAKAISHI, Taigo (DC)
TOKUDA, Yomei (DC)
NIIDA, Haruki (DC)
DORJPALAM, Enkhtuvshin (DC)
MORI, Ryohei ((DC)
KONDO, Yuki (DC)
TSUKIGI, Kaori (MC)
TAKEUCHI, Toshihiro (MC)
ICHII, Kentaro (MC)
MASAI, Toshihiro (MC)
TAMOTO,Yushi(UG)
MIYABE, Daisuke(UG)
SAKO, Akifumi(UG)
FUKUDA, Masahiro(RF)
KAWACHI, Shinichi(RS)
ZHANG, Jian (RS)

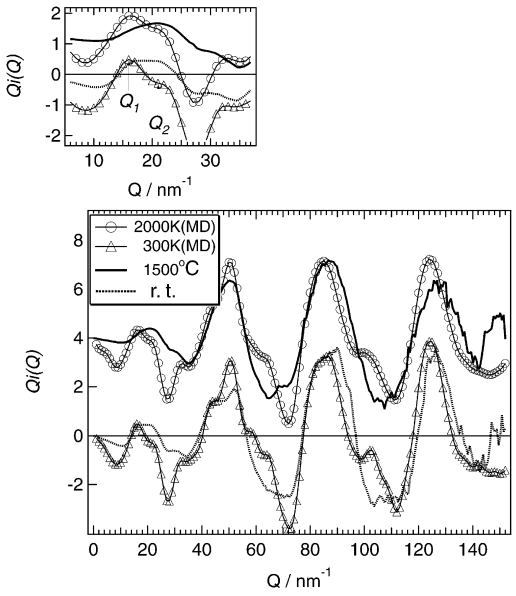

Figure 1. The interference fuctions of $16Na_2O•10CaO•74SiO_2$ glass and melt.

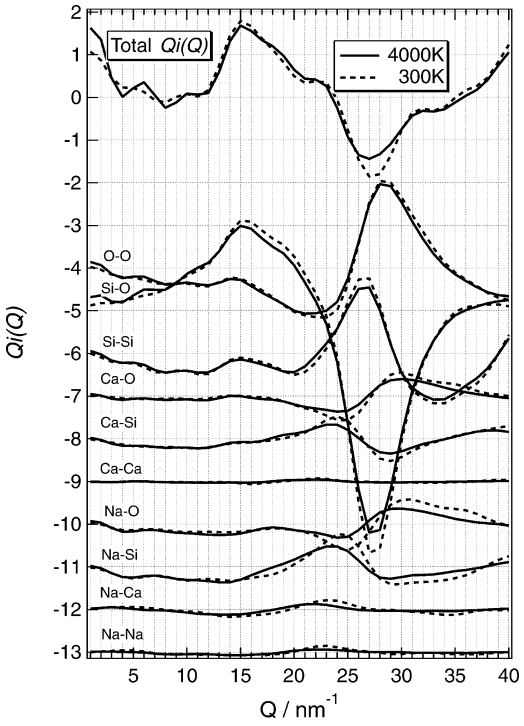

Figure 2. MD results for partial and total interference function of $16Na_2O•10CaO•74SiO_2$ glass and melt.

Namely, the former corresponds to network and the latter to correlations between cation and network of glass. The previous result from MD calculation of pure SiO_2 also shows the FSDP at ~15nm^{-1} which is a contribution of Si-Si, Si-O and O-O pairs[2, 3]. In our MD calculation, the peak at ~21nm^{-1} is shifted to low Q side on increasing temperature. It indicates the expansion of Na(Ca)-Si correlation due to thermal motion. Now we can draw a picture that the distance between the modifier cations and the network former in glass tends to expand with increasing temperature.

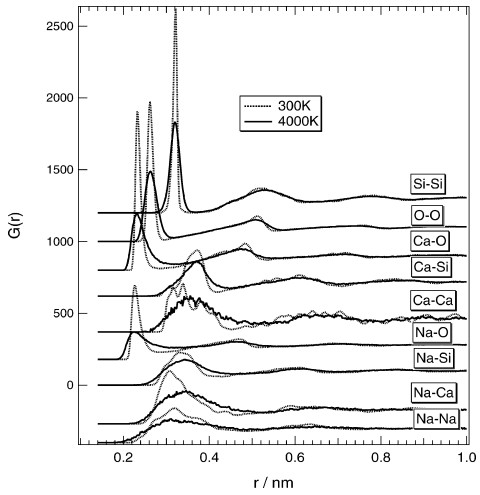

Figure 3. Pair distribution functions of $16Na_2O·10CaO·74SiO_2$ glass and melt derived from MD calculation.

It is surprising that almost no change of Si-O and Si-Si atomic distances was observed between the RDF curves of glass and melt. However, we have observed that the atomic distances of Na-Ca and Ca-Ca were increased by 0.031nm and 0.019nm, respectively, with increasing temperature(see Figure 3). This value is longer than expansion of Si-O at 1000K(0.002nm)[4]. The distinct change of distribution of Na-O and Ca-O correlations that are difficult to be distinguished in experimental *G(r)*with increasing temperature was also observed. This allows us to suggest that the temperature dependence of density cannot be simply explained by the change of local structure of network former and instead the thermal motion of Na^+ and Ca^{2+} ions mainly contributes to the expansion of glass at high temperatures.

In the present study, we have investigated the structure of soda-lime-silicate($16Na_2O·10CaO·74SiO_2$) glass and melt (~1500°C) by X-ray diffraction method in combination with MD calculation. The experimental results clearly show that there is no distinct difference in structure between the present glass and melt, which was also supported by MD calculation. The decrease in density with increasing temperature is due to expansion of atomic distance between Na^+ and Ca^{2+}(Na^+). It is concluded that the increase of correlation length between cations and network with increasing temperature is also responsible for the decrease of density.

References

1. K. Kawamura, *JCPE #P029.*, MXDORTO Program(1995).
2. M. Okuno and K. Kawamura, *J. Non-Cryst. Solids*, **191**, 249-259(1995)
3. H. Iyetomi, P. Vashista and R. K. Kalia , *Phys. Rev*. **B43**, 1726(1991)
4. J. Horbach and W. Kob, *Phys. Rev.*, **B60**, 3169-3181(1999)

Viscoelasticity and Morphology of Soft Polycarbonate as a Substitute for Poly(vinyl chloride)

Tadashi Inoue, Hiroshi Watanabe and Kunihiro Osaki

The soft polycarbonate resins, SPC, were newly developed as a substitute for soft poly(vinyl chloride). The soft polycarbonates are multiblock copolymers composed of bisphenol A polycarbonate, PC, and polydimethylsiloxane, PDMS. SPC resins are clear, transparent, and tough. Viscoelasticity and morphology of the resins were investigated to control physical properties of the resin. Electron microscope and small angle X-ray scattering experiments revealed that the SPC formed microdomain structures. Rheological measurements were used to discuss continuity of PC-rich phase domain, which determined the modulus around the room temperature.

Keywords : Substitute for Poly(vinyl chloride), Polycarbonate, Polydimenthylsiloxane, Viscoelasticity, Strain-Induced Birefringence

Poly(vinyl chloride), PVC, is one of conventional polymeric materials in modern industry. Large amount of PVC is produced to consume chlorine produced in sodium hydrate synthesis process. Its mechanical properties are easily controlled by addition of plasticizers, and therefore PVC is used in many fields; lapping films, sheets for agriculture, building materials like pipes, and so on. However, recently there are some doubts about its safety. Dioxins may be produced by combustion, and additives like octyl phthalate are now known as environmental hormones.

Several approaches to develope substitutes for PVC are in progress. Among these approaches, a reasonable one is to capture properties of plasticized PVC by combination of rubbery and glassy polymers in microscopic level. In order to obtain a transparent material, it should be homogeneous in macroscopic scales unless an isorefractive polymer pair is selected. Obviously, in such an approach, properties of the obtained material would be strongly correlated with the starting polymers, and therefore selection of polymer pair is very important to obtain high performance substitute.

Soft polycarbonate resins, SPC, being multiblock copolymers composed of bisphenol A polycarbonate, PC, and polydimethylsiloxane, PDMS, are recently developed by Idemitsu Kohsan corporation. Neat PC is a very tough engineering plastic and PDMS is an excellent elastomer being chemically and thermally stable. Synthe-

FUNDAMENTAL MATERIAL PROPERTIES — Molecular Rheology —

Scope of research

The molecular origin of various rheological properties of materials is studied. Depending on time and temperature, homogeneous polymeric materials exhibit typical features of glass, rubber, and viscous fluids while heterogeneous polymeric systems exhibit plasticity in addition to these features. For a basic understanding of the features, the molecular motion and structures of various scales are studied for polymeric systems in deformed state. Measurements are performed of rheological properties with various rheometers, of isochronal molecular orientation with flow birefringence, and of autocorrelation of the orientation with dynamic dielectric spectroscopy.

Prof
OSAKI, Kunihiro
(D Eng)

Assoc Prof
WATANABE, Hiroshi
(D Sc)

Instr
INOUE, Tadashi
(D Eng)

Techn
OKADA, Shinichi

Students:
KAKIUCHI, Munetaka (DC)
MATSUMIYA, Yumi (DC)
OGAWA, Takeshi (MC)
UEMATSU, Takehiko (MC)
YAMASHITA, Yasuhiro (MC)
FUKUMA, Eisai (UG)
MORI, Takuya(UG)
TAKAHASHI, Kazuhiro(UG)
OH, Gwan Kyo(RS)

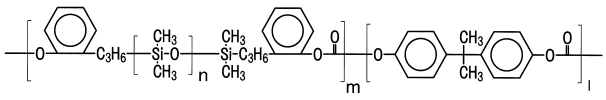

Figure 1. Molecular structure of soft polycarbonate.

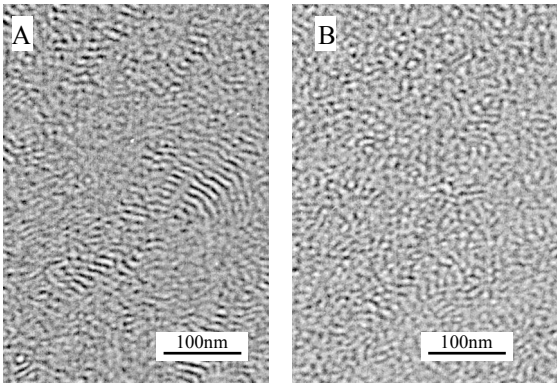

Figure 2. Electron microgram of soft polycarbonates, A and B. Black domains correspond to PDMS rich phase.

sized SPC mimics plasticized PVC; clear, transparent, and tough. Thus, SPC is anticipated to be a good candidate for the substitute. In order to control physical properties and processablility, SPC has been under investigation for a few years in our lab[1].

SPC is synthesized from copolymerization of end phenol-modified poly(dimethyl siloxane), PDMSOH, and bisphenol A. Molecular structure of SPC is shown in Figure 1. Controlling parameters for physical properties of SPC are; content of PDMS(w_{PDMS}), molecular weight of PDMSOH(M_{PDMS}), and total molecular weight(M). As shown later, SPC has microdomain structures. M_{PDMS} affects the miscibility of two microdomains. The reported results were mostly taken with SPC having M_{PDMS} = 1980. Depending on w_{PDMS}, rubber-like (sample A,w_{PDMS} =0.387) and glass-like (sample A,w_{PDMS} =0.552) specimens were obtained.

Figure 2 shows examples of electron microgram of rubber-like (soft) and glass-like (hard) SPC. In both cases, *similar* microdomain structures were observed. For the lower PDMS content polymer(A), lamellar like structure is partially observed. Small angle x-ray scattering experiments, indicating relatively narrow Bragg's peak, also support existence of the microdomain structure.

Details of the microdomain structures were examined through dynamic mechanical measurements using oscillatory deformation. The strain-induced birefringence was also examined to detect structural changes (chain orientation). Figure 3 shows temperature dependence of the complex modulus for the two samples. There are two glass transition temperatures(100°C, -100°C(not shown

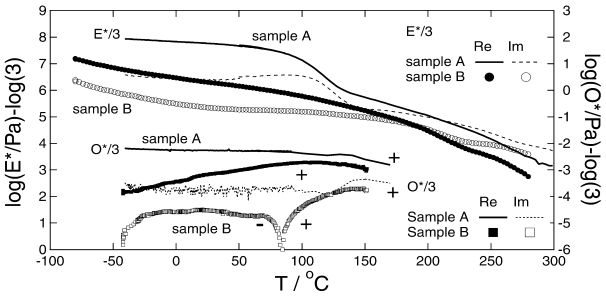

Figure 3. Temperature dependence of the complex modulus, $E^* = E' + iE''$, and the strain optical coefficient, $O^* = O' + iO''$, for SPC.

in Figure 3)), which indicates the system has a phase-separated structure. The higher glass transition temperature is identified with PC and lower one with PDMS. The two glass transition temperatures are almost constant for these polymers. Temperature dependence of modulus around the room temperature is weak, which means that SPC is much more thermally stable than PVC.

The modulus between the two glass temperatures was found to show a steep change around $w_{PDMS} \sim 0.5$. This result suggests that the continuity of the PC-rich phase changes around $w_{PDMS} \sim 0.5$: If PC domains are continuous, glassy PC domains are deformed affinely, and therefore glassy behavior is observed. On the other hand, if the glassy PC domains are not continuous and soft PDMS domains are mainly deformed, rubbery behavior is observed. This speculation is confirmed with dynamic birefringence measurements, which reflects strain of PC domain. (Negative birefringence is due to large deformation of PDMS domains.)

Tensile properties at large deformations were also examined. Strain-stress curve for sample A having higher PDMS content shows rubber-like behavior; the stress increases monotonically with strain. On the other hand, sample B shows the glass-like behavior; stress yielding is observed at few percent elongations. These results also can be explained with continuity of glassy PC domains. Thus, rheological measurements are sensitive to continuity of PC domain, which is hardly discussed with ordinary structural analysis in detail.

In conclusion, continuity of PC domains is a key factor to control mechanical properties of well phase-separated SPC. Effect of miscibility of the two phases will be discussed in near future by using lower M_{PDMS} samples.

References

[1] T. Inoue, K. Osaki, H. Morishita, H. Tamura, and S. Sakamoto, *Zairyo*, **49**, 1298(2000).

Dynamic Heterogeneity of Amorphous Polymers below and above T_g

Toshiji Kanaya and Keisuke Kaji

Dynamic heterogeneity has been investigated for amorphous polymers in terms of non-Gaussian parameter A_0, which is currently believed to be a key to reveal anomalous dynamics near the glass transition. This parameter A_0 was evaluated in incoherent elastic neutron scattering measurements in a wide range of Q (length of scattering vector). Combining the neutron data with the positron annihilation lifetime spectroscopy (PALS) data the spatial scale of the heterogeneous domain or the so-called *cooperatively rearranging region* (*CRR*) has been determined.

Keywords: heterogeneity/ amorphous polymers/ neutron scattering/ non-Gaussian parameter/ positron annihilation lifetime spectroscopy/ cooperatively rearranging region

The glass transition is one of the most important phenomena in condensed matter sciences, especially polymer materials science because polymer materials necessarily include amorphous regions and the properties such as mechanical and thermal properties drastically change at the glass transition temperature T_g. It is now elucidated that the glass transition is not a second order phase transition but a relaxation phenomenon. Therefore, extensive dynamical studies were carried out on amorphous materials using many kinds of techniques to reveal various anomalous but common features of them [1]. A huge amount of data implies that there exists the so-called *cooperatively rearranging region* (*CRR*) in amorphous materials near T_g where molecules or polymer segments must move cooperatively. The existence of *CRR* makes the amorphous materials dynamically very heterogeneous. It is therefore believed that the heterogeneity is a key to solve the anomalous dynamics near T_g.

In a series of works we studied the dynamic heterogeneity of some amorphous polymers below and above T_g using inelastic neutron scattering [2,3,6] and positron annihilation lifetime spectroscopy (PALS) [4,5]. In the neutron scattering measurements, we have evaluated the non-Gaussian parameter which is a measure of the heterogeneity. In addition, we have obtained the size of free volume and its distribution from the PALS experiments. Combining the neutron and PALS data, we proposed a new strategy to evaluate the spatial scale of heterogeneity or *CRR* [5]. In this report, the main results of polyisobutyrene (PIB) and polybutadiene (PB) with T_g =

FUNDAMENTAL MATERIAL PROPERTIES — Polymer Materials Science —

Scope of research

The structure and molecular motion of polymer substances are studied using mainly scattering methods such as neutron, X-ray and light with the intention of solving fundamentally important problems in polymer science. The main projects are: the mechanism of structural development in crystalline polymers from the glassy or molten state to spherulites; the dynamics in disordered polymer materials including low-energy excitation or excess heat capacity at low temperatures, glass transition and local segmental motions; formation process and structure of polymer gels; the structure and molecular motion of polyelectrolyte solutions; the structure of polymer liquid crystals.

Prof
KAJI, Keisuke
(D Eng)

Assoc Prof
KANAYA, Toshiji
(D Eng)

Instr
NISHIDA, Koji

Students
MATSUBA, Go (DC)
MIYAZAKI, Tsukasa (DC)
SAITO, Mitsuru (MC)
TAKAHASHI, Nobuaki (MC)
KITO, Takashi (MC)
KONISHI, Takashi (MC)
OKUYAMA, Tomohiro (MC)
MATSUBARA, Shinya (UG)
YAMANO, Hiroaki (UG)

200 and 170 K, respectively, are summarized.

Firstly we briefly explain about non-Gaussian parameter A_0. Under the so-called Gaussian approximation, an incoherent elastic neutron scattering intensity $I_{el}(Q)$ can be described by

$$\boldsymbol{I_{el}(Q)} = \exp(-\alpha \boldsymbol{Q}^2) \qquad (1)$$

where α is the mean square displacement and Q is the length of scattering vector. If α has a Gaussian distribution $g_G(\alpha)$ due to the dynamic heterogeneity, $I_{el}(Q)$ is given by

$$\boldsymbol{I_{el}(Q)} = \exp(-\overline{\alpha}\boldsymbol{Q}^2 + \overline{\alpha}^2 \boldsymbol{A_0 Q}^4 / 2) \qquad (2)$$

$$\boldsymbol{A_0} = (\overline{\alpha^2} - \overline{\alpha}^2 / \overline{\alpha}^2) \qquad (3)$$

Here, A_0 is a non-Gaussian parameter corresponding to the width of the distribution $g_G(\alpha)$, and hence a measure of the heterogeneity.

The observed incoherent elastic scattering intensities $I_{el}(Q)$ are plotted versus Q^2 in Fig. 1 for PIB, clearly showing non-linear or non-Gaussian behavior. The solid curves in the figure are the best fits of eq. (2) with the observed values, from which the non-Gaussian parameter A_0 and the mean square displacement α were extracted. It was found that the evaluated A_0 increases with decreasing temperature, suggesting PIB becomes more heterogeneous with decreasing temperature. The heterogeneity can be visualized as a normalized distribution of the mean square displacement α/α_{av} as shown in inset of Fig. 1.

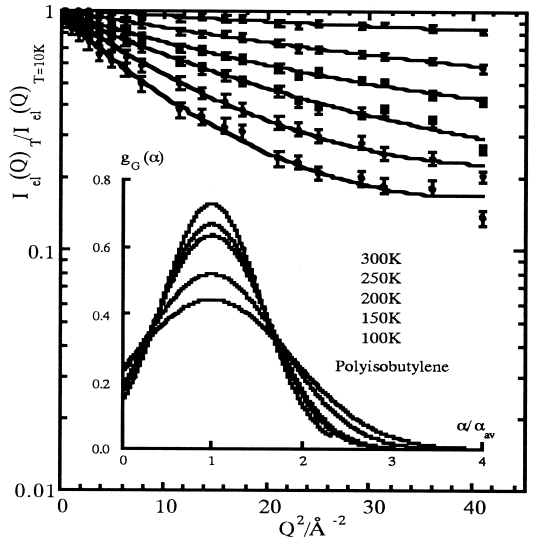

Figure 1. Incoherent elastic scattering intensity $I_{el}(Q)$ from PIB at various temperature, showing non-Gaussian behavior. Inset shows normalized distribution functions of mean square displacement α.

The behaviors of the mean square displacement are suggestive as well. Below T_g, α is proportional to temperature T, meaning that the motion observed here is approximately harmonic vibration, but above about T_g, it shows an excess value $\Delta\alpha$, supporting the onset of relaxational motions above T_g.

The studies of the non-Gaussian parameter showed that the amorphous polymers are heterogeneous, but gave no information about the spatial scale of the heterogeneous domain or *CRR*. In order to evaluate the spatial scale we performed PALS measurements on PB and obtained the average size of free volume V_f as a function of temperature. It was found that the relation of the free volume and the viscosity can be well described by the free volume theory above T_g, meaning that the free volume observed here is related to the structural relaxation. In addition, this relaxational motion must be a cause of the excess mean square displacement $\Delta\alpha$ observed above T_g because the temperature dependence of $\Delta\alpha$ can be also well described by the free volume theory [4]. In the previous paper [5], we have derived a new formula to relate the free volume V_f to the excess mean square displacement $\Delta\alpha$ using the size (radius) ξ of *CRR* as a parameter and evaluated ξ as a function of temperature. It was found that the value ξ increases with decreasing temperature to reach 13 Å at T_g for PB, which is in good agreement with reported values [5]. It should be noted that ξ does not diverge at the Vogel-Fulcher temperature T_0 in contradiction to the fluctuation theory. This finding suggests that *CRR* is frozen in near T_g and the heterogeneity is sustained below T_g, leading to a new idea that the frozen heterogeneity is an origin of the famous Boson peak (localized mode) [5].

[1] Proc. Yukawa International Seminar (YKIS96): *Dynamics of Glass Transition and Related Topics*, ed Odagaki T, Hiwatari Y and Matsui J, 1996, Kyoto,

[2] Kanaya T, Tsukushi I and Kaji K, *Prog. Theor. Phys. Suppl.*, 126, 133 (1997).

[3] Kanaya T, Tsukushi I, Kaji K, Gabys B and Bennington S M, *J. Non-Cryst. Solids*, 235/237, 212 (1998).

[4] Kanaya T, Tsukushi I, Kaji K, Bartos J and Kristiak J, *Phys. Rev.*, E60, 1906 (1999).

[5] Kanaya T, Tsukushi I, Kaji K, Bartos J and Kristiak *J, J. Phys. IV France*, 10, Pr7-317 (2000).

[6] Kanaya T, Buchenau U, Koizumi S, Tsukushi I and Kaji K, *Phys. Rev.*, B61, R6451 (2000).

One- and Two-Dimensional CP/MAS ^{13}C NMR Analyses of Dynamics in Poly(2-hydroxypropyl ether of bisphenol-A)

Hironori Kaji, Toshihiro Tai and Fumitaka Horii

The dynamics of amorphous poly(2-hydroxypropyl ether of bisphenol-A) (PHR), quenched from the melt, has been investigated by one- and two-dimensional solid-state ^{13}C NMR spectroscopy. CP/MAS ^{13}C NMR spectra from –150 to 180 ºC give two specific features: (1) below 23 ºC, resonance lines for C-H carbons of phenylene rings split into two lines; (2) linewidths of resonance lines become broad at 20 - 50 ºC above the glass transition temperature. The feature (1) indicates that phenylene C-H carbons exist in chemically different two sites at low temperatures. These two sites are probably associated with OH ··· π hydrogen bond formation. The coalescence of the resonance lines at elevated temperatures is caused by π flip motion of phenylene rings, which corresponds to the γ relaxation for PHR. The correlation time of the π flip motion is analyzed by the two-site exchange model, and is found to follow the Arrhenius equation. The apparent activation energy is 51 kJ mol^{-1} by assuming an inhomogeneous correlation time distribution described by a Kohlrausch-Williams-Watts (KWW) function with an exponent of 0.2. The feature (2) is caused by the so-called motional broadening, which is originated by enhanced segmental motions. This dynamics corresponds to the α relaxation for PHR and can be described by William-Landel-Ferry (WLF) equation. Two-dimensional CP/MAS ^{13}C exchange NMR experiments confirm the existence of flip angle distribution as well as the distribution of correlation times of phenylene ring π flip motion with a KWW exponent of 0.2.

Keywords : Phenoxy resin / Amorphous polymer / Dynamics / Relaxation / CPMAS ^{13}C NMR

Poly(2-hydroxypropyl ether of bisphenol-A), known as phenoxy resin (PHR), is an amorphous linear polymer and the structure and dynamics have been studied by X-ray diffraction [1], mechanical relaxation [2], and solid-state NMR [3]. Although three relaxations are observed between –100 and –40 ºC, between 20 and 40 ºC, and between 70 and 100 ºC on mechanical relaxation experiments, the molecular origins have not been well understood. In this article, we investigate the dynamics of PHR by analyzing one- and two-dimensional CP/MAS ^{13}C NMR spectra.

PHR films (Union Carbide, grade PKHJ) were prepared by being hot-pressed at 160 ºC under 100 kg cm^{-2}, quenched in ice-water, and dried at room temperature under vacuum for three days. Solid-state ^{13}C NMR measurements were conducted on a Chemagnetics CMX-400 spectrometer operating under a static magnetic field of 9.4 T. The glass transition temperature (T_g) determined by DSC measurements was 80 ºC. No other obvious exothermic and endothermic peaks were observed between –100 and 200 ºC.

Figure 1 shows CP/MAS ^{13}C NMR spectra of PHR ranging from –150 to 180 ºC. We can find two interesting features. One feature is that the resonance lines for C-H carbons of phenylene rings split into two resonance lines at -150 ºC. This indicates that the phenylene C-H carbons exist in chemically different two sites at low temperatures, which would be caused by an OH ··· π hydrogen bond [4] between the hydroxyl group and the phenylene ring. The coalescence of the resonance lines with increasing temperature is originated from phenylene ring π-flip motion. The correlation time of the π-flip motion, whose temperature range corresponds to the mechanical γ relaxation, is determined by using the two-site exchange model [5]. For the analysis, the correlation time distribution with a Kohlrausch-Williams-Watts (KWW) func-

FUNDAMENTAL MATERIAL PROPERTIES — Molecular Dynamic Characteristics —

Scope of Research

The research activities in this subdivision cover structural studies and molecular motion analyses of polymers and related low molecular weight compounds in the crystalline, glassy, liquid crystalline, solution, and frozen solution states by high-resolution solid-state NMR, dynamic light scattering, electron microscopy, X-ray diffractometry, and so on, in order to obtain basic theories for the development of high-performance polymer materials. The processes of biosynthesis, crystallization, and higher-ordered structure formation are also studied for bacterial cellulose.


Prof HORII Fumitaka (D Eng)


Assoc Prof TSUNASHIMA Yoshisuke (D Eng)


Instr KAJI Hironori (D Eng)


Assoc Instr HIRAI Asako (D Eng)


Assoc Instr KUWABARA Kazuhiro (D Eng)


Techn OHMINE Kyoko

Guest Scholar:
HU, Shaohua (Ph.D)

Students:
ISHIDA, Hiroyuki (DC)
MASUDA, Kenji (DC)
MURAKAMI, Miwa (DC)
MAEKAWA, Yasushi (MC)
YAMADA, Shusaku (MC)
FUKE, Kazunori (MC)
NAKAMURA, Hisako (MC)
FUJII, Shigekatsu (UG)
MIZUNO, Megumi (UG)
YANO, Tatsuya (UG)
KOJIMA, Makoto (RF)
SIRASAKA, Hitoshi (RF)

tion with an exponent of $\beta = 0.2$ as well as the flip angle distribution, quantified from the following 2D MAS exchange experiments, are applied. The result, shown by closed squares in Figure 2, indicates that the Arrhenius relation holds with the apparent activation energy, E_a, of 51 kJ mol^{-1}. This value agrees with the previously reported E_a for the π flip motion of phenylene groups for several polymers with bisphenol-A residues, 48 - 56 kJ mol^{-1} [3,6,7]. In contrast, the value of $\beta = 0.2$ is not consistent with that of $\beta = 0.6$ for ^{2}H NMR lineshape analyses of π-flip motion in PHR [3]. However, the value of $\beta = 0.2$ seems to be reasonable because mechanical relaxations and NMR line shape analyses of π-flip motion in cured epoxy resins give $\beta = 0.28$ [8], and CSA lineshape analyses of π-flip motion in PC gives $\beta = 0.154$ [6].

Figure 3 shows 2D CP/MAS ^{13}C exchange NMR spectra for the C4 and C5 carbons of PHR at –120 ºC. While only the diagonal peaks are observed for the mixing time of 10 ms, the exchange signals are clearly observed in the mixing time of 2.0 s. The correlation time of the π-flip motion at –120 ºC is analyzed by the mixing time dependence of the exchange signal intensities, $I(t_m)$. The experimental data cannot be explained by calculated $I(t_m)$ curves with $\beta = 1$ or 0.6. In contrast, the calculated $I(t_m)$ curve with $\tau = 2.0 \times 10^2$ s and $\beta = 0.2$ agree well with the experimental data. It is therefore found that the 2D CP/MAS ^{13}C exchange NMR experiments offer us quantitative information on average correlation times and the width of the correlation time distributions for respective ^{13}C species.

The other feature in Figure 1 is that the linewidths become broad at 20 – 50 ºC above T_g. This is caused by the modulation of MAS and ^{1}H dipolar decoupling efficiency by enhanced segmental motions [9], which correspond to the α relaxation.

The correlation times are analyzed quantitatively from the temperature dependence of the linewidth for each resonance line by assuming the William-Landel-Ferry (WLF) equation. The temperature dependence of correlation times thus obtained is also plotted in Figure 2 as closed circles. It is found that the temperature dependence of the correlation time can be described by WLF equation with typical parameters.

The correlation times at 90 and 120 ºC analyzed from 2D CP/MAS ^{13}C exchange NMR experiments are also shown in Figure 2. The dynamics of each ^{13}C site can be investigated by these simple 1D and 2D solid-state NMR experiments, which are crucial methodology for the elucidation of the origin of relaxations.

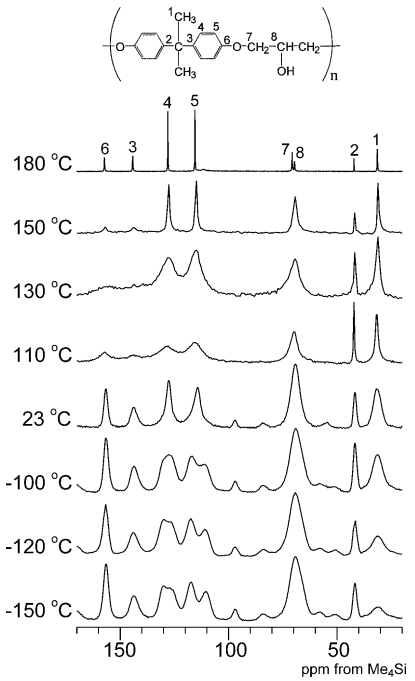

Figure 1. CP/MAS ^{13}C NMR spectra of PHR at different temperatures.

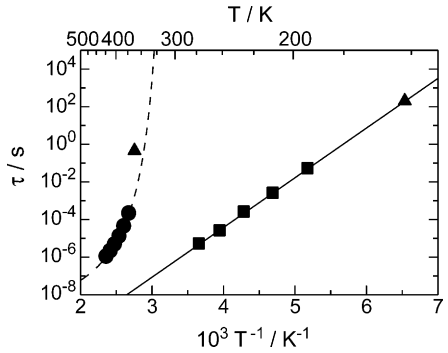

Figure 2. The Arrhenius plot for the correlation time of motion associated with the α and γ relaxations of PHR. ● : motional broadening, ▲ : 2D exchange, ■ : two-site exchange with KWW $\beta = 0.2$

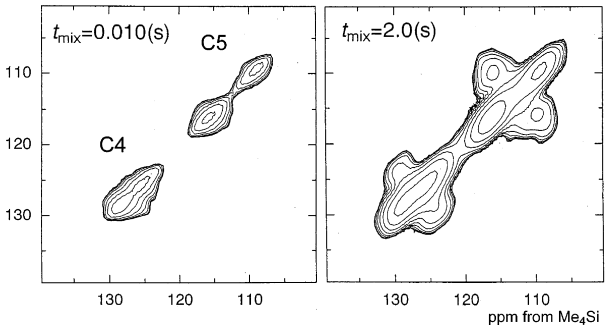

Figure 3. 2D CP/MAS ^{13}C exchange spectra for C4 and C5 carbons of PHR in the glassy state at –120 ºC.

References

1. J. J. del Val et al., *Polymer* **36**, 3625 (1995).
2. R. Erro et al., *J. Polym. Sci. B, Polym. Phys. Ed.* **34**, 1055 (1996).
3. J.-F. Shi et al., *Macromolecues* **29**, 605 (1996).
4. T. Steiner et al., *Acta Cryst.* **B53**, 843 (1997).
5. A. Abragam, *The principles of Nuclear Magnetism*; Clarendon Press: Oxford, 1989.
6. A. K. Roy et al., *Macromolecules* **19**, 1356 (1986).
7. J. Y. Jho and A. F. Yee, *Macromolecules* **24**, 1905 (1991).
8. A. N. Garroway et al., *Macromolecules* **15**, 1051 (1982).
9. K. Takegoshi and K. Hikichi, *J. Chem. Phys.* **94**, 3200 (1991).

Mechanism and Kinetics of RAFT-Based Living Radical Polymerizations of Styrene and Methyl Methacrylate

Atsushi Goto, Koichi Sato, Yoshinobu Tsujii and Takeshi Fukuda

The bulk polymerizations of styrene and methyl methacrylate in the presence of model polymer-dithiocarbonate adducts as mediators and benzoyl peroxide (BPO) as a conventional initiator were kinetically studied. The polymerization rate, hence the concentration of polymer radical $P^{\bullet}$, was proportional to $[BPO]^{1/2}$. The pseudo-first-order activation rate constants k_{act} were determined by the GPC peak-resolution method. The results showed that k_{act} is directly proportional to $[P^{\bullet}]$, indicating that reversible addition-fragmentation chain transfer (RAFT) is the only important mechanism of activation. The magnitude of the exchange rate constant k_{ex} ($= k_{act}/[P^{\bullet}]$) was strongly dependent on both the structures of the dithiocarbonate group and the polymer. The k_{ex} values for the three RAFT systems examined in this work were all very large, explaining why these systems can provide low-polydispersity polymers from an early stage of polymerization.

Keywords: RAFT / Reversible activation / Activation rate constant / Living radical polymerization

There has recently been a surge of interest in living radical polymerization (LRP) techniques as new and facile synthetic routes to well-defined, low-polydispersity polymers. Mechanistically, these techniques are based on the common concept of alternating activation-deactivation processes (Scheme 1a), in which a potentially active (dormant) species P-X is reversibly activated to the active radical $P^{\bullet}$ by, e.g., thermal and chemical stimuli. In the presence of monomer M, $P^{\bullet}$ propagates until it is deactivated by a capping agent X. A number of activation-deactivation cycles allow all the chains to have an almost equal opportunity to grow, resulting in low-polydispersity polymers. This means that the frequency of such cycles, i.e., the magnitude of the activation rate constant k_{act}, fundamentally characterizes the performance of a given LRP.

Recently, a novel LRP using dithio compounds (Scheme 1b: e.g., X = –$SCSCH_3$ and –SCSPh) has been developed.[1] The mechanism of activation is supposed to involve a **r**eversible **a**ddition-**f**ragmentation chain **t**ransfer (RAFT: Scheme 1b) process. The low polydispersity polymers ($M_w/M_n < 1.1$, where M_w and M_n are weight- and number-average molecular weights, respectively) produced in this polymerization even at an early stage of polymerization indicate that these RAFT processes are extremely fast. In this work, we have determined the k_{act} for the RAFT-based polymerizations of styrene and methyl methacrylate (MMA) as a function of polymerization rate R_p and temperature T. In this way, we were able to evaluate the fundamental abilities of these systems, and also experimentally confirm the supposed activation mechanism.

We first examined the polymerization of styrene including a fixed amount of polystyrene (PS)-$SCSCH_3$

ORGANIC MATERIALS CHEMISTRY — Polymeric Materials —

Scope of research

Kinetic and mechanistic analyses are made for better understandings and systematization of the chemical and physicochemical reactions occurring in polymerization systems and for the development of better routes to the synthesis of well-defined polymers. By the application of various polymerization techniques, in particular, living polymerizations, new well-defined polymers or polymer assemblies are prepared, and their structure/properties relationships are precisely analyzed for new polymer-based materials of practical importance. Projects in progress include: (1) kinetics and mechanisms of living radical polymerization. (2) Synthesis of new polymeric materials by living polymerizations and polymer reactions and their structure/properties studies. (3) Synthesis, properties, and applications of high-density polymer brushes.

Prof
FUKUDA, Takeshi
(D Eng)

Instr
TSUJII, Yoshinobu
(D Eng)

Students:
YAMAMOTO, Shinpei (PD)
EJAZ, Muhammad (DC)
GOTO, Atsushi (DC)
MIWA, Nobuhiro (MC)
SATO, Koichi (MC)
HIROSE, Yuichi (MC)
YOSHIKAWA, Chiaki (MC)
MARUTANI, Eizo (UG)
KOH, Kyungmoo (RS)
KWAK, Yungwan (RS)

(0.45 mM) as a probe P_0-X and variable amounts of benzoyl peroxide (BPO: 0–10 mM) as a radical initiator. For all the examined values of $[BPO]_0$, the mean polymerization rate $R_p/[M]$ (= $k_p[P^\bullet]$, where k_p is the propagation rate constant) was found to be constant. The plot of $(R_p/[M])^2$ vs $[BPO]_0$ was almost linear, which is relevant with the conventional (RAFT agent-free) system.

The k_{act} was determined by the gel permeation chromatographic (GPC) peak-resolution method, which focuses on an early stage of the polymerization containing P_0-X. When P_0-X is activated, the released $P_0^\bullet$ will propagate until it is deactivated to give a new adduct P_1-X. Since P_0-X and P_1-X are generally different in chain length and its distribution, they may be distinguished by GPC. By following the change in [P_0-X], k_{act} will be determined. A lower $[P_0\text{-X}]_0$ leads to a larger number of monomer units added to $P_0^\bullet$ during an activation-deactivation cycle. In fact, with a sufficiently low $[P_0\text{-X}]_0$ (0.45 mM), the GPC curves were composed of two definite peaks such as shown in Figure 1, which allowed accurate resolution. Thus, we could unequivocally follow the [P_0-X] and obtain well-defined values of k_{act}.

The mechanism of activation, i.e., the cleavage of the C-S bond, is supposed to be RAFT (rate constant = k_{ex}: Scheme 1b). However, thermal homolysis (rate constant = k_d: Scheme 1c) might contribute as well. When both processes are involved, k_{act} takes the form

$$k_{act} = k_d + k_{ex}[P^\bullet] \quad (1)$$

Figure 2 shows the plot of k_{act} against $R_p/[M]$ (= $k_p[P^\bullet]$). Evidently, the data points form a straight line passing through the origin, showing that $k_d = 0$ and the slope of the curve gives C_{ex} (= k_{ex}/k_p) = 180. This result suggests that the main mechanism of activation in this system is the RAFT process rather than thermal dissociation. With the known value of k_p (340 M^{-1} s^{-1}), k_{ex} is estimated to be

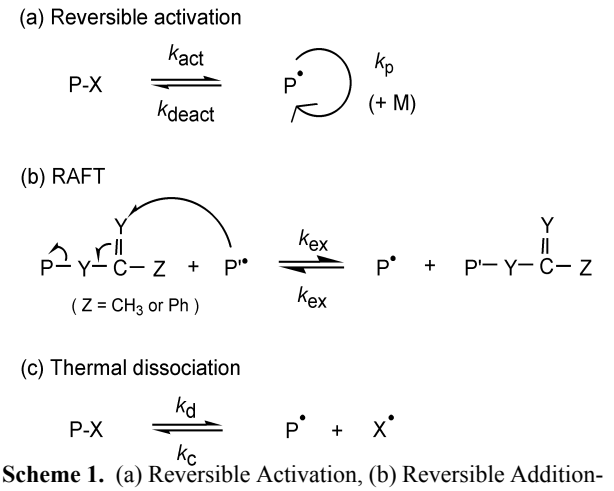

Scheme 1. (a) Reversible Activation, (b) Reversible Addition-Fragmentation Chain Transfer (RAFT), and (c) Thermal Dissociation.

Table 1. Comparison of C_{ex} (60 °C)

P-X	C_{ex}
PS-$SCSCH_3$	180
PS-SCSPh	6000 ± 2000[a]
PMMA-SCSPh	140
PS-I[2]	4.0
PMMA-macromonomer[3]	0.20

[a] Preliminary result at 40 °C.

61000 M^{-1} s^{-1}. The temperature dependence of C_{ex} was found to be given by

$$C_{ex} = 3.1 \exp(+11.5 \text{ kJ mol}^{-1}/RT) \quad (2)$$

We also determined k_{act} in the styrene/PS-SCSPh system and the MMA/PMMA-SCSPh system. The corresponding C_{ex} values are summarized in Table 1. The results clearly show that C_{ex} is strongly dependent on both the structures of carbonate and polymer (alkyl) moiety. In comparison with the C_{ex} values for other exchanging chain transfer-type LRP systems (PS-iodide[2] and PMMA-macromonomer[3] systems), those for the examined RAFT systems are exceptionally large. This explains why these RAFT systems can yield low-polydispersity polymers from an early stage of polymerization.

References

(1) Chiefari, J. et al. *Macromolecules* **1998**, *31*, 5559.
(2) Goto, A. et al. *Macromolecules* **1998**, *31*, 2809.
(3) Moad, C. L. et al. *Macromolecules* **1996**, *29*, 7717.

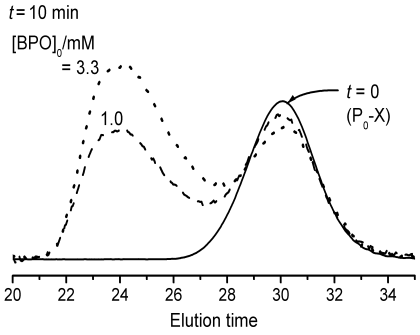

Figure 1. Examples of GPC chromatograms in the styrene/PS-$SCSCH_3$(P_0-X) system (60 °C): $[P_0\text{-X}]_0$ = 0.45 mM; $[BPO]_0$ as indicated in the figure.

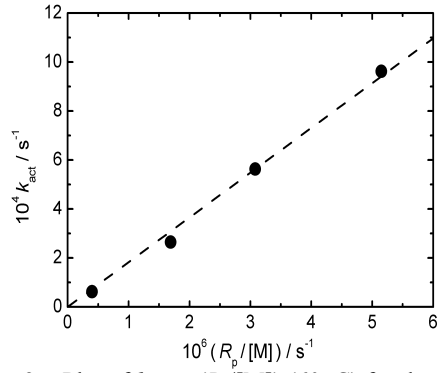

Figure 2. Plot of k_{act} vs $(R_p/[M])$ (60 °C) for the styrene/PS-$SCSCH_3$ system.

Novel π-Conjugated Systems: The First Silatropylium Ion and Planar Cyclooctatetraene Annelated with Bicyclic Frameworks and New Derivatives of Fullerene C_{60}

Koichi Komatsu, Tohru Nishinaga, Yasujiro Murata, Akira Matsuura, Yoshiteru Izukawa, and Noriyuki Kato

The first silylium ion with cyclic π-conjugation, the silatropylium ion, was prepared, which was made possible by annelation with three bicyclo[2.2.2]octene frameworks and steric protection of the silylium-ion center by a mesityl group. The presence of cyclic π-conjugation through the p-orbital of silicon was confirmed by NMR measurements. The first planar cyclooctatetraene was synthesized by cuprate mediated cyclotetramerization of 2,3-diiodobicyclo[2.1.1]hexene, and its structure determined by X-ray crystallography. On the other hand, a thermal reaction of fullerene C_{60} with phthalazine in solution afforded a C_{60} derivative with an eight-membered-ring opening on the surface while the reaction conducted in the solid state gave a novel adduct with two C_{60} cages incorporated in a bicyclic framework.

Keywords: silylium ion / Hückel aromaticity / cyclooctatetraene / fullerene / rearrangement

1. The First Silatropylium Ion[1] and Planar Cyclooctatetraene[2] Stabilized by Bicycloannelation.

The problem of generation or isolation of the silyl cation in the condensed phase has been among the central issues of organosilicon chemistry. So far the reports on a silylium ion having no coordination with the solvent or counteranion are quite limited. Furthermore, there has been no example on the silylium ion incorporated in cyclic π-conjugation. As one of such π-conjugated silylium ions, the silatropylium ion is of great interest, but its presence either in solution or in gas phase has been highly questioned from the theoretical viewpoint.

In the present study, the first silatropylium ion was made possible by applying the annelation with rigid bicyclic frameworks and the protection of the silicon atom by the sterically demanding mesityl group.

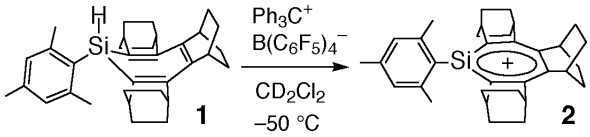

Thus the hydride abstraction from mesitylsilacycloheptatriene **1** in CH_2Cl_2 at low temperature successfully afforded the silatropylium ion **2**, which was confirmed by NMR measurements. In cation **2** the ^{29}Si NMR signal (δ 142.9) was downfield shifted from **1** by 192.2 ppm, and so were the ^{13}C NMR signals for the seven-membered ring carbons. Furthermore, the down-field shift of the ^1H NMR signals of the bridgehead protons of the bicyclic frameworks indicated the presence of a diamagnetic ring current. Thus, the silatropylium ion **2** is con-

ORGANIC MATERIALS CHEMISTRY — High-Pressure Organic Chemistry —

Scope of Research

Fundamental studies are being conducted for creation of new functional materials with novel structures and properties and for utilization of high pressure in organic synthesis. The major subjects are: synthetic and structural studies on novel cyclic π-systems having σ-π conjugation; synthesis of redox-active dehydroannulenes; chemical transformation of fullerene C_{60}; mechanochemical reactions of fullerenes.

Prof
KOMATSU
Koichi
(D Eng)

Instr
MORI
Sadayuki
(D Eng)

Instr
NISHINAGA
Tohru
(D Eng)

Instr
MURATA
Yasujiro
(D Eng)

Students:
MATSUURA, Akira (DC)
FUJIWARA, Koichi (DC)
WAKAMIYA, Atsushi (DC)
ITO, Miho (MC)
NODERA, Nobutake (MC)
INOUE, Ryouta (MC)
SUZUKI, Mitsuharu (MC)
MURATA, Michihisa(UG)
YAMAZAKI, Daisuke(UG)

sidered as a new example of a positively charged aromatic π-conjugated system containing silicon.

Cyclooctatetraene (COT) is known as a tub-shaped molecule. However, annelation with a highly strained system such as bicyclo[2.1.1]hexene (BCH) is expected to cause planarization of the COT ring, which is of great interest from the viewpoint of antiaromaticity and realization of a novel electronic structure.

When 2,3-diiodobicyclo[2.1.1]hexene was monolithiated and treated with CuI, the COT **4** annelated with four BCH units was obtained in 21% yield together with benzene **3** in 34% yield. The structure of novel COT **4** was determined by X-ray crystallography: **4** has a completely planar eight-membered ring with remarkable bond alternation (1.331 Å and 1.500 Å with the shorter bonds exocyclic to bicycloannelation). The planarization of the COT ring in **4** results in elevation of a HOMO level and reduction of HOMO-LUMO gap as shown by the long-wavelength absorption (459 nm) and extremely low oxidation potentials ($E_{1/2}(1)$ +0.07 V vs Fc/Fc^+, $E_{pa}(2)$ +0.76 V). The antiaromaticity in COT **4** is greatly reduced due to the bond alternation and also σ-π interaction.

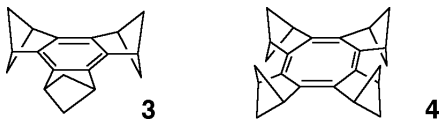

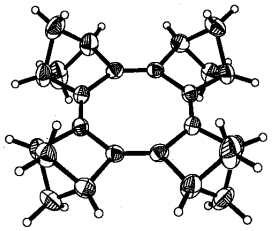

X-ray structure of COT **4**

2. Thermal Reactions of C_{60} with Phthalazine.[3]

The mechanochemical solid-state reaction using a high-speed vibration milling technique has been successfully utilized in our group for the organic functionalization of fullerene C_{60}.

In a present study, it was demonstrated that the thermal reactin of C_{60} with phthalazine (**5**) takes totally different courses depending on the reaction phase.

A reaction of C_{60} with **5** in a solution phase at 255 ºC, in 1-chloronaphthalene afforded a new compound **7** with an eight-membered-ring opening on the C_{60} surface as a single product in 57% yield. The structure was confirmed by ^1H and ^{13}C NMR and MS spectroscopy. This compound has 60 π-conjugated carbons with sp^2 hybridization, and its magenta-colored solution exhibits an electronic spectrum which is quite similar to that of C_{60} itself.

On the other hand, when the reaction was conducted in the solid state with high-speed vibration milling for 1 h and then heated at 200 ºC for 2 h, a totally different product **8** was formed in 41% yield, which had two C_{60} cages incorporated in a bicyclic framework. The structure was confirmed by ^1H and ^{13}C NMR and MS spectroscopy.

These reactions are supposed to take place through a common intermediate **6**, which either undergoes the intramolecular rearrangement to give **7** in solution or is subjected to the [4+2] cycloaddition with C_{60} to give **8** in the solid state where no solvent molecules intervene.

In the dimeric compound **8** the two C_{60} cages are rigidly held at such close ploximity with the distance of two six-membered rings of around 3.0 Å. Reflecting this, **8** readily underwent an intramolecular [2+2] cycloaddition in solution under irradiation of the visible light to give the dimer **9**.

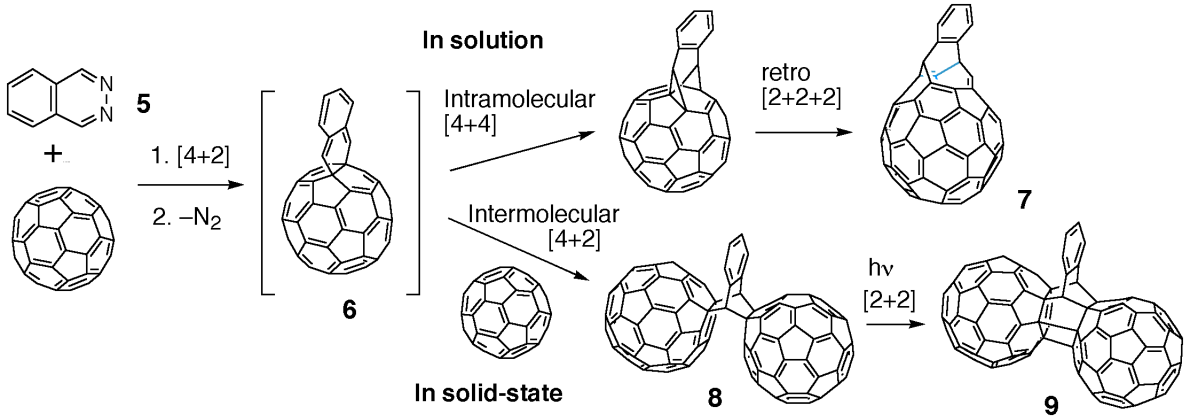

References

1. Nishinaga T, Izukawa Y, Komatsu K, *J. Am. Chem. Soc.*, **122**, 9312 (2000).
1. Matsuura A, Komatsu K, *J. Am. Chem. Soc.*, **123**, 1768 (2001).
2. Komatsu K, Murata Y, Kato N, *Fullerene 2000*, **9**, 20 (2000).

Stereoselective Formation of Cyclopropylsilane through Intramolecular Rearrangement of [(Allyloxy)dimesitylsilyl]lithiums

Atsushi Kawachi, Hirofumi Maeda and Kohei Tamao

A [(*sec*-allyloxy)dimesitylsilyl]stannane having a phenyl group on the olefin part reacts with *n*-BuLi in THF to give a cyclopropylsilane as a single diastereomer, in contrast to the [2,3]-sila-Wittig rearrangement affording an allylsilane, previously observed for a substrate having an alkyl group on the olefin part. The substituent effect is revealed by *ab initio* calculations in terms of the regioselectivity in the reaction of silyllithiums with an olefin.

keywords: silyllithiums / sila-Wittig rearrangement / cyclopropanation reaction / cyclopropylsilane

Previously we demonstrated the [2,3]-sila-Wittig rearrangement [1], the silicon analogs to the [2,3]-Wittig rearrangement: the [(*tert*-allyloxy)diphenylsilyl]lithiums [2] generated from the [(*tert*-allyloxy)diphenysilyl]stannane and *n*-BuLi underwent the [2,3]-rearrangement to afford the lithium allylsilanolates. During the course of this study, we have found that when a phenyl group is attached to the terminus of the olefin, the reaction mode of the rearrangement changes in such a way that a cyclopropylsilane is formed in a stereoselective manner, in contrast to the [2,3]-sila-Wittig rearrangement observed for substrates having alkyl group(s) on the olefin part [2].

(*E*)-[(*sec*-allyloxy)dimesitylsilyl]stannane (*E*)-**1** having a phenyl group on the olefin was treated with *n*-BuLi (1.2 mol amt.) in THF at 0 ºC for 3 h, as shown in Scheme 1. The reaction was then quenched with a 5% aqueous solution of NH4Cl to afford the cyclopropylsilane **2** in 68% yield as a single diastereomer. It was found that (*Z*)-**1** afforded the same diastereomer **2** in 79% yield. The relative configuration of **2** was determined by the X-ray diffraction analysis of the single crystals [4], as shown in Figure 1. Both the phenyl group and the methyl group are *trans* to the silyl group. This product is thus designated as (*r-Si-trans, trans*)-**2**.

The formation of the cyclopropylsilane can be rationalized as shown in Scheme 1. The silyllithium **3** generated in situ undergoes intramolecular addition to the olefin on the β-carbon (C(β)) in the initial step. The result-

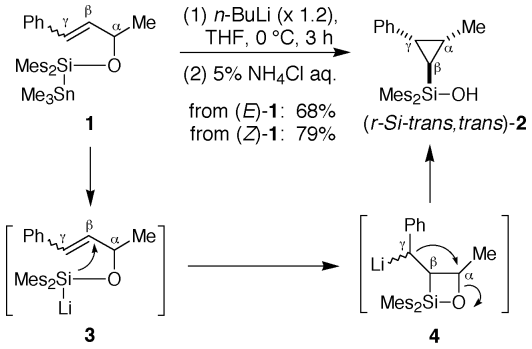

Scheme 1.

SYNTHETIC ORGANIC CHEMISTRY — Synthetic Design —

Scope of research

(1) Synthesis, structural studies, and synthetic applications of organosilicon compounds, such as pentacoordinate silicon compounds, functionalized silyl anions, and functionalized oligosilanes. (2) Design and synthesis of novel π-conjugated polymers containing silacyclopentadiene (silole) rings, based on new cyclization reactions and carbon-carbon bond formations mediated by the main group and transition metals. (3) Chiral transformations and asymmetric synthesis via organosulfur and selenium compounds, especially via chiral episulfoniun and episelenonium ions.

Prof TAMAO, Kohei (D Eng)

Assoc Prof TOSHIMITSU, Akio (D Eng)

Instr KAWACHI, Atsushi (D Eng)

Instr YAMAGUCHI, Shigehiro (D Eng)

RANGAPPA, Kanchugarakoppal Subbegowda (Guest Scholar); CHO, Yeon Seok (Guest Res Assoc); NAKAMOTO, Masaaki (Res Assoc); AKIYAMA, Seiji (DC); MAEDA, Hirofumi (DC); TSUJI, Hayato (DC); SHIRASAKA, Toshiaki (DC); ITAMI, Yujiro (DC); SAEKI, Tomoyuki (MC); HIRAO, Shino (MC); MINAMIMOTO, Takashi (MC); KANETA, Yasuhiro (MC); MIKI, Takashi (MC); OISHI, Yohei (UG); FUJIMURA, Hirokazu (UG)

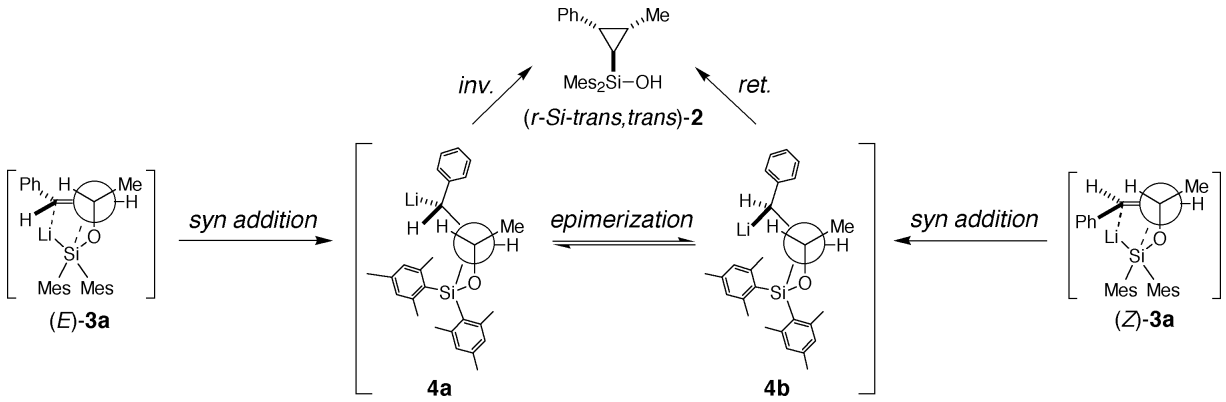

Scheme 2.

ing 1-oxa-2-sila-cyclobutane **4** is so reactive due to the ring strain that it readily suffers a nucleophilic substitution on the α-carbon (C(α)) by the benzyllithium moiety, resulting in the ring cleavage of the oxasilacyclobutane and the formation of the cyclopropane ring during the second step.

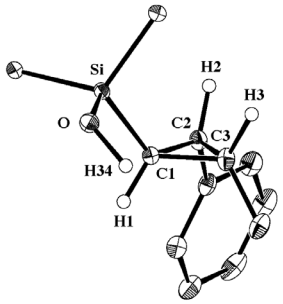

Figure 1. Crystal structure of (*r-Si-trans,trans*)-**2**•H_2O. The H_2O molecule and hydrogen atoms except for H1, H2, H3, and H34 are omitted for clarity.

The stereoselective formation of (*r-Si-trans, trans*)-**2** was followed as shown in Scheme 2, which includes the Newmann projections of **3** and **4** along the C(α)-C(β) bond axis. The silyllithium (*E*)-**3**, coming from (*E*)-**1**, favors the conformer (*E*)-**3a** to avoid the steric repulsion between the phenyl group and the mesityl group(s). The syn addition of (*E*)-**3a** to the olefin gives **4a**. The cyclization in **4a** with inversion of configuration at the lithiated benzylic carbon provides (*r-Si-trans,trans*)-**2**. Alternatively, **4a** may undergo epimerization at the lithiated carbon to give another epimer **4b**. The cyclization in **4b** with retention of configuration at the lithiated benzylic carbon also provides (*r-Si-trans,trans*)-**2**. In a similar manner, the conformer (*Z*)-**3a**, coming from (*Z*)-**1**, also provides the same (*r-Si-trans,trans*)-**2** as a single diastereomer via the common intermediates **4a** and/or **4b**. We cannot determine the reaction stereochemistry, inversion or retention, because the stereochemical courses of the benzyllithium derivatives are sensitive to several factors such as the nature of the leaving group.

The observed regioselectivity of the reaction of the silyllithium to the olefin was rationalized by ab initio molecular orbital calculations (MP2/6-31G**//HF/3-21G) of the model compounds **5** and **6**, as shown in Figure 2 [5]. The alkyl-substituted compound **5** exhibits the maximum of the molecular orbital coefficient in the LUMO on C(γ) and thus accepts the nucleophilic attack at this position, resulting in the sila-Wittig rearrangement. In contrast, the phenyl-substituted compound **6** exhibits the maximum of the molecular orbital coefficient in the LUMO on C(β) and thus accepts the nucleophilic attack on C(β), resulting in the cyclopropylsilane formation.

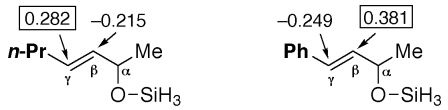

5 **6**

Figure 2. Molecular orbital coefficients on LUMO of the model compounds **5** and **6**.

In summary we have demonstrated the stereoselective formation of the cyclopropylsilane based on the intramolecular rearrangement of the [(allyloxy)silyl]lithiums.

References

1. (a) Kawachi A, Doi N, and Tamao K, *J. Am. Chem. Soc.*, **119**, 233 (1997). (b) Kawachi A and Tamao K, *Bull. Chem. Soc. Jpn.*, **70**, 945 (1997).
2. The term *tert*-allyl means that the allylic carbon is tertiary. The term *sec*-allyl is used in a similar way in this paper.
3. Kawachi A, Maeda H, Tamao K, *Chem. Lett.*, 1216 (2000).
4. The crystal includes one H_2O molecule per **2**. Crystal data for (*r-Si-trans,trans*)-**2**•H_2O: $C_{28}H_{36}O_2Si$; M = 432.68; Rigaku RAXIS-IV imaging plate area detector; crystal size 0.25 x 0.25 x 0.25 mm; monoclinic, space group $P2_1/c$ (No. 14), $Z = 4$, $a = 8.5408(6)$ Å, $b = 17.948(2)$ Å, $c = 15.996(2)$ Å, $\beta = 93.875(7)°$, $V = 2446.3999$ Å^3, $D_{calcd} = 1.175$ g/cm^3; $T = 173$ K; $2\theta_{max} = 55.1°$. The structure analysis is based on 5108 reflections, 4443 observed ($I>3.00\sigma(I)$), and 281 parameters. $R = 0.071$, $R_W = 0.083$.
5. All calculations were performed with the Gaussian 94 program package.

A Chiral Nonracemic Enolate with Dynamic Axial Chirality: Direct Asymmetric Alkylation of α-Amino Acid Derivatives

Takeo Kawabata, Hideo Suzuki, Yoshikazu Nagae, Jianyong Chen and Kaoru Fuji

The structure of enolate was long believed to be achiral. However, a chiral nonracemic enolate with a racemization barrier of 16 kcal/mol at -78 ºC was found to be the crucial intermediate for the asymmetric α-methylation of **1** to give **2** in 81% ee and 96% yield. The asymmetric α-methylation occurs in other amino acid derivatives (Val, Leu, Trp, His, Tyr, Dopa) in 78-93% ee.

Key words: chiral enolate / dynamic chirality / asymmetric synthesis / amino acid / axial chirality

The structure of enolate was long believed to be achiral because all four substituents are on the same plane as the enolate double bond. For example, enolates generated from α-amino acid derivatives are seemingly achiral when substituents R^1 - R^4 are achiral (**A**). However, we propose that some enolate structures are intrinsically chiral. As shown in **B**, an enolate with axial chirality along the C(1)-N axis is expected if R^3 is different from R^4. An enolate with a chiral nitrogen is shown in **C**, where tight coordination of nitrogen to a metal cation creates a stereogenic nitrogen atom. Racemization of these chiral enolates takes place so readily through simple C(1)-N bond rotation that the chirality is not static, but dynamic. These enolates can exist in chiral nonracemic forms for a limited time at low temperatures. We describe here experimental evidence for a chiral nonracemic enolate with dynamic axial chirality, as exemplified in **B**. Through the intrinsically chiral enolate intermediate, asymmetric α-methylation of various α-amino acid derivatives can occur in highly enantioselective manner.

We anticipated that the choice of R^3 and R^4 in **B** or **C** would have the key role for the asymmetric induction, so we screened the substituents at the nitrogen atom of phenylalanine. We found that substrates possessing *t*-butoxycarbonyl (Boc) and methoxymethyl (MOM)

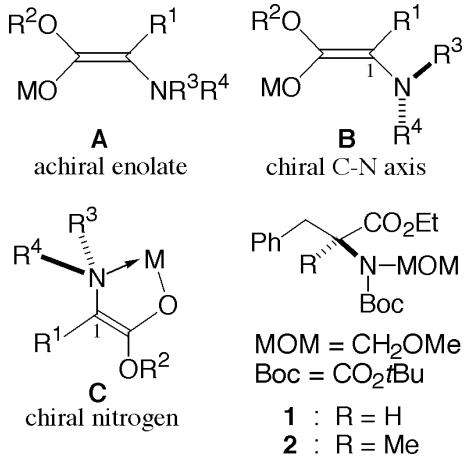

SYNTHETIC ORGANIC CHEMISTRY — Fine Organic Synthesis —

Scope of Research

The research interests of the laboratory include the development of new synthetic methodology, molecular recognition, and total synthesis of natural products. Programs are active in the areas of use of chiral leaving groups for an asymmetric induction, asymmetric alkylation of carbonyl compounds based on "memory of chirality", development of new type of chiral nucleophilic catalysts, utilization of 8,8'-disubstituted 1,1'-binaphthyls as a chiral controller, visualization of molecular length by functionalized phenolphthalein, use of homooxacalixarene for molecular recognition, syntheses of molecular switch.

Professor FUJI Kaoru (D Pharm SC)

Assoc Prof KAWABATA Takeo (D Pharm SC)

Instructor TSUBAKI Kazunori (D Pharm SC)

Technician TERADA Tomoko

Secretary:
IZAWA, Yukako
Lecturer (part-time):
BAGUL, Trusar D. (Ph. D)
Guest Research Associate:
MARX, Karsten H. (Ph. D); CHEN, Jianyong (Ph. D); STRAGIES Roland (Ph. D)
Students:
MOMOSE, Yashima (DC); OHNISHI, Hiroshi (DC); NURUZZAMAN, Mohammad (DC); OTSUBO, Tadamune (DC); YOSHIDA, Hiroshi (MC); TANAKA, Hiroyuki (MC); SUZUKI, Ryutaro (MC); MUKOYOSHI, Koichiro (MC); KAWAKAMI, Shinpei (MC); FUKAYA, Takayuki (MC); KUSUMOTO, Tomokazu (MC); MORIMOTO, Tatsuya (MC)

groups at the nitrogen gave satisfactory results. Treatment of phenylalanine derivative **1** with potassium hexamethyldisilazide (KHMDS) in toluene-THF (4:1) at −78 ºC for 30 min followed by methyl iodide gave α-methylated product **2** in 96% yield and 81% ee.

Intermediary enolate was trapped with *t*-butyldimethylsilyl (TBS) triflate to give *Z*-enol silyl ether **3** and its *E*-isomer in a 2 : 1 ratio in combined isolated yields of 85%. The rotational barrier of the C(1)-N bond of **3** was determined to be 16.8 kcal/mol (365K) by variable-temperature NMR. The restricted bond rotation brings about axial chirality in **3** along the C(1)-N axis, as shown in **D**. On the other hand, the rate of racemization of the potassium enolate intermediate was determined to be 5.3 x 10^{-4}/min at −78 ºC through the periodic quenching of the enolate generated from **1** and KHMDS with methyl iodide. The barrier of racemization of the enolate was calculated to be 16.0 kcal/mol, which matches the rotational barrier of the C(1)-N bond of **3**. This suggests that the chirality of the potassium enolate also originates in the restricted rotation of the C(1)-N bond. It is concluded that *a chiral nonracemic enolate with axial chirality* ***E*** *is the origin for the present asymmetric induction*. The half-life of racemization of the chiral enolate was 22 h at −78 ºC, which is sufficiently long for the chiral enolate to undergo asymmetric methylation [1].

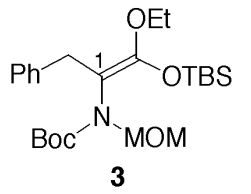

3

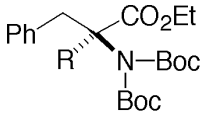

4 : R = H
5 : R = Me

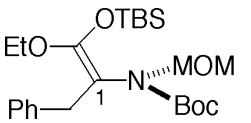

D

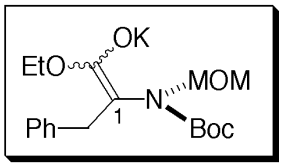

E

Support for this novel mechanism was obtained from the reactions of di-Boc derivative **4**. Upon α-methylation, **4** gave racemic **5** in 95% yield. The result is consistent with the conclusions above, since the enolate generated from **4** can *not* be axially chiral along the C-N axis.

Asymmetric α-methylation also occurred enantioselectively (78 ~ 93% ee) in various α-amino acid derivatives in the absence of any external chiral sources (Table 1). The stereochemical course of α-methylation was retention [2].

The protocol for the asymmetric α-alkylation was applied to isoleucine and *allo*-isoleucine derivatives **6** and **8** that possess chiral centers at both C(2) and C(3). α-Methylation of **6** gave **7** as a major product whereas **8** gave **9** predominantly, although both **6** and **8** have (*S*)-chiral center at C(3). This indicates that chirality at C(2) in **6** and **8** was preserved in the corresponding enolate intermediates and the induced chirality made a major contribution in the stereochemical course of the reaction, while chirality at the adjacent chiral center C(3) had little effect [3].

Table 1. Asymmetric α-Methylation of *N*-MOM-*N*-Boc-α-Amino Acid Derivatives.[a)]

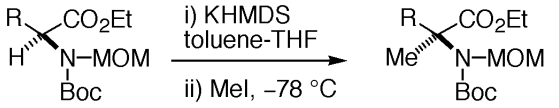

Entry	R	Yield [%]	ee [%]	Configuration
1	$PhCH_2$ –	96	81	*S*
2	*t*-BuOCO, N, N, CH_2 –	83	93	-
3	$MeOCH_2O$, CH_2 –	94	79	*S*
4	MeO, MeO, CH_2 –	95	80	*S*
5	CH_2 –, N, CH_2OMe	88	76	-
6	Me_2CH –	81	87	*S*
7	Me_2CHCH_2 –	78	78	*S*

a) A substrate (0.5 mmol) was treated with 1.1 mol eq of KHMDS in toluene-THF (4 : 1) at -78 °C for 30 min (for entries 1-5) or 60 min (for entries 6 and 7) followed by 10 mol eq of methyl iodide for 16 - 17 h at –78 °C.

In conclusion, a chiral nonracemic enolate with dynamic axial chirality was shown to be the crucial intermediate for direct asymmetric α-alkylation of α-amino acid derivatives. Some other enolates with a restricted bond rotation should have axial chirality with an intrinsic barrier to racemization. Because the rotational barrier is controllable by introducing substituents or protective groups, asymmetric induction based on the present strategy would have further applicability in enolate chemistry.

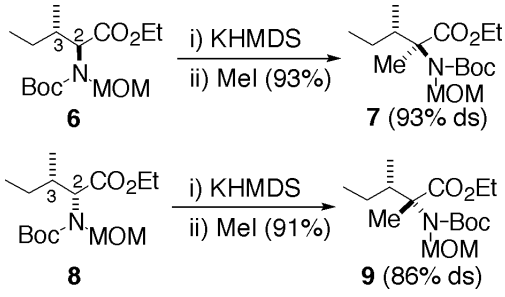

6 **7** (93% ds)

8 **9** (86% ds)

References

1. Kawabata T, Suzuki H, Nagae Y, Fuji K: *Angew. Chem. Int. Ed.*, **39**, 2155-2157 (2000).
2. Kawabata T, Fuji K: *J. Syn. Org. Chem. Jpn.*, **58**, 1095-1099 (2000).
3. Kawabata T, Chen J, Suzuki H, Nagae Y, Kinoshita T, Chancharunee S, Fuji K: *Org. Lett.*, **2**, 3883-3885 (2000).

Synthesis of a Stable Stibabismuthene; the First Compound with an Antimony-Bismuth Double Bond

Takahiro Sasamori, Nobuhiro Takeda and Norihiro Tokitoh

Condensation reaction of an overcrowded dihydrostibine with dibromobismuthine using 1,8-diazabicyclo[5.4.0]undec-7-ene as a base afforded the first stable stibabismuthene, the formation of which was evidenced by the UV-vis and Raman spectra and its chemical reactivity.

Keywords: stibabismuthene/steric protection/antimony/bismuth/double bond

In recent years there has been much interest in compounds with a double bond between heavier group 15 elements. Since the first isolation of a stable diphosphene (Mes*P=PMes*; Mes* = 2,4,6-tri-*t*-butylphenyl) in 1981, a number of examples of kinetically stabilized diphosphenes (RP=PR) and diarsenes (RAs=AsR) have been isolated and fully characterized.[1] Recently, we have succeeded in the synthesis and characterization of the first stable distibene (TbtSb=SbTbt)[2] and dibismuthene (TbtBi=BiTbt),[3] even heavier congeners of azo compounds, by taking advantage of an efficient steric protection group, 2,4,6-tris[bis(trimethylsilyl)methyl]phenyl (Tbt) group. Very recently, Power *et al*. also synthesized another type of stable distibene and dibismuthene substituted by bulky 2,6-$Ar_2C_6H_3$ groups (Ar = mesityl or 2,4,6-triisopropylphenyl).[4] As for the case of heteronuclear double-bond compounds between heavier group 15 elements, several phosphaarsenes and phosphastibenes have been synthesized as stable compounds.[1,5] However, there is no examples of a heteronuclear doubly bonded system between antimony and bismuth, *i. e.* stibabismuthene. Although the successful results on the kinetic stabilization of distibene and dibismuthene (TbtE=ETbt; E = Sb, Bi) naturally prompted us to apply the Tbt group to the synthesis of stable stibabismuthene, we were apprehensive that the extremely low solubility of the Tbt-substituted doubly bonded system of heavier group 15 elements may prevent us from the examination of the possible synthetic approaches and also the spectroscopic detection of the reaction products. On the other hand, during the course of our investigation on the kinetic stabilization of low-coordinated highly reactive species we have developed another bulky aromatic substituent, 2,6-bis[bis(trimethylsilyl)methyl]-4-[tris(trimethylsilyl)methyl]phenyl (Bbt) group,[6] which is expected to be a potentially more useful steric protection group than Tbt group. In fact, a new distibene and dibismuthene substituted by Bbt groups, which have relatively high solubility compared with TbtE=ETbt (E = Sb, Bi), were successfully synthesized and characterized. We now report the successful application of the Bbt group to the synthesis of the first stable stibabismuthene, BbtSb=BiBbt (**1**).

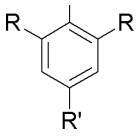

Tbt: R = R' = $CH(SiMe_3)_2$
Bbt: R = $CH(SiMe_3)_2$, R' = $C(SiMe_3)_3$

BIOORGANIC CHEMISTRY — Organoelement Chemistry —

Scope of research

Major research interests of our laboratory are in the chemistry of the compounds having a novel bonding containing heavier main group elements and/or transition metals, such as aromatic compounds containing heavier group 14 elements, double-bond compounds containing heavier main group elements and/or transition metals, and metallacyclopropabenzenes containing group 14 elements. These compounds are synthesized as stable compounds by taking advantage of bulky substituents and their properties are investigated in detail. Mechanism of biochemical reactions and organic synthesis mediated by biocatalysts are also studied.


Prof TOKITOH, Norihiro (D Sc)


Assoc Prof NAKAMURA, Kaoru (D Sc)


Instr SUGIYAMA, Takashi (D Sc)


Instr KAWAI, Yasushi (D Sc)


Instr TAKEDA, Nobuhiro (D Sc)


Assoc Instr YAMAZAKI, Norimasa (D Sc)


Techn HIRANO, Toshiko

Students: INABA, Yoshikazu (RS); MATSUO, Takashi (DC); ODA, Seiji (DC); HAYASHI, Motoko (DC); ITOH, Kenji (DC); SASAMORI, Takahiro (DC); YAMAGUCHI, Hitomi (DC); NAGATA Kazuto (DC); NAKATA Norio (DC); YAMANAKA, Rio (DC); OHTA, Mitsuko (MC); SASAKI, Takayo (MC); HORI Mariko (MC); KAJIWARA Takashi (MC); SHINOHARA, Akihiro (MC)

Condensation reaction of $BbtBiBr_2$ with $BbtSbH_2$, which was prepared by the reaction of $BbtSbBr_2$ with $LiAlH_4$, in the presence of 1,8-diazabicyclo[5.4.0]undec-7-ene (DBU) in THF at -95 ºC afforded stibabismuthene **1** as red-purple crystals quantitatively. Stibabismuthene **1** showed satisfactory spectral data, as discussed below.

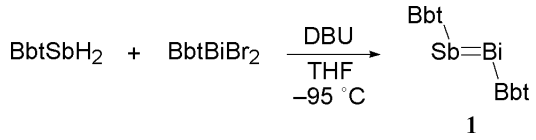

1

In the Raman spectrum (in the solid state) of **1**, a strong line attributable to the Sb-Bi stretching was observed at 169 cm^{-1}. This frequency lies between the value of the Sb-Sb stretching vibration in TbtSb=SbTbt (207 cm^{-1})[2] and that of the Bi-Bi stretching vibration in TbtBi=BiTbt (135 cm^{-1}),[3] and is higher than the Sb-Sb and Bi-Bi stretching frequencies for Ph_2E-EPh_2 (E=Sb, Bi). The UV/vis spectrum of **1** in hexane shows two absorption maxima at 709 nm (ε 200) and 516 nm (ε 7500), which are most likely assignable to the forbidden n→π* and the allowed π→π* transitions of the Sb=Bi chromophore, respectively. These results are consistent with the characteristic red-shifts in the electronic spectra of previously reported heavier congeners of azo compounds, and the λ_{max} value for π→π* transition of **1** is in the middle between that of BbtSb=SbBbt (**2**) [λ_{max} 490 nm (ε 6000)] and that of BbtBi=BiBbt (**3**) [λ_{max} 537 nm (ε 6000)]. These spectral data suggest that **1** features a double bond between antimony and bismuth even in solution as well as in the solid state. The reason of the superfluous red-shifts for the n→π* transition of **1**, which is 39 nm longer than that of **3** [λ_{max} 670 nm (sh, ε 20)], is not clear at present.

The molecular structure of stibabismuthene **1** was also supported by the X-ray crystallographic analysis, but the definite structural parameters for **1** have not been obtained yet due to the inevitable disorder of the antimony and bismuth atoms, which cannot be solved by the data collection with a number of different single crystals of **1** even at low temperature (-180 ºC).

Stibabismuthene **1** is stable at ambient temperature in hydrocarbon solvents in the absence of air and light. When a solution of **1** in benzene-d_6 was heated at 70 ºC, **2** and **3** were formed very slowly as judged by ^{1}H NMR spectroscopy. Heating the solution of **1** at 80 ºC for 20 days led to the formation of a mixture of **1**, **2** and **3** with the ratio of 1:1.4:1.1, respectively. On the other hand, when a solution of **1** in benzene-d_6 was irradiated with a medium pressure mercury lamp (100 W) in a sealed Pyrex NMR tube at room temperature, the disproportionation reaction was completed in 4 h to give a 1:1 mixture of **2** and **3**. The results of the thermal and photochemical disproportionation reactions of **1** into the homonuclear double-bond species **2** and **3** can be regarded as a chemical evidence for the formation of stibabismuthene **1**.

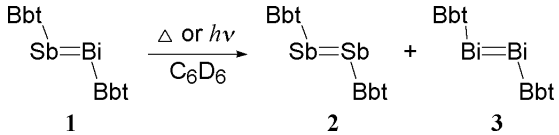

1 **2** **3**

Taking the previous reports on the reactivities of diphosphenes[7] into consideration, two different pathways can be postulated for the disproportionation reactions of stibabismuthene **1**. The first one is the dimerization of **1** by heating or irradiation followed by the decomposition of the resulting four-membered dimer **4** into the homonuclear double-bond species **2** and **3** (path **A**), while the other one is based on the dissociation of **1** giving the corresponding monovalent species, *i. e.*, stibinidene **5** and bismuthinidene **6**, both of which might undergo ready dimerization leading to the formation of **2** and **3**, respectively (path **B**).

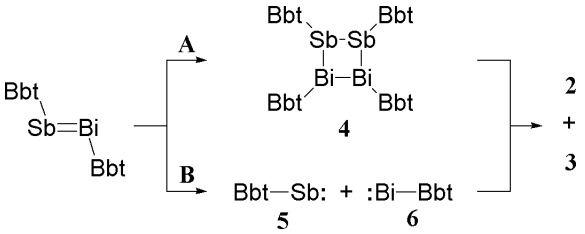

Although we have examined the thermolysis and photolysis of **1** in the presence of 2,3-dimethyl-1,3-butadiene in expectation of trapping the intermediary monovalent species **5** and **6**, no [4+1] cycloadducts of **5** and **6** but only distibene **2** and dibismuthene **3** were obtained in high yields. Since we have already found that the stibinidene **5** generated by thermal cycloreversion of the corresponding overcrowded stibolene derivative readily undergoes [4+1] cycloaddition with 2,3-dimethyl-1,3-butadiene to give the stable stibinidene adduct,[6] the disproportionation reactions of stibabismuthene are not rationalized by the mechanism via stibinidene and bismuthinidene intermediates but most likely interpreted in terms of the association-dissociation mechanism via the head-to-head dimerization of **1**.

In summary, we have succeeded in the synthesis of the first stable stibabismuthene **1** by taking advantage of kinetic stabilization afforded by a new and effective steric protection group, Bbt. Further investigations on the physical and chemical properties of stibabismuthene and synthesis of other variations of heteronuclear doubly bonded systems between heavier main group elements are currently in progress.

References

1. For a recent review see: P. P. Power, *Chem. Rev.*, 1999, **99**, 3463.
2. N. Tokitoh, Y. Arai, T. Sasamori, R. Okazaki, S. Nagase, H. Uekusa and Y. Ohashi, *J. Am. Chem. Soc.*, 1998, **120**, 433.
3. N. Tokitoh, Y. Arai, R. Okazaki and S. Nagase, *Science*, 1997, **277**, 78.
4. B. Twamley, C. D. Sofield, M. M. Olmstead and P. P. Power, *J. Am. Chem. Soc.*, 1999, **121**, 3357.
5. B. Twamley and P. P. Power, *Chem. Commun.*, 1998, 1979.
6. N. Tokitoh, T. Sasamori and R. Okazaki, *Chem. Lett.*, 1998, 725 and references cited therein.
7. M. Yoshifuji, T. Sato and N. Inamoto, *Bull. Chem. Soc. Jpn.*, 1989, **62**, 2394.

Artificial Zinc Finger Peptide Containing a Novel His_4 Domain

Yuichiro Hori, Kazuo Suzuki, Yasushi Okuno, Makoto Nagaoka, Shiroh Futaki and Yukio Sugiura

Zinc finger constitutes one of the most common DNA binding motifs. Although zinc finger proteins consisting of Cys_2His_2, Cys_3His, Cys_4, and Cys_6 domains are known in nature, a novel His_4 zinc finger protein has never been observed. Herein, we have created the first artificial His_4-type zinc finger protein (H_4Sp1) engineered by Cys to His mutations of the Cys_2His_2-type zinc finger transcription factor Sp1. The CD features of the single finger H_4Sp1f2 and three-finger H_4Sp1 clearly demonstrate the folding of the mutant His_4 peptides by complexation with Zn(II). The NMR study of Zn(II)-H_4Sp1f2 reveals that some distortions of the helical region occur due to Zn(II) coordination. The gel mobility shift assay and DNase I footprinting analysis strongly show the binding of Zn(II)-H_4Sp1 to the GC-box site of duplex DNA. The methylation interference pattern of Zn(II)-H_4Sp1 binding significantly resembles that of the corresponding C_2H_2Sp1 binding. The present artificial peptide H_4Sp1 is the first example of a zinc finger containing the His_4 domain. Of special interest is the fact that the zinc finger domains of H_4Sp1 are folded (although not identical to the native structure) and bind DNA similar to wild type C_2H_2Sp1.

Key words: Zinc finger/ Sp1/ Designed metallofinger/ DNA binding

Metalloproteins play important roles in gene regulation, and some metal ions also participate in the transcriptional stage by protein-mediated metallation. In particular, zinc ion is essential as a structural factor for zinc finger proteins, which constitute one of the most common DNA binding motifs. Zinc finger proteins acquire DNA binding ability by Zn(II)-complexation. In nature, Cys_2His_2-, Cys_3His-, Cys_4-, and Cys_6-type zinc fingers exist. Among them, the Cys_2His_2-type zinc finger motif especially possesses the following fascinating characteristics; (1) a compact ββα fold is acquired by Zn(II)-coordination to bind the asymmetric DNA sequence, (2) one finger recognizes 3 to 4 base pairs by the side chains of amino acids located on the recognition helix, and (3) extended recognition can be attained by tandem repeating. The mini ββα fold of the Cys_2His_2-type zinc finger motif is an attractive framework for designing a novel metallofinger motif. At the present stage, no newly designed metallofingers that have evident DNA recognition ability are known. In addition, zinc finger proteins containing the His_4 domain have never been found or engineered. Herein, we have created the first novel His_4-type zinc finger protein by Cys to His mutations of a Cys_2His_2-type zinc finger in transcription factor Sp1.

In order to clarify the structural alteration of the zinc finger domain by Cys to His mutations, the H_4Sp1f2-Zn(II)

BIOORGANIC CHEMISTRY — Bioactive Chemistry —

Scope of research

The major goal of our laboratory is to elucidate the molecular basis of the activity of various bioactive substances by biochemical, physicochemical, and synthetic approaches. These include studies on the mechanism of sequence-specific DNA cleavage by antitumor or carcinogenic molecules, studies on the DNA recognition of zinc-finger proteins, and model studies on the action of ion channels. In addition, artificial designed peptides have also been developed as useful tools in molecular biology and potentially in human medicine.

Prof
SUGIURA,Yukio
(D Pharm Sci)

Assoc Prof
FUTAKI, Shiroh
(D Pharm Sci)

Instr
NAGAOKA, Makoto
(D Pharm Sci)

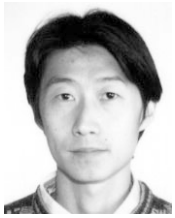

Assoc Instr
OKUNO, Yasushi
(D Pharm Sci)

Guest Research Associate
ZHANG, Youjun (D Sc)
Students
ARAKI, Michihiro (DC)
IMANISHI, Miki (DC)
MATSUSHITA, Keizo (DC)
SUZUKI, Tomoki (DC)
NOMURA, Akiko (DC)
UNO, Yumiko (MC)
OHASHI, Wakana (MC)
TAKADA, Naoko (MC)
HORI, Yuichiro (MC)
KIWADA, Tatsuto (MC)
DOI, Yoshihide (MC)
NAKASE, Ikuhiko (MC)
NOMURA, Wataru (MC)
SHIRAISHI, Yasuhisa (UG)
NIWA, Miki (UG)
MIYAGI, Shinichi (UG)

complex was investigated using two-dimensional NMR techniques. In contrast to C_2H_2Sp1f2, a 3D structural model of H_4Sp1f2 showed the twisting of an extended strand in the Pro2-Trp7 region and helical unwinding around Asp18-Gln21, as indicated by the disappearance of the $C_\alpha H_i$-NH_{i+3} NOEs between them. The twisting detected in the Pro2-Trp7 region probably occurs in order to accommodate a tetrahedral binding geometry enforced by zinc coordination constraints.

To examine whether the folding of H_4Sp1 is Zn(II)-dependent as well as that of H_4Sp1f2, CD studies were carried out. The mutant protein H_4Sp1 was constructed from C_2H_2Sp1 by Cys to His mutations of all three of the zinc finger domains. The CD spectrum of H_4Sp1 in the Zn(II)-free buffer was characteristic of the random coil. In the presence of Zn(II), the negative CD signal bands near 203 nm and 222 nm clearly increased, demonstrating the folding of H_4Sp1 by Zn(II)-complexation. The CD feature of Zn(II)-H_4Sp1 was different from that (207 and 226nm) of Zn(II)-C_2H_2Sp1 to some degree, suggesting that the zinc finger domain of H_4Sp1 did not form the structure identical to that of the wild type C_2H_2Sp1.

The results of the gel mobility shift assays clearly showed that Zn(II)-H_4Sp1 was bound to the DNA fragment (41 bp) containing an Sp1 recognition site GC box (5'-GGGGCGGGGCC-3'). From the evidence for the monomeric binding of the C_2H_2-type zinc finger to the single binding site, the binding mode of Zn(II)-H_4Sp1 is also monomeric because the mobility of the shifted band was the same as that of Zn(II)-C_2H_2Sp1. However, the DNA binding affinity of H_4Sp1 for the GC box was lower than that of C_2H_2Sp1. Furthermore, the Zn(II)-dependent DNA binding ability of H_4Sp1 was shown by the decrease in the DNA binding by EDTA. From the result of the DNase I footprinting analysis of Zn(II)-H_4Sp1 for a 148-bp DNA fragment containing the GC box, H_4Sp1 almost protected the residues of the GC box at 2.4 μM from DNase I cleavage in the presence of Zn(II). These results strongly indicate that the H_4Sp1 still retained the DNA binding ability in spite of the Cys to His mutation.

Previous studies have demonstrated that C_2H_2Sp1 can bind DNA by interacting with Co(II), Cd(II), and Ni(II) as well as Zn(II). To clarify whether the present H_4Sp1 gains the DNA binding ability by various metal complexations, H_4Sp1 was reconstructed with Zn(II), Ni(II), Cu(II), Co(II), or Cd(II) from insoluble fractions during the purification step, and a gel mobility shift assay was conducted. While Zn(II)-reconstituted H_4Sp1 was really bound to a GC-box fragment, under this experimental condition, the DNA binding activity was not detected in the case of Ni(II)-, Cu(II)-, Co(II)-, and Cd(II)-reconstituted H_4Sp1. From the CD studies of the H_4Sp1f2, only the Zn(II) binding to its His_4 domain highly induced an ordered conformation with the secondary structure. Therefore, these results indicate that effective folding by Zn(II) binding is essential for the DNA binding ability of H_4Sp1.

When Zn(II)-H_4Sp1 was bound to the GC-box fragment (41 bp), its methylation interference pattern was compared with that of Zn(II)-C_2H_2Sp1. In the case of H_4Sp1, strong base contacts with G(2), G(3), G(4), and G(6) in the guanine-rich strand (G-strand) and G(5') in the cytosine-rich strand (C-strand) were detected and also weak contacts with G(1) and G(7) in the G-strand and G(11') in the C-strand were observed. The interference feature remarkably resembled that of the wild type C_2H_2Sp1, indicating similar DNA binding modes between H_4Sp1 and C_2H_2Sp1.

The Cys to His conversion generates a larger metal coordination sphere because the size of the His residue is larger than that of the Cys residue as opposed to the case. Although the Cys to His mutation results in a decreased DNA binding affinity, the present peptide H_4Sp1 maintains the DNA binding ability. In spite of the structural alteration or distortion of the zinc finger domain as clearly indicated by the CD and NMR evidence of H_4Sp1f2, it is of special interest that specific interactions between the recognition helix of the finger 2 and its subsite, 5'-GCG-3', are retained. In addition, fingers 1 and 3 of H_4Sp1 also preserve the DNA recognition ability of the wild type C_2H_2Sp1. Several reasons are considered for the fact that H_4Sp1 and C_2H_2Sp1 show similar DNA recognition, despite the somewhat different helical conformation between their zinc finger domains. First, the DNA binding to Zn(II)-H_4Sp1 may cause an additional structural change and result in a specific DNA recognition analogous to Zn(II)-C_2H_2Sp1. Indeed, it is known that the specific DNA binding induces a structural alteration in the basic region of GCN4. Second, Zn(II)-H_4Sp1 may recognize DNA bases in a different manner from Zn(II)-C_2H_2Sp1. Namely, the mutant peptide H_4Sp1 compensates for specific contacts with particular bases by a directional change in the side chain that is essential for DNA recognition. As a result, the recognition helix of Zn(II)-H_4Sp1 may be located in a different orientation to DNA from that of Zn(II)-C_2H_2Sp1.

In conclusion, this paper describes the preparation, structure, and DNA binding properties of an engineered His_4 mutant of the zinc finger protein Sp1. We present the NMR structure for a single mutated zinc finger (H_4Sp1f2) from Sp1 and the DNA binding data for a three domain mutant (H_4Sp1). The CD characteristics of H_4Sp1f2 and H_4Sp1 are also compared with those of C_2H_2Sp1f2 and C_2H_2Sp1. Interestingly, the His_4 domain is folded and recognizes the GC-box DNA. The development of such a novel peptide may also lead to a new zinc finger type or other metal finger domain. Additionally, the present results suggest that a His_4-type zinc finger protein may also exist in nature.

α-Synuclein and Neurodegeneration

Seigo Tanaka, Masanori Takehashi, Naomi Matoh and Kunihiro Ueda

α-Synuclein is implicated in pathogenesis of various neurodegenerative diseases, but the molecular mechanisms of its action might be different. In Alzheimer's disease (AD), NAC (non-Aβ component of AD amyloid) is produced from α-synuclein, and then interacts with Aβ protein to form amyloid in senile plaques. In Parkinson's disease (PD) and Dementia with Lewy bodies (DLB), a full-length or partially truncated form of α-synuclein is a constituent of LB, that is an inclusion found in degenerating neurons. Recently, oligodendroglial cytoplasmic inclusion in multiple system atrophy was reported to be immunoreactive with anti-α-synuclein antibody. Therefore, α-synuclein is suggested to be a common mediator of neurodegenerative diseases.

Keywords : α-Synuclein / Alzheimer's disease / Parkinson's disease / Amyloid / Lewy body

I. Introduction

Amyloid deposition in the senile plaque cores is one of the major neuropathological features in the AD brain. NAC was originally identified in senile plaques as a protein other than Aβ. NAC consisting of at least 35 amino acids is supposed to be produced from a precursor protein (α-synuclein). NAC is located in the most hydrophobic portion of the α-synuclein molecule. The α-synuclein has seven incompletely repeated KTKEGV motifs and no signal peptide sequence nor N-linked glycosylation sites.

Recently, two types of mutation, Ala30Pro and Ala53Thr, in the α-synuclein gene were found in some families of PD. Furthermore, α-synuclein was found to accumulate in Lewy body (LB) that is a hallmark of idiopathic PD. These findings suggest a possible role of α-synuclein in pathogenesis of both PD and AD.

II. Physiological functions of α-synuclein

α-Synuclein has been found in association with synaptic vesicles in the rat brain by immunoelectron microscopy. In order to clarify its physiological functions, we transiently transfected α-synuclein cDNA into PC12 and COS7 cells. We found the α-synuclein to be distributed in the cytosol and neurites of differentiated PC12 cells. A confocal laser microscopic study showed colocalization of α-synuclein with a synaptic marker, synaptophysin, indicating possible role(s) of α-synuclein in synaptic function.

III. Amyloidogenicity of NAC

NAC and Aβ protein are reportedly colocalized in the core of senile plaques (Figure 1). The ratio of NAC to Aβ in senile plaques has been estimated to be less than 1:10. Structural analysis has shown that NAC has a strong ten-

BIOORGANIC CHEMISTRY — Molecular Clinical Chemistry —

Scope of research

This laboratory was founded in 1994 with the aim of linking (bio)chemical research and clinical medicine. Thus, the scope of our research encompasses the structure, function and regulation of various biomolecules, the pathophysiological significance of bioreactions in relation to human diseases, and the application of molecular techniques to clinical diagnosis and therapy. Our current interest is focused on poly(ADP-ribosyl)ation, nuclear localization of proteins in association with apoptosis, and the molecular etiology of Alzheimer's disease and other neurodegenerative disorders.

Prof
UEDA, Kunihiro
(D Med Sc)

Assoc Prof
TANAKA, Seigo
(D Med Sci)

Instr
ADACHI, Yoshifumi
(D Med Sci)

Guest Scholar
BANASIK, Marek (D Med Sci)
Guest Res Assoc
STROSZNAJDER, Robert (Ph D)
Students
CHU, Dong (DC)
TAKEHASHI, Masanori (DC)
BAHK, Songchul (DC)
CHEN, Liping (DC)
TAKANO, Emiko (RF)
MATOH, Naomi (RS)
IIDA, Shinya (RS)
HAYASHI, Naoko (RS)
KAWAKAMI, Tomomi (UG)
NAKANO, Mariko (UG)

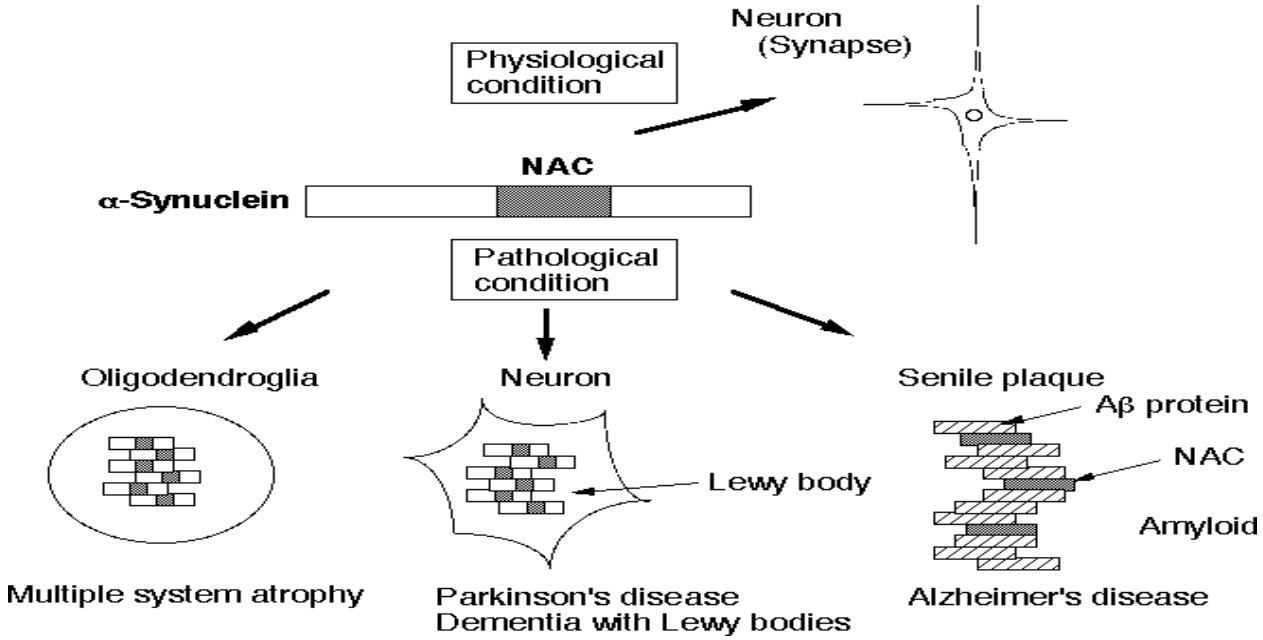

Figure 1. α-Synuclein and neurodegenerative diseases.

dency to form a β-sheet structure. We confirmed that fibrils are easily formed from synthetic NAC peptides, and stained with Congo red to give green images suggestive of amyloid under polarized light. We then analyzed kinetics of amyloid fibril formation by monitering thioflavine T fluorescence. Formation of $A\beta_{1\text{-}40}$ fibrils was facilitated, with no nucleation phase, by the addition of NAC fibrils preformed, suggeting that NAC fibrils could serve as a nucleus for the amyloid formation. In order to analyze the process of NAC production from α-synuclein, we labeled α-synuclein metabolically with [^{35}S]methionine in transfected COS7 cells. The half-life of ^{35}S-labeled α-synuclein in COS7 cells was longer than 24 hours. We could not detect any proteolytic products in the cell lysate nor in the culture medium. Although exact steps of α-synuclein processing remains to be clarified, it is possible that α-synuclein is released from damaged neurites and extracellularly proteolysed to produce NAC.

IV. Neurotoxicity of NAC amyloid

We found NAC to induce mitochondrial dysfunction in neuronally differentiated PC12 cells at 100 nM, which is comparable to the cytotoxic effect of $A\beta_{25\text{-}35}$. This finding was confirmed by nuclear stainings with Hoechst 33258 and propidium iodide (PI); the former staining all cells and the latter, dead cells. Some nuclei were condensed and others were swollen, indicating that the cytotoxicity was a mixture of apoptotic and necrotic effects. In order to clarify the molecular mechanism by which NAC exerted the toxic effects, we screened several chemicals for protective effects against NAC toxicity. We found that two antioxidants, propylgallate and N-*t*-butylphenylnitrone, effectively reduce the NAC cytotoxicity, suggesting a role of reactive oxygen species in the toxic event.

V. α-Synuclein and Lewy body

DLB is considered to be the second commonest form of degenerative dementia in old ages after AD. The antibodies against N- and C-terminal portions of α-synuclein stained positively Lewy bodies (LBs), indicating that full-length α-synuclein is a constituent of LB (see Figure 1). Full-length as well as C-terminal truncated forms of α-synuclein have been biochemically demonstrated in LBs. Recombinant α-synuclein was shown to form amyloid-like fibrils *in vitro*, and the fibril formation to be accelerated by mutations found in familial PD (Ala30Pro and Ala53Thr). Cytochrome c, a component of the mitochondrial electron transport chain, was suggested to contribute to the oxidative stress-induced aggregation of α-synuclein. Since cytochrome c is a mediator of apoptotic signals, the formation of LB might be facilitated by cytochrome c released in apoptotic cells in neurodegenerative diseases.

References

1. Tanaka, S., Takehashi, M., Matoh, N., and Ueda, K. In *"Neuroscientific Basis of Dementia"* (C. Tanaka, P. L. McGeer, and Y. Ihara, eds.), Birkhäuser Verlag, Basel (2000), pp. 137-141

Identification of Catalytic Nucleophile of *Escherichia coli* γ-Glutamyltranspeptidase by Mechanism-Based Affinity Label

Jun Hiratake, Makoto Inoue, Hideyuki Suzuki, Hidehiko Kumagai and Kanzo Sakata

γ-Glutamyltranspeptidase (EC 2.3.2.2) is the enzyme involved in glutathione metabolism and catalyzes the hydrolysis and transpeptidation of γ-glutamyl compounds such as glutathione and its derivatives. The reaction is thought to proceed via a γ-glutamyl-enzyme intermediate where a hitherto unknown catalytic nucleophile is γ-glutamylated. Neither affinity labeling nor site-directed mutagenesis of conserved amino acids has succeeded so far in identifying the catalytic nucleophile. We describe here the identification of the catalytic nucleophile of *Escherichia coli* γ-glutamyltranspeptidase by a novel mechanism-based affinity labeling agent, 2-amino-4-(fluorophosphono)butanoic acid (**1**), a γ-phosphonic acid monofluoride derivative of glutamic acid. Compound **1** rapidly inactivated the enzyme in a time-dependent manner (k_{on} = 4.83 × 10^4 $M^{-1}sec^{-1}$). The inactivation was competitive with respect to the substrate. The inactivated enzyme did not regain its activity after prolonged dialysis, suggesting that **1** served as an active-site-directed affinity label by phosphonylating the putative catalytic nucleophile. Ion-spray mass spectrometric analyses revealed that one molecule of **1** phosphonylated the one molecule of small subunit. LC/MS experiments of the proteolytic digests of the phosphonylated small subunit identified the N-terminal peptide Thr391-Lys399 as the phosphonylation site. Subsequent MS/MS experiments of this peptide revealed that the phosphonylated residue was Thr-391, the N-terminal residue of the small subunit. We conclude that the N-terminal Thr-391 is the catalytic nucleophile of *E. coli* γ-glutamyltranspeptidase. This result strongly suggests that γ-glutamyltranspeptidase is a new member of N-terminal nucleophile hydrolase family.

Keywords: *E. coli* γ-Glutamyltranspeptidase/ Glutathione metabolism/ Mechanism-based affinity labeling/ Phosphonofluoridate/ Catalytic nucleophile/ Phosphonylation/ Ion-spray MS/ N-Terminal nucleophile hydrolase family/

γ-Glutamyltranspeptidase (γ-GGT, EC 2.3.2.2) catalyzes the cleavage of γ-glutamyl bond of glutathione and related γ-glutamyl compounds to transfer the γ-glutamyl group either to water or to amino acids and peptides to complete hydrolysis or transpeptidation, respectively. This enzyme is widely distributed among the living organisms from bacteria to mammals and plays important roles in glutathione metabolism. Despite the physiological importance of this enzyme, details of the catalytic mechanism still remain unclear. The reaction catalyzed by γ-GGT is thought to proceed via a γ-glutamyl-enzyme intermediate followed by nucleophilic substitution by water, amino acids, or peptides (Scheme 1). Although a hydroxy group of a Ser or Thr is proposed as the γ-glutamylation site, the catalytic nucleophile has remained to be identified either by chemical modification or by site-directed mutagenesis. Here we designed 2-amino-4-(fluorophosphono)butanoic acid **1**, a γ-phosphonic acid monofluoride derivative of glutamic acid, as a novel affinity labeling agent to trap the catalytic nucleophile of *E. coli* γ-GGT. Compound **1** is expected to bind covalently to the catalytic nucleophile in a mechanism-based manner, forming a transition-state like adduct in the enzyme active site (Scheme 1).

Compound **1**, sysnthesized from 2-amino-4-phosphonobutanoic acid in four steps, was relatively stable under acidic conditions (pH 5.5, $t_{1/2}$ = 21.6 h) at which the enzyme exhibited the maximal activity.

MOLECULAR BIOFUNCTION — Chemistry of Molecular Biocatalysts —

Scope of research

Our research aims are to elucidate the chemistry-function relationships of various biocatalysts (enzymes) in combination with organic chemistry, molecular biology and X-ray crystallography. The biochemical and physiological roles of enzymes and hormone receptors are also studied from the chemical point of view. Main subjects are (1) Chemical, biochemical and molecular biological studies on β-primeverosidase, a major tea aroma-producing β-glycosidase concerned with tea-manufacturing process, and on its original physiological roles in tea plants, (2) Design and synthesis of transition-state analogues and mechanism-based inhibitors of ATP-dependent ligases and glycosidases to probe the enzyme mechanisms, (3) Development of a new method for functional cloning of plant hormone receptors and biochemical studies on plant hormone biosynthesis, (4) X-Ray crystallography of firefly luciferase and Maize pyruvate phosphate dikinase, (5) Development of a novel lipase with altered reaction specificity by directed evolution.

Prof
SAKATA, Kanzo
(D Agr)

Assoc Prof
HIRATAKE, Jun
(D Agr)

Instr
MIZUTANI, Masaharu
(D Agr)

Instr
SHIMIZU, Bun-ichi
(D Agr)

INOUE, Makoto (DC), FUJII, Ryota (DC), MA, Seung-Jin (DC), AHN, Young-Ock (DC), EMA, Jun-ichi (MC), NAKANISHI, Tsugumi (MC), SATO, Tadashi (MC), INOUE, Kazuko (MC), INOUE, Toshiki (MC), KATO, Masahiro (MC), SAITO, Shigeki (MC), UTSUNOMIYA, Yuji (MC), OHNISHI, Toshiyuki (RS), ASADA, Junko (UG, RS), UEMURA, Miyuki (secretary)

Scheme 1

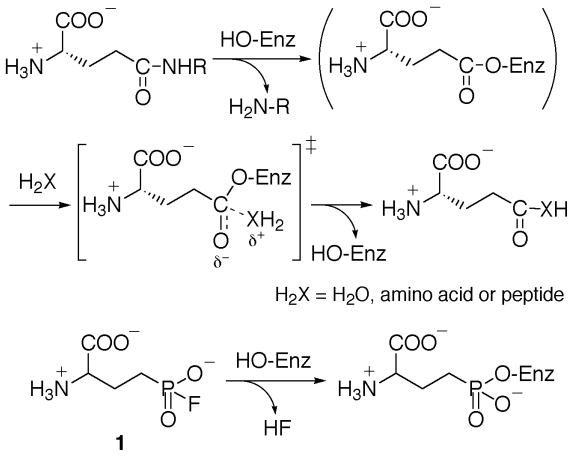

1

The enzyme was rapidly and competitively inhibited by **1** in a time-dependent manner (Figure 1). No regain of enzyme activity was observed after prolonged dialysis (10 days), suggesting that the enzyme active site was covalently modified with **1.**

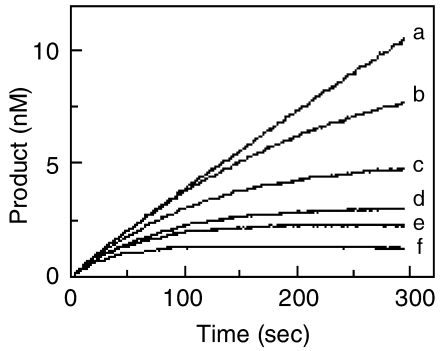

Figure 1. Time-dependent inhibition of *E. coli* γ-glutamyltranspeptidase by **1.** The enzymatic reaction was carried out in the presence of the following concentrations of **1**: (a) 0, (b) 0.17, (c) 0.33, (d) 0.5, (e) 0.67 and (f) 1.0 μM.

The inactivated enzyme was analyzed by ion-spray mass spectrometry. The *E. coli* γ-GGT is composed of two subunits with a molecular mass of 20,010 and 39,196 Da for the small and large subunit, respectively. Mass analyses revealed that the molecular mass of the small subunit increased from 20,014 Da (unmodified enzyme) to 20,178 Da (modified enzyme) (Figure 2). The observed mass increase of 164 Da corresponded well to the expected mass increase of 165 Da caused by the phosphonylation by **1**, indicating that one molecule of **1** was attached covalently to the small subunit.

The small subunit of each unmodified and modified enzyme was digested by lysyl endopeptidase C, and the resulting proteolytic digests were analyzed by LC/MS to find that the N-terminal peptide of the small subunit (Thr391-Lys399, 1049.7 Da) was phosphonylated to increase its molecular mass by 165 Da.

Finally, the phosphonylated residue in the N-terminal peptide was identified by MS/MS analysis. The $(M + 3H)^{3+}$ ions at *m/z* 350.7 (unmodified peptide) and 405.9 (phosphonylated peptide) were subjected to collision-induced decay (CID). The resulting CID spectrum and the amino acid sequence of the N-terminal peptide Thr391-Lys399 are depicted in Figure 3. The CID spectrum of the $(M + 3H)^{3+}$ precursor ion at *m/z* 405.8

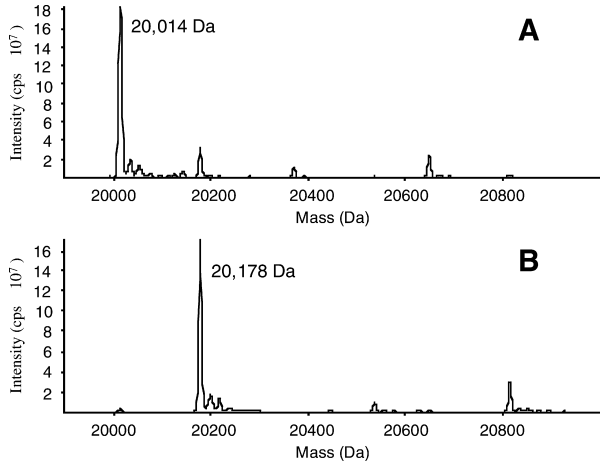

Figure 2. Reconstructed mass spectra of the small subunit. (A) Small subunit from the unmodified enzyme. (B) Small subunit from the modified enzyme.

(phosphonylated peptide) was the same as that of the unmodified peptide, except for the precursor ion (Figure 3C). Thus, the mass increase of 165 Da was observed only in the precursor ion. This result has clearly shown that compound **1** phosphonylated the N-terminal residue of the small subunit, that is, Thr-391. In addition, two fragment ions (*m/z* 184.1 and 516.4) served as a good indication of β-elimination of 2-amino-4-phosphonobutanoic acid (m/z 183) from the phosphonylated N-terminal peptide Thr 391-Lys399.

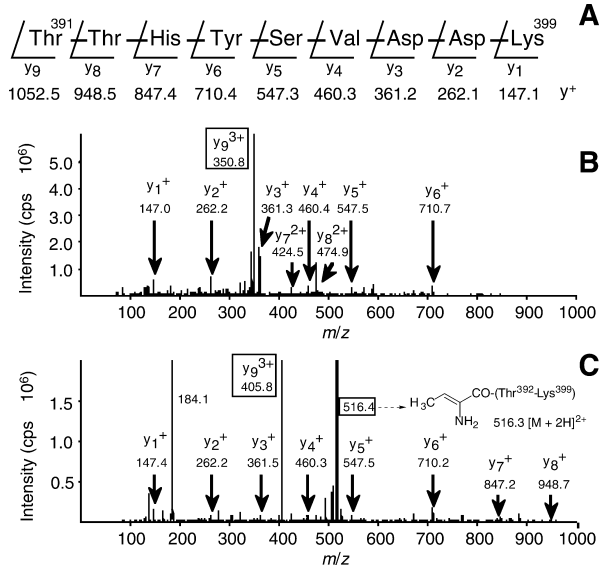

Figure 3. MS/MS analysis of the peptide Thr391-Lys399. (A) Predicted product ions of type y. (B) CID spectrum of the *m/z* 350.7 precursor ions (Thr391-Lys399) from the unmodified enzyme. (C) CID spectrum of the *m/z* 405.9 precursor ions (Thr391-Lys399) from the modified enzyme.

Thus, the N-terminal Thr 391 was identified as the catalytic nucleophile of *E. coli* γ-GGT. This result, along with sequence similarity and a chracteristic post-translational processing of this enzyme, strongly suggested that *E. coli* γ-GGT is a member of N-terminal nucleophile hydrolases, a recently recognized new hydrolase family.

Referencce: M. Inoue, J. Hiratake, H. Suzuki, H. Kumagai, K. Sakata *Biochemistry* **2000**, *39*, 7764-7771.

Novel Mechanism of Enzymatic Hydrolysis Involving Cyanoalanine Intermediate Revealed by Mass Spectrometric Monitoring of an Enzyme Reaction

Nobuyoshi Esaki, Tatsuo Kurihara, Yong-Fu Li and Susumu Ichiyama

L-2-Haloacid dehalogenase from *Pseudomonas* sp. YL catalyzes the hydrolytic dehalogenation of L-2-haloalkanoic acids to produce the corresponding D-2-hydroxyalkanoic acids. Asp10 of the enzyme functions as a catalytic nucleophile: the residue attacks the α-carbon of the substrate to form an ester intermediate, which is subsequently hydrolyzed to release the product. Surprisingly, replacement of Asp10 by Asn did not completely inactivate the enzyme. We found that Asn10 of the D10N mutant enzyme is spontaneously deamidated to yield Asp, though slowly, causing increasing activity of the D10N preparation. We also revealed by mass spectrometric monitoring of the enzyme reaction that the D10N mutant enzyme itself catalyzes the hydrolytic dehalogenation: Asn10 attacks the substrate to form an imidate, and a proton and D-lactic acid are eliminated to produce a nitrile (a β-cyanoalanine residue), followed by hydrolysis to reproduce Asn10. This is the first report of the function of Asn to catalyze nucleophilic substitution through its dynamic structural change that includes conversion to a β-cyanoalanine residue as an intermediate structure.

Keywords: 2-Haloacid dehalogenase/ Ion-spray mass spectrometry/ Cyanoalanine residue

L-2-Haloacid dehalogenase from *Pseudomonas* sp. YL (L-DEX YL) catalyzes the hydrolytic dehalogenation of L-2-haloalkanoic acids, producing the corresponding D-2-hydroxyalkanoic acids. The enzyme is involved in biodegradation of xenobiotic compounds such as a herbicide, 2,2-dichloropropionic acid. The enzyme is also useful as an industrial biocatalyst for the synthesis of optically active hydroxyalkanoic acids. We have studied the reaction mechanism of L-DEX YL in detail, and revealed that the reaction proceeds as follows [1, 2]. Asp10 of the enzyme nucleophilically attacks the α-carbon of the substrate to release a halide ion and produce an ester intermediate, which is subsequently hydrolyzed to release a D-2-hydroxyalkanoic acid and regenerate Asp10. We performed mutagenesis studies on L-DEX YL, and surprisingly found that replacement of Asp10 by Asn did not completely inactivate the enzyme, whereas replacement by Ala, Gly, Ser, or Glu resulted in total inactivation [3].

MOLECULAR BIOFUNCTION — Molecular Microbial Science —

Scope of research

Structure and function of biocatalysts, in particular, pyridoxal enzymes and enzymes acting on xenobiotic compounds, are studied to elucidate the dynamic aspects of the fine mechanism for their catalysis in the light of recent advances in gene technology, protein engineering and crystallography. In addition, the metabolism and biofunction of sulfur, selenium, and some other trace elements are investigated. Development and application of new biomolecular functions of microorganisms are also studied to open the door to new fields of biotechnology. For example, molecular structures and functions of psychrophilic enzymes and their application are under investigation.

Prof
ESAKI, Nobuyoshi
(D Agr)

Assoc Prof
YOSHIMURA, Tohru
(D Agr)

Instr
KURIHARA, Tatsuo
(D Eng)

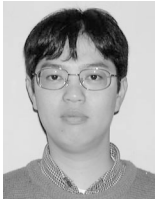

Instr
MIHARA, Hisaaki
(D Agr)

Assoc Instr (part-time): UO, Takuma
Technician: SEKI, Mio; UTSUNOMIYA, Machiko
Students: YOSHIMUNE Kazuaki (DC); KATO, Shin-ichiro (DC); NAKAYAMA Daisuke (DC); WEI, Yun-Lin (DC); YOW, Geok-Yong (DC); KENNEDY R. Alexander J. D. (MC) MORI, Kensuke (MC); NAKANO Michiko (MC); SAITO Megumi (MC); TAKAHATA, Hiroyuki (MC); HIZUKURI Yoshiyuki (MC); IGARASHI Motoki (MC); KURATA Atsushi (MC); OKUBO Fumi (MC); ASHIDA Hiroyuki (RF); KASHIWA Masami (RF); KAKUTANI Ryou (RS)

In the present study, we analyzed the mechanism of dehalogenation catalyzed by the L-DEX YL D10N preparation by ion-spray mass spectrometry [4].

We found that the activity of the D10N preparation increased in a time- and temperature-dependent manner. When determined immediately after purification of the enzyme, it showed about 1% activity of the wild-type enzyme activity, whereas it showed 26% activity of the wild-type enzyme activity when stored at room temperature for about a month. Amino acid sequencing of the enzyme preparation showing 26% activity revealed the occurrence of Asp at the position of Asn10. These results indicate that the side chain amide of Asn10 is slowly deamidated to produce carboxylate.

We next examined whether the D10N mutant enzyme itself is involved in the dehalogenation by ion-spray mass spectrometry. Although the D10N preparation is contaminated by the wild-type enzyme produced by the spontaneous deamidation of Asn10 as described above, the wild-type enzyme content in the fresh preparation is considered to be less than 1% of the total enzyme molecules judging from the enzyme activity of the preparation. Thus it is possible to monitor the structural change of D10N itself by mass spectrometry, because the small amount of the wild-type enzyme does not interfere with the mass spectra of D10N, which is present abundantly. We first confirmed that the control enzyme not incubated with the substrate showed a peak at 26,180 Da (M), which is virtually identical to the molecular mass (26,178 Da) predicted from the primary structure of the D10N enzyme, and then incubated the enzyme preparation with L-2-chloropropionate as a substrate to monitor the structural change of the enzyme. After 10 s of the incubation, the original peak at around 26,178 Da disappeared, and new peaks appeared at 26,253 Da (M+73) and 26,162 Da (M-18). Over a period from 10 s to 1 min, the relative abundance of the M+73 species decreased, and the M-18 species increased. From 20 s to 40 min, the enzyme occurred predominantly as the M-18 species. The original peak (M) reappeared and increased over a period of 30-60 min, and became predominant by 60 min.

We determined the N-terminal amino acid sequence of the M+73 species, and found that the Asn10 was modified. To analyze the modification at position 10 by mass spectrometry, we constructed D10N/L11K double mutant enzyme: lysyl-endopeptidase treatment of this enzyme produces a short peptide fragment containing Asn10, which is small enough for determination of accurate molecular mass. We confirmed that the mutation at position 11 did not alter the reactivity of the D10N enzyme as judged by structural change of the enzyme revealed by mass spectrometry. D10N/L11K incubated with L-2-chloropropionate was digested with lysyl endopeptidase, and the resultant peptide containing Asn10 was analyzed by tandem MS/MS. We found that the modification causing the 73-Da increase occurred at Asn10, and revealed that an imidate structure was produced as a reaction intermediate (Fig. 1): we found that the M+73 species was artificially produced by hydrolysis of the imidate (M+72) under a low-pH condition employed in the present experiment to terminate the enzyme reaction.

We next analyzed the structure of the M-18 species. The M-18 species derived from D10N/L11K was digested with lysyl endopeptidase, and the peptide containing Asn10 was analyzed by tandem MS/MS. We found that Asn10 was specifically modified in such a way as its molecular mass becomes 18-Da lower than the original value. The most probable structure formed at residue number 10 is a β-cyanoalanine residue as shown in Fig. 1.

To examine if the final step of the reaction is the reconversion of β-cyanoalanine residue into Asn as shown in Fig. 1, D10N/L11K was incubated in $H_2{}^{18}O$ in the presence of L-2-chloropropionate for 60 min. After the incubation, we analyzed the molecular mass of the peptide containing Asn10, and found that an ^{18}O atom was incorporated in Asn10. This result indicates that the nitrile undergoes the nucleophilic attack of a water molecule to produce the side chain amide of Asn10.

In colclusion, we revealed a unique structural change of L-DEX YL D10N that occurs through the mechanism shown in Fig. 1: Asn10 nucleophilically attacks the substrate to form the imidate, and a proton and D-lactic acid are eliminated to produce the nitrile. This is the first report showing that Asn functions as a catalytic nucleophile in enzymatic hydrolysis where β-cyanoalanine residue is produced as a reaction intermediate.

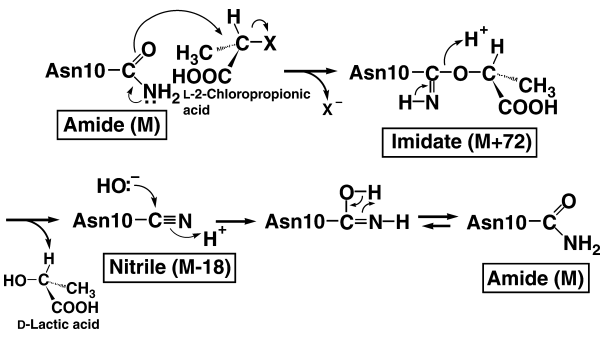

Figure 1. Structural change of D10N involving an imidate and a nitrile as reaction intermediates.

References

1. Liu, J.-Q., Kurihara, T., Miyagi, M., Tsunasawa, S., Nishihara, M., Esaki, N. and Soda, K. (1997) J. Biol. Chem. 272, 3363-3368

2. Li, Y.-F., Hata, Y., Fujii, T., Hisano, T., Nishihara, M., Kurihara, T. and Esaki, N. (1998) J. Biol. Chem. 273, 15035-15044

3. Kurihara, T., Liu, J.-Q., Nardi-Dei, V., Koshikawa, H., Esaki, N. and Soda, K. (1995) J. Biochem. 117, 1317-1322

4. Ichiyama, S., Kurihara, T., Li, Y.-F., Kogure, Y., Tsunasawa, S. and Esaki, N. (2000) J. Biol. Chem. 275, 40804-40809

Crystal Structure of a NifS Homologue CsdB from *Escherichia coli*

Tomomi Fujii and Yasuo Hata

Escherichia coli CsdB is a dimeric NifS-homologue belonging to the fold-type I family of PLP-dependent enzymes, and catalyzes the decomposition of L-selenocysteine into selenium and L-alanine with specificity higher than that for a substrate of cysteine. The structure of the enzyme has been determined at 2.8 Å resolution by an X-ray crystallographic method. The subunit of CsdB comprises a large domain, a small domain, and an N-terminal segment. A remarkable structural feature of CsdB is that an α-helix in the lobe extending from the small domain to the large domain in one subunit of the dimer interacts with a β-hairpin loop protruding from the large domain of the other subunit. Cys364, which is essential for the activity toward cysteine but not toward selenocysteine, is clearly seen on the loop of the extended lobe (Thr362–Arg375) although the corresponding loop (Ser321–Arg332) is disordered in the *Thermotoga maritima* NifS-like protein, which is closely related to the cysteine-specific NifS and whose crystal structure has recently been determined as the second example.

Key words: X-ray crystallography / CsdB / NifS-like protein / iron-sulfur cluster / PLP

CsdB, the *csdB* gene product from *Escherichia coli*, is a PLP-dependent protein, which decomposes L-selenocysteine, L-cysteine sulfinic acid and L-cysteine into selenium, sulfur dioxide and sulfur, respectively, and L-alanine [1]. This enzyme shares 23% sequence identity with the NifS protein, that catalyzes the decomposition of L-cysteine and functions in the nitrogen fixation system of *Azotobacter vinelandii* by supplying sulfur to stabilize or repair the iron-sulfur cluster of the nitrogenase component protein. In order to clarify structure-function relationships of a family of NifS-like proteins, three-dimensional structure of the *E. coli* CsdB has been determined by X-ray crystallographic analysis [2].

The crystals of CsdB were grown by a hanging drop vapor diffusion method using sodium acetate as a precipitant. Two heavy-atom derivatives were prepared by soaking the crystals into phenyl mercury acetate and potassium tetracyanoplatinate. Diffraction data were collected on an R-AXIS IIc imaging-plate detector system using CuKα radiation produced by a RU-300 generator. The structure of CsdB was solved by the multiple isomorphous replacement with anomalous scattering and density modification techniques. The polypeptide chain was traced based on the bones generated by truncating the map. The structure was refined at 2.8 Å resolution. The subunit structure of CsdB is composed of a polypeptide chain of Phe3–Gly406, one PLP, and one acetate.

The overall fold of the CsdB subunit (Figure 1) is similar to those of the fold-type I family of PLP-dependent enzymes, represented by an aspartic acid

MOLECULAR BIOLOGY AND INFORMATION — Biopolymer Structure —

Scope of research

Our research aims are to elucidate structure-function relationships of biological macromolecules, mainly proteins, by using physicochemical methods such as spectroscopic and X-ray diffraction methods. The following attempts have been mainly made in our laboratory for that purpose. (1) X-ray diffraction studies on protein structures in crystal and in solution are carried out by crystallographic and/or small-angle X-ray scattering techniques to elucidate structure-function relationships of proteins. (2) Molecular mechanism for myosin assembly is studied by proteolytic method, electron microscopy, and computer analysis of the amino acid sequence.

Assoc Prof
HATA,
Yasuo
(D Sc)

Instr
HIRAGI,
Yuzuru
(D Sc)

Instr
FUJII,
Tomomi
(D Sc)

Students:
KURIHARA, Eiji (DC)
HASEGAWA, Junya (MC)
Research Assistant:
AKUTAGAWA, Tohru

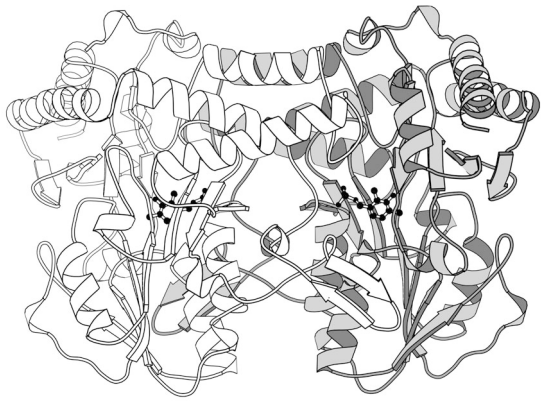

Figure 1. The dimeric molecule of CsdB viewed perpendicularly to the molecular two-fold axis. The figure, showing a pair of subunits shaded differently, was drawn with program MOLSCRIPT [5].

aminotransferase (AAT), especially to that of a phosphoserine aminotransferase (PSAT) which belongs to the class V of fold-type I enzymes. The subunit consists of three parts: the large domain of an α/β fold containing a seven-stranded β-sheet flanked by helices, the small domain containing a four-stranded β-sheet with three α-helices, and the N-terminal segment.

The circumstances of active site in CsdB, AAT, and PSAT are almost similar among one another. PLP has the C4' atom connected with the Nζ atom of Lys226, providing the Schiff base to form an internal aldimine. The O3' and N1 atoms of PLP hydrogenbond with the Nε2 atom of Gln203 and with Asp200, respectively. The most striking difference in the interactions between the protein and PLP lies in the stacking mode of the aromatic residue and the pyridine ring of PLP. In CsdB, the imidazole ring of His123 is stacked against the pyridine ring of PLP, whereas the indole ring of the Trp residue in AAT and PSAT. The expected binding mode of a substrate selenocysteine to the active site of CsdB was considered based on the crystal structures of complexes of AAT or PSAT with their substrate analogues. In the model of the CsdB complex, the α-carboxyl group of the substrate is recognized with Arg379 and Asn175. The selenium at the γ-position of the substrate is close to the side chain of Cys364.

CsdB has several structural features which are different from those of other families of enzymes. A β-hairpin loop (residues 256 – 267) protruding from one subunit of the dimer interacts with an α-helix in a lobe (residues 366 – 371) extending from the small domain to the large domain of the other subunit. These two portions of the β-hairpin loop and the lobe form one side of a limb of an active site in the enzyme. Cys364, which is essential for the activity toward L-cysteine but not toward L-selenocysteine [3], lies on the extended lobe which has an ordered conformation. This structure is not found in other 'fold-type I' PLP dependent enzymes.

The CsdB structure in Figure 2 shows the regions (A – D) markedly different in sequence between CsdB and NifS. The β-hairpin loop (region C) in CsdB is deleted in NifS. In contrast to this deletion, 10 residues are inserted in NifS between the residues corresponding to Met366

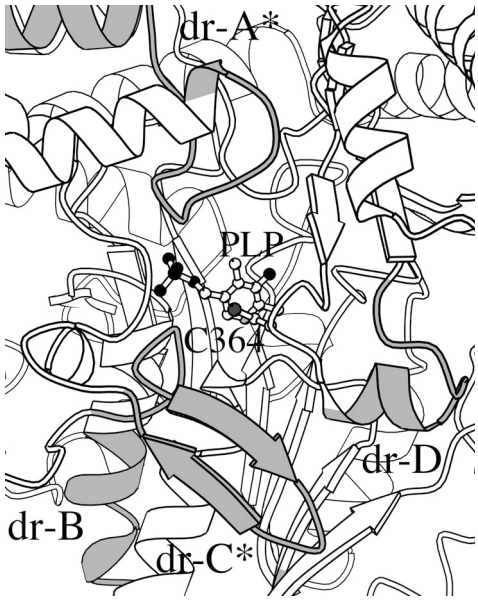

Figure 2. Schematic representation of CsdB showing differences in sequence between CsdB and NifS. These regions are shaded and labeled "dr-B" for residues 99 – 115 and "dr-D" for residues 366 – 376 in one subunit, and "dr-A*" for residues 34 – 60 and "dr-C*" for residues 251 – 268 from the other subunit. PLP and Cys364 are depicted as ball-and-stick models. Helices and β-strands are represented by spirals and arrows. The figure was drawn with program BOBSCRIPT [6].

and Pro367 on α-helix of the extended lobe in CsdB (region D). The region just follows the putative catalytic residue Cys364. Therefore, the extended lobe anchoring the catalytic cysteine residue seems to be much larger in NifS than in CsdB and to have a different structure as well as a different location of the catalytic cysteine residue. Recently, the crystal structure of *Thermotoga maritima* NifS-like protein (tmNifS), which is closely related to the cysteine-specific NifS, has been determined as the second example [4]. However, the loop of tmNifS corresponding to the extended lobe of CsdB is disordered. The extending lobe is the most remarkable structural feature common to the NifS homologues and probably a prerequisite for their function.

This project has been carried out in collaboration with the division of Molecular Biofunction – Molecular Microbial Science –, Institute for Chemical Research.

References

1. Mihara H, Maeda M, Fujii T, Kurihara T, Hata Y, and Esaki N, *J. Biol. Chem.*, **274**, 14768-14772 (1999).
2. Fujii T, Maeda M, Mihara H, Kurihara T, Esaki N, and Hata Y, *Biochemistry*, **39**, 1263-1273 (2000).
3. Mihara H, Kurihara T, Yoshimura T, and Esaki N, *J. Biochem.*, **127**, 559-567 (2000).
4. Kaiser JT, Clausen T, Bourenkow GP, Bartunik H-D, Steinbacher S, and Huber R, *J. Mol. Biol.*, **297**, 451-464 (2000).
5. Kraulis PJ, *J. Appl. Crystallogr.*, **24**, 946-950 (1997).
6. Esnouf RM, *J. Mol. Graphics Modell.*, **15**, 132-134 (1997).

Upstream Regions Required for Expression Control of the *Arabidopsis* floral homeotic gene *PISTILLATA*

Takashi Honma

PISTILLATA is a B-class floral organ identity gene required for the normal development of petals and stamens in *Arabidopsis thaliana*. Its expression is induced in the stage 3 flowers (early expression) and is maintained until anthesis (late expression). To explore in more detail the developmentally regulated gene expression of *PISTILLATA*, the author dissected its upstream DNA region followed by analyzing the promoter activity with transgenic plants carrying various mutations in meristem and organ identity genes. The results indicate that *LEAFY* and *UNUSUAL FLORAL ORGANS* induce *PISTILLATA* expression in a flower-independent manner through a distal promoter, and that *PISTILLATA* together with *APETALA3* maintain *PISTILLATA* expression in the later stages of flower development through a proximal promoter.

Keywords: *Arabidopsis thaliana*/ Flower development/ Homeotic gene/ Transcriptional control

The *Arabidopsis* flower consists of the four type organs: sepals, petals, stamens and carpels. These organs develop by proliferation of cells in meristem. The developmental fate of meristem is controlled by the floral homeotic genes. When the activity of a homeotic gene is lost, conversions of one organ type to other occur. Their functional difference allow us to classify these genes into (i) the meristem identity genes which establish the floral meristem and (ii) the organ identity genes which are required for appropriate organ development in their respective place in the flower.

The organ identity genes *PISTILLATA* (*PI*) and *APETALA3* (*AP3*) are necessary for petal and stamen development. The loss of either gene function result in similar phenotypes, with petals being transformed into sepals and stamens into carpels [1]. Both genes encode the MADS-box transcription factors that are capable of forming a heterodimer and bind to DNA containing the consensus sequence $CC(A/T)_6GG$ [2, 3]. Therefore, the PI/AP3 complex appears to have a role as the regulator essential for petal and stamen development.

PI transcripts become first detectable after the sepal primordia begin to form at stage 3 [2]. During the petal and stamen primordia emerge, *PI* transcripts continue to be detected in both petals and stamens throughout the flower development. *PI* expression is regulated in two

MOLECULAR BIOLOGY AND INFORMATION — Molecular Biology —

Scope of research

Attempts have been made to elucidate structure-function relationships of genetic materials and various gene products. The major subjects are mechanisms involved in signal transduction and regulation of gene expression responsive to environmental stimuli, differentiation and development of plant organs, and plant-microbe interaction. As of December 2000, study is being concentrated on the roles of homeodomain proteins and DDK response regulators of higher plants in developmental and signal transduction processes.

Prof
OKA, Atsuhiro
(D Sc)

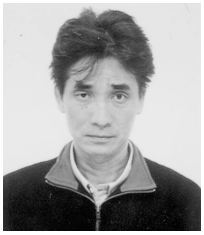

Assoc Prof
AOYAMA, Takashi
(D Sc)

Assoc Instr
HONMA, Takashi

Students:
OHGISHI, Maki (DC)
SAKAI, Hiroe (DC)
LIANG, Yajie (DC)
OHASHI, Yohei (DC)
MURAMOTO, Takuya (RF, D Sc)
IWAKOSHI, Shintaro (RS)

steps; the establishment of initial expression and the maintenance of their expression by PI and AP3 proteins (autoregulation). Genetic analysis has proposed that the initial expression is induced by combinations of the meristem identity genes, *LEAFY* (*LFY*) and *UNUSUAL FLORAL ORGANS* (*UFO*), and after once established, *PI* expression in the petals and stamens is maintained by the activities of PI and AP3 proteins [2, 4, 5].

In order to define the regulatory elements in the *PI* promoter region, various deletions in the 1.5-kb region upstream of *PI* were generated and then connected to a reporter gene that had been made by an in-frame translational fusion of *PI* with the *uidA* gene coding for the β-glucuronidase (GUS). The author introduced these constructs (*PI::GUS* series) into the *Arabidopsis* genome, and flowers of the resulting transgenic plants were stained for GUS enzyme activity. *PI::GUS* transgenic lines carrying a promoter DNA region to nt -498 (or to more) from the *PI* translation initiation site showed petal- and stamen-specific GUS expression pattern, similar to the localization of *PI* transcript. An additional deletion to nt -399 led to alteration of GUS expression in the stage 3 flowers (early expression), suggesting that this -498 to -399 region contains a *cis* element(s) required for early expression occurring in response to induction signals (the distal region). In *PI::GUS* transgenic lines containing up to nt -266, the level of GUS expression in petals and stamens (late expression) was reduced. Further deletions up to nt -233 entirely abolished GUS expression. These results suggest that the deletions to nt -266 and to nt -233 remove *cis* elements essential for the late expression (the proximal region), partially and entirely, respectively.

In order to define *cis* elements responsive to the PI/AP3 complex in the *PI* promoter region, each of the above deletion derivatives of *PI::GUS* was introduced into the loss- and gain-of-function alleles of *PI* and *AP3*. In the loss-function alleles of *PI* or *AP3*, the early expression mediated by the distal region remained but the late expression mediated by the proximal region disappeared. These results indicate that the early *PI* expression is independent of *PI* and *AP3* and that the late expression requires the functional *PI* and *AP3* gene products. In the gain-function alleles of *PI* and *AP3* (35S-*PI* and 35S-*AP3*), strong GUS activity mediated by the proximal region was observed in any of the flower organs. It was thus concluded that the proximal promoter contains the *cis* elements that respond to the autoregulatory signals of the PI/AP3 complex.

To test whether the early and late expression of *PI* are influenced by *LFY* and *UFO*, the deletion derivatives of *PI::GUS* were similarly introduced into the loss- and gain-of-function alleles of *LFY* and *UFO*. In plants deficient in *LFY*, GUS expression mediated by the distal region in the stage 3 flowers was completely eliminated. In contrast, defects in *UFO* did not influence GUS expression promoted by either of the distal and proximal regions. These results suggest that *LFY* affects the early but not the late expression of *PI*, and that *PI* expression is not highly influenced by the *UFO* mutations. In the gain-of-function allele of *LFY* (35S-*LFY*), partial ectopic GUS expression was observed, depending on the distal *PI* promoter. Furthermore, 35S-*LFY* plants carrying simultaneously introduced 35S-*UFO* showed GUS expression mediated by the distal region in the whole plant body; however, GUS expression directed by the proximal region was restricted within the flower organs. These results indicate that the coexistence of *LFY* and *UFO* is sufficient to induce *PI* expression in a flower-independent manner and that the *cis*-acting elements responsive to LFY/UFO are located in the distal region of the *PI* promoter.

In summary, I have demonstrated that the *PI* promoter consists of discrete *cis*-acting elements; one in the distal region is responsive to induction signals mediated by the meristem identity genes *LFY* and *UFO*, and the other element in the proximal region is responsive to autoregulatory signals produced by the PI/AP3 complex [6].

References

1. Bowman, J. L., Smyth, D. R. and Meyerowitz, E. M. *Plant Cell,* **1**, 37-52 (1989).
2. Goto, K. and Meyerowitz, E. M. *Genes Dev*., **8**, 1548-1560 (1994).
3. Jack, T., Brockman, L. L. and Meyerowitz, E. M. *Cell,* **68**, 683-697 (1992).
4. Weigel, D. and Meyerowitz, E. M. *Science,* **261**, 1723-1726 (1993).
5. Levin, J. Z. and Meyerowitz, E. M. *Plant Cell,* **7**, 529-548 (1995).
6. Honma, T. and Goto, K. *Development,* **127**, 2021-2030 (2000).

Classification and Analysis of Eukaryotic ABC Transporters in Complete Eukarya Genomes

Yoshinobu Igarashi and Minoru Kanehisa

The ABC(ATP-Binding Cassette) transporters form a major class of active transporters which are widespread in archaea, bacteria, and eukarya. Most of eukaryotic ABC transporters are involved in exporting antibiotic drugs. In this study, first, we identified the eukaryotic ABC transporters in three complete eukarya genomes, *S.cerevisie*, *C.elegans* and *D.melanogaster*. Next, we classified the eukaryotic ABC transporters into the clusters of orthologs and paralogs using the hierarchical cluster analysis. In addition, we built Hidden Markov Models (HMMs) for individual clusters, and identified the orthologs of individual clusters in othrer genomes by using the HMMs.

Keywords: ABC transporter / Hidden Markov Model / Bioinformatics

Accumulation of genome information is increasing at an accelerative tempo, recent years, and already, the genomes of 6 archaea, 28 eubacteria, and 3 eukarya were determined. These sequences facilitate the analysis of the genome comparison, the analysis of evolutionary relationships and the reconstruction of pathways. However, frequently, the annotation of the proteins and genes sequenced by the genome projects are still based on only the simple sequence similarity. The systematic analysis of genome comparison or evolutionary relationships can carry out producing the more detailed annotations which are never obtained only from the simple sequence similarity. Furthermore, such systematic analysis can be used to avoid the wrong annotations which tend to be produced from the evaluation of only sequence similarity.

The structure of a prokaryotic ABC transporter usually consists of three components. A typical transporter consists of two integral membrane proteins each having six transmembrane segments, two peripheral proteins that bind and hydrolyze ATP, and a periplasmic (or lipoprotein) substrate binding protein. Many of the

MOLECULAR BIOLOGY AND INFORMATION — Biological Information Science —

Scope of research

This laboratory aims at developing theoretical frameworks for understanding the information flow in biological systems in terms of genes, gene products, other biomolecules, and their interactions. Toward that end a new database is being organized for known molecular and genetic pathways in living organisms, and computational technologies are being developed for retrieval, inference and analysis. Other studies include: functional and structural prediction of proteins from sequence information and development of sequence analysis tools.

Prof
KANEHISA, Minoru
(D Sc)

Assoc Prof
GOTO, Susumu
(D Eng)

Instr
NAKAYA, Akihiro
(D Sc)

Students:
PARK, Keun-joon (DC)
IGARASHI, Yoshinobu (DC)
KATAYAMA, Toshiaki (DC)
NAKAO, Mitsuteru (DC)
YOSHIZAWA, Akiyasu (DC)
OKUJI, Yoshinori (DC)
KATO, Masaki (MC)
ITOH, Masumi (MC)
LEVCHENKO, Maria (RS)
Research Fellow:
SATO, Kazushige (RF)
HATTORI, Masahiro (RF)

genes for the three components form operons as in fact observed in known archaea and bacteria genomes[1].

On the other hand, in a typical eukaryotic ABC transporter, the membrane spanning protein and the ATP-binding protein are fused, forming a polypeptide with the membrane spanning domain and the ATP-binding domain.

In prokaryotic ABC transporters, the ATP-binding protein component is the most conserved, the membrane protein component is somewhat less conserved, and the substrate-binding component is most divergent in terms of the sequence similarity[2][3]. Therefore, in eukaryotic ABC transporters, it could also be expected that ATP-binding domain is the most conserved domain.

In this analysis, we first searched and compared the eukaryotic ABC transporters in three eukarya complete sequenced genomes, *S.cerevisiae*, *C.elegans* and *D.melangaster*. We identified ATP-binding domains and other domains in the candidate sequences using the hidden Markov model in Pfam5.0. Then, in order to confirm whether these candidate sequences also have the membrane spanning domain simultaneously, we predicted the membrane spanning domains using SOSui transmembrane prediction program[4]. The prediction results of SOSui program were used as the reference for removing false positive eukaryotic ABC transporters from candidate sequences by manual operation. Then, eukaryotic ABC transporters of 24 in *S.cerevisiae*, 46 in *C.elegans*, 50 in *D.melanogaster* were identified (Table 1). We counted alternatively spliced proteins as one entry.

Next, they were classified into orthologs and paralogs from sequence similarity and domain structure according to the hierarchical cluster analysis. These transporters were classified into orthologs and paralogs from the sequence similarity of the ATP-binding domain and the domain structure, i.e., the ordering of the two domains. The resulting set of clusters (families) is shown in Table 1.

Furthermore, hidden Markov models were built using individual clusters, and they were used to search for similar sequences in other genomes in the KEGG/GENES database.

By the HMM search in bacteria, archaea and eukarya, we identified a specific ATP-binding domain group, whose homologs are found in only plants and fungi. The HMM for this ATP-binding domain group was constructed by the members of *S.cerevisiae* only, and they belong to multidrug resistance family (family 4 in table 1). Each sequence of this family has two ATP-binding domains, and the homologs of C-terminal side ATP-binding domain are found in bacteria and other eukarya, but the homologs of N-terminal side ATP-binding domain are found in only *S.pombe*, *C.albicans* and *A.thaliana*. Therefore, it is possible that N-terminal side of the sequences may have a function special to the medicine tolerance of fungi and plant cells.

Table1: The number of eukrayotic ABC transporters in *S.cerevisiae*, *C.elegans* and *D.melanogaster*

	family	*S.cer*	*C.ele*	*D.mel*
1	p-glycoprotein	4	21	9
2	multidrug resistance associated protein	7	7	14
3	peroxisomal membrane transporter	2	5	4
4	multidrug resistance (white protein homolog)	10	7	14
5	ABC-2 type?	0	5	8
6	miscellaneous	1	2	1
		24	46	50

Acknowledgments

This work was supported by grants from the Ministry of Education, Science, Sports and Culture of Japan, the Science and Technology Agency of Japan, and the Japan Society for the Promotion of Science. The computational resource was provided by the Supercomputer Laboratory, Institute for Chemical Research, Kyoto University.

References

1. Tomii K. and Kanehisa M., *Genome Research*, **8**, 1048 - 1059 (1998)
2. Saurin W. and Dassa E., *Protein Sci*, **3**, 325 - 344 (1994).
3. Tam R. and Saier M.H. Jr., *Microbiol Rev*, **57**, 320 - 346 (1993)
4. Hirokawa T, Boon-Chieng S, Mitaku S, *Bioinformatics*, **14**, 378-379 (1998)

The Stretcher Operation of KSR

Takashi Sugimura, Akio Morita, Hiromu Tonguu, Toshiyuki Shirai, Yoshihisa Iwashita, Hirokazu Fujita and Akira Noda

The electron ring KSR has been utilized as a pulse stretcher of the 100 MeV S-band electron linac. The duty factor of the electron beam has been increased drastically more than 90% from 2×10^{-5}.

Keywords: electron ring/ KSR/ slow extraction/ RFKO/ duty factor

An S-band electron linac with the maximum energy of 100 MeV has been operated since October 1995. This linac has been used for experiments such as Parametric X-Ray radiation from the crystal and resonant transition radiation from the foils of dielectric substance. The pulse width and the repetition rate of the linac, however, are limited at 1μsec and 20Hz, respectively, which results in the beam duty factor of 2×10^{-5} at maximum. In order to avoid the pile up of the signals from the detectors, we are forced to reduce the peak current of the output beam from the linac, which causes reduction of the average current. So the idea of using the KSR as a pulse stretcher was proposed so as to improve this situation, while KSR is also to be utilized as a synchrotron light source with the maximum energy of 300 MeV[1,2]. The total layout of KSR is shown in Figure 1, where main devices for beam injection and extraction are indicated.

In the stretcher mode, the electron beam from the linac is injected into the ring through the inflector and extracted from the ring through the electrostatic septum (ESS) with the repetition rate of 1 Hz[3]. After the injection, the transverse RF electric field resonating with the betatron oscillation is applied in the horizontal direction (RF knock out, RF-KO). The stable beam with small amplitude is driven to the separatrix, which is the boundary between the stable and unstable regions for the third order resonance in the horizontal transverse phase space. The beam becomes unstable and its amplitude increases as shown in Figure2 along the branches of the separatrix. With this method, the separatrix is fixed throughout the whole process and the direction of the extracted beam

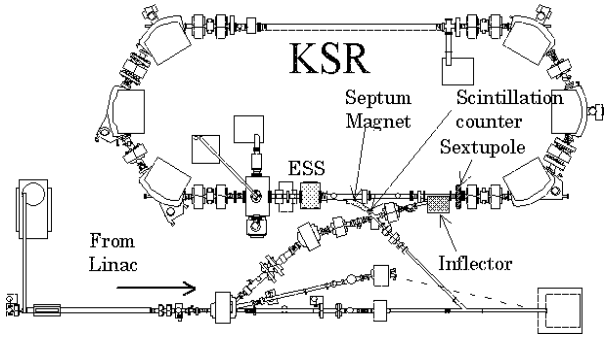

Figure 1. The layout of the KSR. Main devices for the beam injection and extraction are shown.

NUCLEAR SCIENCE RESEARCH FACILITY — Particle and Photon Beams —

Scope of research

Particle and photon beams generated with accelerators and their instrumentations both for fundamental research and practical applications are studied. The following subjects are being studied: Beam dynamics related to space charge force in accelerators: Beam handling during the injection and extraction processes of the accelerator ring:radiation mechanism of photon by electrons in the magnetic field: R&D to realize a compact proton synchrotron dedicated for cancer therapy: Control of the shape of beam distribution with use of nonlinear magnetic field: and Irradiation of materials with particle and photon beams.

Prof
NODA, Akira
(D Sc)

Assoc Prof
IWASHITA, Yoshihisa
(D Sc)

Instr
SHIRAI, Toshiyuki

Techn
TONGUU, Hiromu

Lecturer(part-time):
NAKAJIMA, Kazuhisa(KEK)
Students:
SUGIMURA, Takashi(DC)
KIHARA, Takahiro (DC)
URAKABE, Eriko (DC)
MORITA, Akio (DC)
NAKAMURA, Syu(MC)
FADIL, Hicham(MC)
YAMAZAKI, Atsushi(RS)

The work is supported by Grant-in-Aid for Scientific Research (A) from Ministry of Education, Science, Sports and Culture of Japan with contract No. of 09304042.

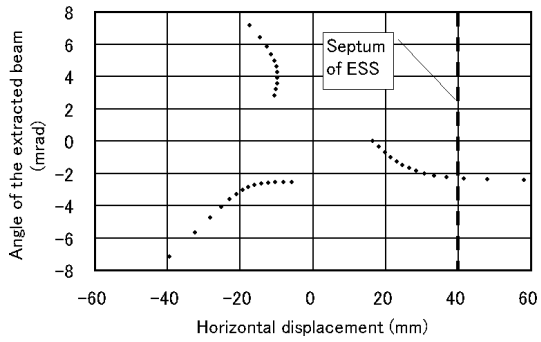

Figure 2. Phase space plot of the beam at the entrance of ESS.

does not change, while the ordinary method, so far utilized, reduces the separatrix size, which inevitably results in the variation of the extracted beam direction. The turn separation, which is the amplitude increase of betatron oscillation in 3 turns, is estimated to be 3.2 mm in the present case and the extraction efficiency is calculated to be 97% for the extraction system using the electrostatic septum with septum thickness of 0.1 mm.

The extraction channel consists of two devices. One is the Electrostatic septum and the other is a magnetic septum (see Figure 3,4).

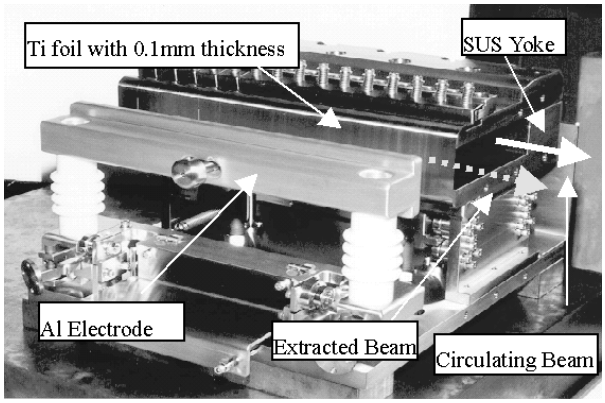

Figure 3. The electrostatic septum. The circulating beam passes through the inside of the yoke, and the beam exceeding 40mm in its oscillation amplitude is deflected outward by 20.5 mrad with the electric field applied between the Ti foil and the Al electrode, and then guided to the septum magnet located downstream.

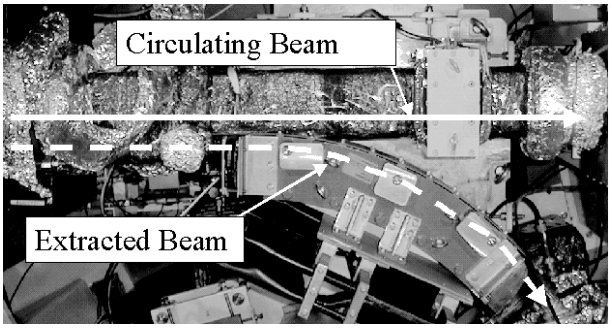

Figure 4. The magnetic septum.After the deflection of the ESS, septum thickness of 22.6 mm is provided for the septum magnet. With the field of 0.5T and the pole length of 550 mm the extracted beam is deflected as large as 45° and is guided to the extraction beam line.

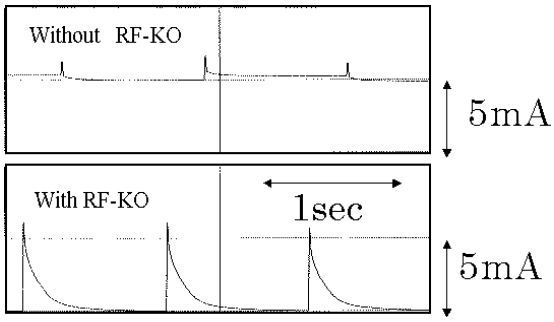

Figure 5. Output signal of the DCCT. The axes of abscissa and ordinate are time and the circulating beam current in KSR,respectively. Without RF-KO, the circulating beam does not decrease. With RF-KO, circulating beam decreases slowly with extraction procedure.

Observations of a beam current in the ring and an extracted beam spill were performed with the beam energy of 80 MeV. Figure 5 shows the output signal of the DCCT (DC current transformer) with and without RF-KO. This figure shows that the beam current in KSR decreases slowly by RF-KO. A scintillation counter was set just after the exit of the magnetic septum as shown in Figure 1 and the extracted beam was measured. Figure 6 shows the first measurement of the pulse rate of scintillation counter for the first 800 ms. It was confimed that the beam extraction continues during almost 1sec after the injection.

The stretcher ring KSR utilizing the slow extraction with an RF-KO and the third order resonance is found to work as designed. This is the first slow extraction experiment with this scheme for the electron beam under the radiation damping.

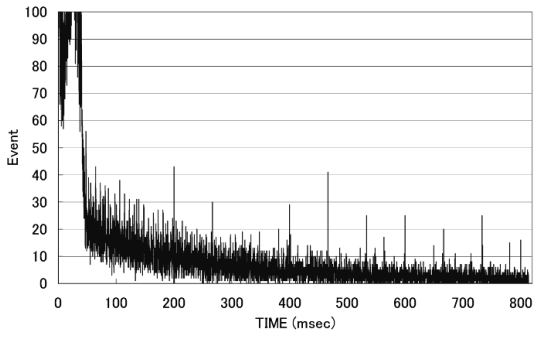

Figure 6. Pulse rate of the extracted beam. A background has been subtracted. The further fine tuning is required to realize the flat beam spill.

References

[1] A.Noda et al., "Stretcher Mode of KSR", Proc. of the 11th symposium on Accelerator Science and Technology.(1997) 59.

[2] A.Noda et al., "Slow extraction system of stretcher ring, KSR", Proc. of the European Particle Accelerator Conference,(1998) 2120.

[3] A.Noda et al., "Electrostatic septum for slow extraction at KSR", Beam Science and Technology. (1998) 31.

Coherent Time Evolution of Highly Excited Rydberg States in Pulsed Electric Field: Opening a New Scheme for Stringently Selective Field Ionization

M. Tada, Y. Kishimoto, M. Shibata, K. Kominato, C. Ooishi, T. Saida, T. Haseyama and S. Matsuki

Coherent time evolution of highly excited Rydberg states in Rb ($98 \leq n \leq 150$) under pulsed electric field in high slew rate regime was investigated with the field ionization detection. We observed for the first time a discrete transition of the threshold ionization field with slew rate, the behavior of which depends also on the position of the low l states relative to the adjacent manifold. The experimental results strongly suggest that the coherent interference effect plays decisive role for such transitional behavior, and bring us a new, quite effective scheme for the stringently selective field ionization.

Keywords : Rydberg atoms/selective field ionization/pulsed electric field/dark-matter axion search

Highly excited Rydberg states in the ramped electric field is one of the most interesting system for investigating the coherence effects in the time evolution of a quantum systems[1]. With increasing principal quantum number n, more numbers of the Rydberg Stark states are coherently excited along the increasing electric field, thus the coherence effects becoming more and more important factors to the behavior of the Rydberg states[2]. In spite of this promising feature and also of their potential applicability to the wide area of fundamental physics research including cavity QED and quantum computations, the Rydberg states with high $n > 80$ have not been investigated in detail, partly because of the difficulty in selectively detecting a particular state from many close-lying states[2].

We here investigated the time evolution of highly excited Rydberg states in Rb ($98 \leq n \leq 150$) under pulsed electric field in high slew rate regime[3]. Thermal atomic beam of Rb is introduced into the laser interaction region where the Rb atoms are excited to a highly excited Rydberg state via the two-step laser excitation process from the ground $5s_{1/2}$ state through the second excited $5p_{3/2}$ state. The excited Rydberg state is then fed to the field ionization region, 40 mm apart from the laser interaction region, and ionized with a pulsed electric field in high slew rate regime. The resulting electrons liberated with the field ionization process are detected with a channel electron multiplier. All the data acquisi-

NUCLEAR SCIENCE RESEARCH FACILITY — Beams and Fundamental Reaction —

Scope of research

Atoms, nuclei, and dark matter particles in the Universe are studied with quantum electronic methods: Current research subjects are 1) search for a cosmological dark-matter candidate particle, axion, in the Universe with the Rydberg-atom cavity detector, 2) highly excited Rydberg atoms in an electric field and their applications to fundamental physics research, and 3) nuclear magnetism in 3-5 semiconductors with laser-assisted Overhauser process and optical pumping.

Assoc Prof
MATSUKI, Seishi
(D Sc)

Research Fellow:
HASEYAMA Tomohito (D Sc)

Students:
TADA, Masaru (DC)
KISHIMOTO, Yasuhiro (DC)
SHIBATA, Masahiro (DC)
KOMINATO Kentaro (DC)
OOISHI, Chikara (DC)
SAIDA, Tomoya (MC)

tion and analyses were performed on-line as well as off-line with a LabVIEW DAQ system.

In Fig. 1 shown is typical field ionization spectra of 111*s*,111*p*, and 109*d* states: The upper part shows the originally obtained raw spectra, while the lower part represents the resulting spectra by taking derivative of the above raw spectra. Fig. 2 shows the comparison of the spectral change of the *s* and *p* states with varying slew rate, where the spectra of these states taken independently were superimposed to each other. These spectra show clearly that the field ionization for both the *s* and *p* states has a single threshold, which does not vary continuously but change discretely with the slew rate applied. Note also that this slew rate dependence is quite different for the *s* and *p* states: For example, the *s* state threshold value is 5.2 V/cm at the slew rate of 11 V/(cm μs), while that of the *p* state is 1.7 V/cm, almost 200% difference. This is to be compared to the case of the purely adiabatic transition process at which the expected difference is only 5 %.

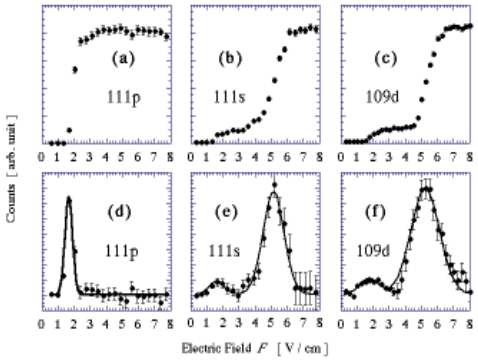

Figure 1. Typical field ionization spectra of *s*, *p* and *d* states.

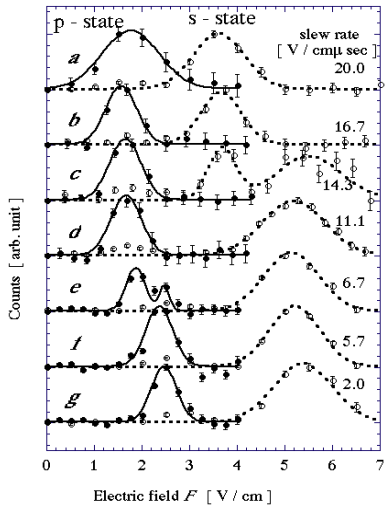

Figure 2. Slew rate dependence of the field ionization threshold for the 111*s* and 111*p* states.

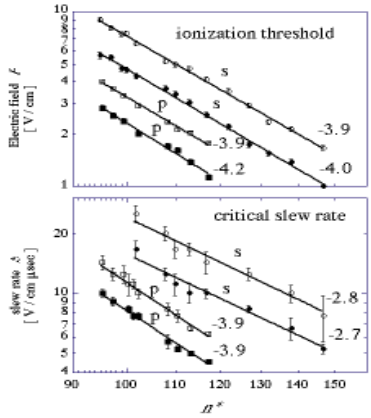

Figure 3. Dependence of the field ionization threshold values and the slew rate on the principal quantum number n^*.

This transitional behavior observed for the first time here has also quite regular *n* dependence as shown in Fig. 3 where the threshold field and the corresponding slew rate are plotted as a function of the effective principal quantum number n^*. This regular dependence thus indicates that the transitional behavior is quite general and strongly suggests that the coherent interference effects in the time evolution play the decisive role to the field ionization processes. Also the experimental results show that the transitional behavior of the low *l* states depends on the position relative to the adjacent manifold and the stringently selective ionization are applicable for a wide range of highly excited Rydberg states, thus opening a quite effective way to utilize such highly excited Rydberg states for the investigations of and applications to fundamental physics research. One of the interesting application for such selective field ionization is a realization of ultra low noise microwave detector in which a single microwave photon is detected one by one with the Rydberg atoms in a well cooled cavity: This is one of the underlying aim of the present study and such a detector was developed and is being utilized to search for dark matter axions in our galactic halo[4].

References

1. D. A. Harmin, Phys. Rev. **A49** (1994) 1933.
2. T. M. Gallagher, *Rydberg atoms* (Cambridge Univ. Press, Cambridge, 1994) and references therein.
3. M. Tada *et al*., Preprint archive, Physics/0010071(2000).
4. S. Matsuki and K. Yamamoto, Phys. Lett. **B263** (1991) 523; I. Ogawa, S. Matsuki and K. Yamamoto, Phys. Rev. **D53** (1996) R1740; K. Yamamoto and S. Matsuki, Nucl. Phys. **B72** (1998) 132; M. Tada *et al*., Nucl. Phys. **B72** (1998) 164; S. Matsuki *et al*., Proc. 2nd Int. Workshop on the Identification of Dark Matter in theUniverse, Buxton, 1998 (World Scientific, Singapore,1999) p.441.

Purification of Terminal Uridylyltransferase from the *Crithidia* Kinetoplast-Mitochondrion

Hiroyuki Sugisaki

Terminal uridylyltransferase is a candidate responsible for a post-transcriptional RNA editing process of mitochondrial transcripts in kinetoplastid protozoans. The activity was solubilized by detergent lysis of mitochondria of *Crithidia fasciculata* isolated by the Renografin density gradient floatation centrifugation, and the enzyme was partially purified using chromatography on phosphocellulose, DEAE-cellulose and Sephadex G200 columns. The major activity of the purified enzyme was to add more than 30 uridylates to the 3'-OH end of guide RNA molecules, required magnesium cations and acted in a UTP dependent manner.

Keywords: kinetoplastid protozoan/ RNA editing / guide RNA

Several species of mitochondrial mRNA in kinetoplastid protozoans such as *Crithidia*, *Leishmani*a, and *Trypanosoma* are extensively edited after transcription. The location of editing domains, number of editing sites within a single domain and number of uridine (U) residues to be added or deleted at each editing site are very specific to individual mRNA. As to the mechanism of RNA editing, a model that small RNA, named guide RNA (gRNA), specify the sequence alternation has been proposed, based on the finding that the intergenic regions of maxicircle contain some sequences that can pair with edited mRNA sequences if G:U pairs are allowed. This model was experimentally supported by detection of small RNA species with poly(U) tails that can hybridized to the corresponding regions of the maxicircles and minicircles[1, 2].

In the current model of the editing pathway, the gRNA also serves as the U donor for the editing process via the poly(U) tails of gRNA molecules. This model, which draws analogies from RNA splicing, proposes that editing occurs through multiple rounds of trans-esterification which predicts mRNA-gRNA chimeric molecules as the reaction intermediates. Such chimeric RNAs could also be formed by a mechanism that utilizes endonuclease and RNA ligase. Both chimeric models propose that the role of uridylyltransferase (TUTase) activity is to add the non-coded poly(U) tails to the gRNAs. In the enzyme cascade model, on the other hand, TUTase would be also responsible for uridylate addition to the liberated 3' end in the editing sites which was generated by specific endonuclease for the editing reaction[1, 2]. To examine the function of TUTase in the editing reaction, I first attempted to purify the enzyme.

For assaying TUTase activity, enzyme fraction was

RESEARCH FACILITY OF NUCLEIC ACIDS

Scope of research

The following is the current major activities of this facility.
With emphasis on regulatory mechanisms of gene expression in higher organisms, the research activity has been focused on analysis of signal structures at the regulatory regions of transcriptional initiation and of molecular mechanisms involved in post-transcriptional modification by the use of eukaryotic systems appropriate for analysis. As of December 1994, studies are concentrated on the molecular mechanism of RNA editing in mitochondria of kinetoplastids.

Assoc Prof
SUGISAKI, Hiroyuki
(D Sc)

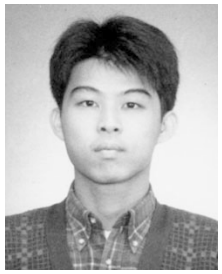

Instr
KAWASHIMA, Shuichi

Techn
YASUDA, Keiko

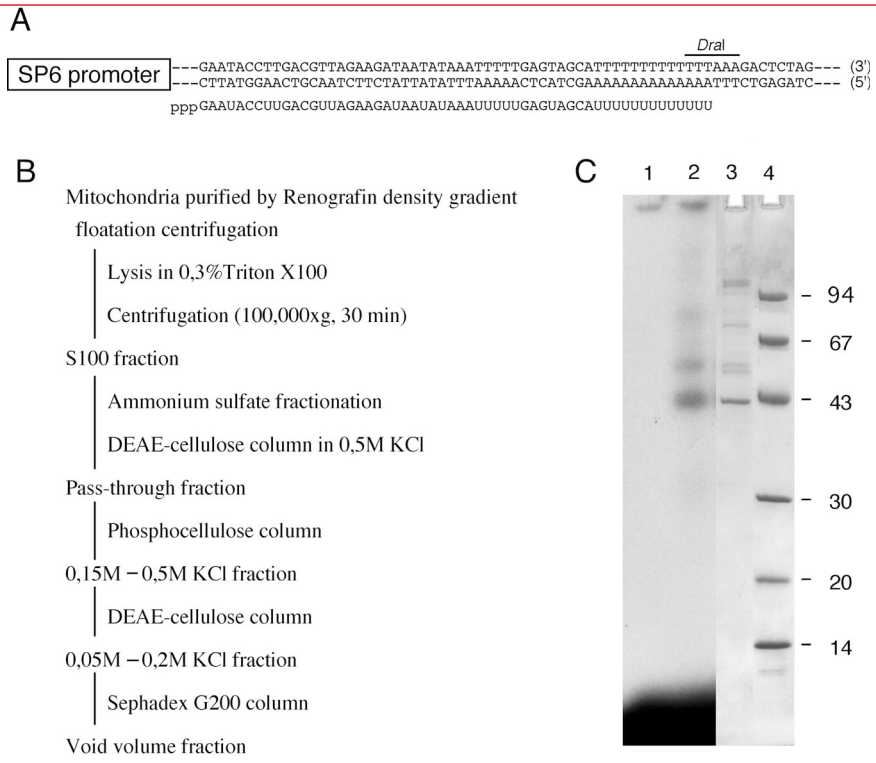

Figure 1. (A) The sequence of Cyb-I gRNA. Below the sequence of the structural gene for Cyb-I gRNA downstream of the promoter for SP6 RNA polymerase in pKS920, the sequence of the transcript on the *Dra*I-digested plasmid is shown. (B) Purification procedures of TUTase from purified mitochondria of *C. fasciculata*. (C) Identification of proteins interacted with ^{32}P-labelled Cyb-I gRNA by the UV irradiation method. ^{32}P-labelled Cyb-I gRNA was incubated with the Sephadex G-200 fraction (lane 2). After UV irradiation, the reaction mixture was digested with RNase A and subjected to SDS-PAGE. Lane 1 is of no enzyme fraction control. The Sephadex G-200 fraction was resolved by gradient SDS-PAGE (10-20%), and stained with Coomasie Brilliant Blue (lane 3). By the side of the marker lane (lane 4), molecular weights (x10^3) of marker are given.

incubated in the reaction mixture containing 0.02M Tris-HCl, pH 7.9, 0.1mM EDTA, 1mM DTT and0.05mM UTP in the presence of ^{32}P-labelled gRNA (Cyb-I gRNA). The gRNA was synthesized *in vitro* on *Dra*I-digested pKS920 carrying the promoter for SP6 RNA polymerase and the structural gene for gRNA responsible for the RNA editing process on the 5'-terminal region of the transcript of the apocytochrome b cryptogene in the presence of (α^{32}P)UTP (Figure 1A). The reaction mixtures were electrophoresed on a polyacrylamide-urea gel and the activity for transfer of uridylates from UTP to the 3'-OH end of the RNA was determined.

Crithidia cells were grown in the brain heart infusion medium containing hemin. After treated with digitonin, the cells were disrupted in a Polytron. The kinetoplast-mitochondrial fraction was isolated by Renografin isopycnic floatation centrifugation, lysed in 0.05M Tris-HCl, pH7.5, 0.1mM EDTA and 1mM DTT containing 0.3% Triton X-100 and centrifuged for 30 min at 100,000xg. The procedures to purify TUTase from the S100 fraction are summarized in Figure 1B.

The Sephadex G200 fraction showed a major band at 43kDa in molecular weight and a few faint bands at 50, 75, and 100 kDa in SDS-polyacrylamide gel electrophoresis (SDS-PAGE) (Figure 1C, lane 3). TUTase certainly recognizes the 3'-OH end of gRNA. To identify the molecular weight of TUTase, the enzyme fraction was incubated with ^{32}P-labelled Cyb-I gRNA to form the TUTase-gRNA complexes. After UV irradiation to form the covalent linkage between TUTase and gRNA in the complexes, the reaction mixtures were digested with RNase, and subjected to SDS-PAGE. The result of analysis is shown in Figure 1C, lanes 1 and 2. The 43 kDa protein was mainly labelled with ^{32}P and the 50 kDa protein was faintly labelled. Therefore, the 43 kDa or 50 kDa protein would be TUTase or a subunit of TUTase which interacted with 3'-OH of gRNA. The major activity of the purified enzyme was to add more than 30 uridylates to the 3'-OH end of gRNA molecules, requireed magnesium cations and acted in a UTP dependent manner.

References

1. Sollner-Webb B, *Science*, 273, 1182-1183 (1996)
2. Simpson L, *"mRNA editing"*. In *Eukaryotic MessengerRNA Processing* (Krainer, A., Ed.) *Frontiers inMoecular Biology*, IRL Press, London, 335-376.

LABORATORIES OF VISITING PROFESSORS

SOLID STATE CHEMISTRY — Structure Analysis —

Vis Prof
MAEKAWA, Sadamichi
(D Sc)

Professor
MAEKAWA, Sadamichi (D Sc)
Institute for Materials Research, Tohoku University
(2-1-1 Katahira, Aoba-ku, Sendai 980-8577)

Lectures at *ICR*
Spin Liquid State around a Doped Hole in Insulating Curates
Effect on Stripes on Electronic States in Undoped $La_{2-x}Sr_xCuO_4$

Vis Prof
OGATA, Masao
(D Sc)

Professor
OGATA, Masao (D Sc)
Department of Pysics
The University of Tokyo
(7-3-1 Hongo, Bunkyo-ku, Tokyo 113-0033)

Lectures at *ICR*
The Basic Theory on the High-Tc Superconductor 1
The Basic Theory on the High-Tc Superconductor 2

FUNDAMENTAL MATERIAL PROPERTIES — Composite Material Properties —

Vis Prof
MATSUI, Michikage
(D Eng)

Vis Assoc Prof
KAWASE, Takeshi
(D Sc)

Professor
MATSUI, Michikage (D Eng)
General Manager, Industrial Textile Development Center, Teijin Ltd
(3-4-1 Mimihara, Ibaraki, Osaka 567-0006)

Lectures at *ICR*
Basic Studies and Industrial Applications of Melt Spinning, Wet Spinning, and Dry Spinning
High-Speed Spinning of Poly(ethylene terephthalate) and Poly(ethylene naphthalate)
Pursuit of Aesthetics and Development of *Shin-Gosen* Fabrics
Development and Industrial Applications of High Strength and High Modulus Aramid Fibers and Carbon Fibers
Functional Fibers for Health and Comfort

Associate Professor
KAWASE, Takeshi (D Sc)
Department of Chemistry, Graduate School of Science, Osaka University
(1-1 Machikaneyamacho, Toyonaka 560-0043)

Lectures at *ICR*
Supramolecular Chemistry of Curved Conjugated System — Complex Formation between the Belt-shaped Conjugated Molecule and Fullerenes

SYNTHETIC ORGANIC CHEMISTRY — Synthetic Theory —

Vis Prof
KUWAJIMA, Isao
(D Sc)

Vis Assoc Prof
NEMOTO, Hisao
(D Sc)

Professor
KUWAJIMA, Isao (D Sc)
Kitasato Institute
(Kitasato 1-15-1, Sagamihara 228-8555)

Lectures at *ICR*
Current Natural Product Synthesis

Associate Professor
NEMOTO, Hisao (D Sc)
Faculty of Pharmaceutical Sciences
Tokushima University
(Sho-machi 1, Tokushima 770-8505)

Lectures at *ICR*
Molecular Design and Synthesis of Novel Functional Molecules

PUBLICATIONS

STATES AND STRUCTURES

I. Atomic and Molecular Physics

Ito Y, Tochio T, Vlaicu A. M, Mutaguchi K, OoHASHI H, Shigeoka N, Nakata Y, Akahama Y, Uruga T and Emura S: DOUBLE-ELECTRON EXCITATION ABOVE Xe K-EDGE, In *the Abst. of 8th International Symposium on Radiation Physics*, 146, June 5-9 (2000)

Vlaicu A. M, Ito Y, Mukoyama T and Bastug: M-SHELL SATELLITE STRUCTURE OF $_{74}$W X-RAY EMISSION LLINES, In *the Abst. of 8th International Symposium on Radiation Physics*, 326, June 5-9 (2000)

Ito Y: High Resolution X-ray Emission Spectroscopy, In *the Abst. of 16th International Conference on the Application of Accelerators in Research and Industry CAARI 2000*, FC2, November 1-4 (2000) (invited)

Ito Y, Vlaicu A. M, Tochio T, Mutaguchi K, OoHASHI H, Shigeoka N, Shoji T, Harada J, Emura S and Uruga T: High Energy Tunable X-ray Spectroscopy in Spring-8, In *the Abst. of International Workshop on Physical Properties of Matter by X-ray Absorption and Emission Spectroscopy*, 32-37, July 24-26 (2000)

Vlaicu A. M, Tochio T, Shigeoka N, OoHASHI H, Mutaguchi K, Ito Y, Emura S, Uruga T, Shoji T and Taniguchi K: Resonant Excitation of $_{74}$W L 2 visible satellite in SPRING-8, In *the Abst. of International Workshop on Physical Properties of Matter by X-ray Absorption and Emission Spectroscopy*, 49-51, July 24-26 (2000)

Yamaguchi K, Forray R, Ito Y and Emura S: Linear inverse problem solution of spherical wave XAFS equation, In *the Abst. of The 11th International Conference on X-ray Absorption Fine Structure*, P1-013, July 26-31 (2000)

Ito Y, Tochio T, Vlaicu A. M, Mutaguchi K, OoHASHI H, Shigeoka N, Nakata Y, Akayama Y, Uruga T and Emura S: Multielectron transitions in x-ray absorption spectra of Xe, In *the Abst. of The 11th International Conference on X-ray Absorption Fine Structure*, P1-030, July 26-31 (2000)

Vlaicu A. M, Ito Y, Shigeoka N, OoHASHI H, Mutaguchi K, Mukoyama T, Melissa G, Wayne S and Fred S: [MO] double electron transitions above $_{74}$W M edge, In *the Abst. of The 11th International Conference on X-ray Absorption Fine Structure*, P1-032, July 26-31(2000)

Tochio T, Vlaicu A. M, Shigeoka N, OoHASHI H, Mutaguchi K, Ito Y, Mukoyama T, Nishihata Y, Uruga T and Emura S: The copper K $_{1, 2}$ emission spectra measurement by monochromatic x-ray excitation, In *the Abst. of The 11th International Conference on X-ray Absorption Fine Structure*, P3-007, July 26-31 (2000)

Ito Y, Tochio T, Vlaicu A. M, Mutaguchi K, OoHASHI H, Shigeoka N, Nakata Y, Akahama Y, Uruga T and Emura S: Double-electron excitation in Xe, In *the Abst. of Spring-8 User Experiment Report*, No.4, 8 (2000)

Nishihata Y, Ito Y, Vlaicu A, Emura S, Mizuki J, Inami T, Uruga T, Yoshikado S, Shoji T, OoHASHI H, Nakanishi Y and Mutaguchi K: EXAFS study on the Debye-Waller factor of perovskite crystals, In *the Abst. of SPring-8 User Experiment Report*, **No.4**, 19 (2000)

Iwazumi T, Nakamura T, Shoji H, Kobayashi K, Kishimoto S, Katano R, Isozumi Y and Nanao S: Magnetic circular Dichroism of Gd 3d-2p and 4d-2p X-ray emission in ferromagnetic Gd-Co amorphous, *J. Phys. Chem. Solids*, **61**, 453-456 (2000)

Ohsawa D, Masaoka S, Katano R and Isozumi Y: Resolution of position-sensitive proportional-counter with a resistive anode wire of carbon fiber, *Applied Radiation and Isotopes*, **52**, 943-954 (2000)

Masaoka S, Katano R and Isozumi Y: Electric discharge of helium-filled proportional counter at liquid helium temperature, *Nucl. Instrum. Methods Phys. Res. B*, **160**, 172-181 (2000)

Nakamura T, Shoji H, Nanao S, Iwazumi T, Kishimoto S, Katano R and Isozumi Y: Magnetic circular Dichroism of the x-ray-emission spectra for the 2p→1s decay in Co metal, *Phys. Rev. B*, **62**, 5301-5304 (2000)

Isozumi Y, Masaoka S, Katano Y, Shimizu H: Helium-filled Proportional Counter and its new Application, *Housyasen*, **26**, 3-13 (2000) (in Japanese)

Nakamatsu H and Mukoyama M: Assignment of Ce XANES spectra for CeO_2 and $CeO_{1.75}$ and effect of oxygen vacancy, *Adv. Quantum Chem.*, **37**, 111-125 (2000)

Sekine R, Tanaka K, Onoe J, Takeuchi K, Nakamatsu H: Analysis of chemical bond in metal clusters: I. Alkali metal and alkaline earth metals, *Adv. Quantum Chem.*, **37**, 237-254 (2000)

Varga S, Fricke B, Nakamatsu H, Mukoyama M, Anton J, Geschke D, Heitmann A, Engel E and Bastug T: Four-component relativistic density functional calculations of heavy diatomic molecules, *J. Chem. Phys.*, **112**, 3499-3506 (2000)

Tanaka K, Sekine R, Onoe J, Nakamatsu H: On Role of the 3d Atomic Orbital in Chemical Bonding for Sulfur Fluorides, *Adv. Quantum Chem.*, **37**, 375-383 (2000)

Nakamatsu H: Description of Molecular Orbital Method Suitable for Theoretical NEXAFS Spectra, *J. Jpn. Soc. Synchro. Rad. Res.*, **13**, 128-136 (2000) (in Japanese)

Tsuji J, Kojima K, Ikeda S, Nakamatsu H, Mukoyama T and Taniguchi K: Li K Absorption Spectra of Various Li Compounds, *Advances in X-Ray Chemical Analysis*, Japan, **31**,149-158 (2000) (in Japanese)

Kondo R, Sekine R, Onoe J, Nakamatsu H: Geometric and Electronic Structures of V and Cr Clusters, *J. Surf. Sci. Soc. Jpn.*, **21**, 462-467 (2000)

Hirata M, Bastug T, Tachimori S, Sekine R, Onoe J and Nakamatsu H: Relativistic Density Functional Calculations for Potential Energy Curves of Uranyl Nitrate hydrate, *Adv. Quantum Chem.*, **37**, 325-333 (2000)

Hirata M, Tachimori S, Sekine R, Jun Onoe J, Nakamatsu H: Electronic structures and chemical bonding of actinyl nitrates dihydrates, *Adv. Quantum Chem.*, **37**, 335-351 (2000)

II. Crystal Information Analysis

Hashimoto S, Ogawa T, Isoda S and Kobayashi T: Electron Diffraction Analysis of Polymorph Structure in Ultra Thin Film of Vanadyl Phthalocyanine on KBr (001), *J. Electron Microscopy*, **48**, 731-738 (1999)

Yoshida K, Isoda S, Tsujimoto M, Yaji T, Nemoto T and Kobayashi T: Combined Microscopic Analyses of Organic Hetero-interface, *J. Elecron Microcopy*, **48**, 739-745 (1999)

Suga T, Isoda S, Kobayashi T, Isogai M and Engel M: Structure and UV-VIS Spectra of Nitrido (phthalocyanato) Rhenium (V) (ReNPc) Thin Film, *Mol. Cryst.& Liq. Cryst.*, **337**, 377-380 (1999)

Yoshida K, Isoda S, Kobayashi T, Sato N and Shirotani I: Dependence of Optical Absorption Spectra on Structures of Bis (1,2-benzoquinonedioximato) Pt (II) Thin Films, Mol. *Cryst.& Liq. Cryst.*, **342**, 121-126 (2000)

Koshino M, Kurata H, Isoda S and Kobayashi T: Branching Ratio and L_2+L_3 Intensities of 3d-Transition Metals in Phthalocyanines and the Amine Complexes, *Micron*, **31**, 373-380 (2000)

Fujiwara E, Irie S, Nemoto T, Isoda S and Kobayashi T: A Scanning Tunneling Microscopy Study on the Monolayer Epitaxy of [Cyano (ethoxycarbonyl) methylene]-4,5-dimethyl-2-ylidene-1,3-dithiole on the (0001) Graphite Surface and its dynamic feature, *Surface Science*, **459**, 390-400 (2000)

Fujiwara E, Isoda S, Hoshino A, Kobayashi T and Yamashita Y: Substituent Effect on Epitaxy of Mono-molecular Layer on HOPG, *Mol. Cryst. &Liq. Cryst.*, **349**, 215-218 (2000)

Yaji T, Isoda S, Kawase N, Kobayashi T and Takeda K: Relaxation of the Stress Produced by Photopolymerization of a Diacetylene Crystal, *Mol. Cryst. & Liq. Cryst.*, **349**, 107-110 (2000)

Kobayashi T: Structure Analysis, 2. Organic Materials, Dennshi-Kenbikyo, **35**, 167-168 (2000) (in Japanese)

III. Polymer Condensed States Analysis

Kohjiya S, Horiuchi T, Miura K, Kitagawa M, Sakashita T, Matoba Y and Ikeda Y: Polymer Solid Electrolyte from Amorphous Poly[epichlorohydrin-*co*-(ethylene oxide)] / Lithium Perchlorate Complex, *Polym. Int.*, **49**, 197-202 (2000)

Kohjiya S and Ikeda Y: Reinforcement of General-Purpose Grade Rubbers by Silica Generated *in situ, Rubber Chem. Technol.*, **73**, 534 - 550 (2000)

Kohjiya S and Ikeda Y: Reinforcement of Natural Rubber by Silica Generated *in situ, Proc. Japan Acad.*, **76B**, 29-34 (2000)

Nishimoto Y, Takagi S, Kohjiya S and Kuroda S: Properties of Sealing Materials Used for the Compressed Air Energy Storage Gas Turbine (CASE-G/T), *Nippon Gomu Kyokaishi*, **73**, 225-232 (2000) (in Japanese)

Ikeda Y, Wada Y, Matoba Y, Murakami S and Kohjiya S: Elastomeric Comb-Shaped High Molecular Mass Poly(oxyethylene) for Polymer Electrolyte: Morphology and Ionic Conductivity, *Rubber Chem. Technol.*, **73**, 720-730 (2000)

Kohjiya S *et al.*: Encyclopedia of Rubber, Asakurasyoten (2000) (in Japanese)

Murakami S, Elinor L B and Kohjiya S:Structural Development of PEN/PET Blend Film during Drawing at High Temperature, *J. Soc. Mat. Sci., Japan*, **49**, 1263-1269 (2000) (in Japanese)

Ohta M, Hyon S H, Kang Y B, Oka M, Tsutsumi S, Murakami S and Kohjiya S: Wear Properties and Mechanical Properties of Slightly Cross-Linked Ultra-High Molecular Weight Polyethylene Crystallized Under Uniaxial Compression, *J. Soc. Mat. Sci., Japan*, **49**, 1301-1305 (2000) (in Japanese)

Kawamura T, Urayama K, Fukahori Y and Kohjiya S: Analysis of Strain Energy Density Function of Elastomers, *J. Soc. Rubber Ind., Jpn.*, **73**, 6-13 (2000) (in Japanese)

Urayama K, Yokoyama K and Kohjiya S: Low-temperature Behavior of Deswollen Poly(dimethylsiloxane) Networks, *Polymer*, **41**, 3273-3278 (2000)

Pralle M, Urayama K, Tew G, Neher D, Wegner G and Stupp S: Piezoelectricity in Polar Supramolecular Materials, *Angew. Chem. Int. Ed.*, **39**, 1486-1489 (2000)

De Sarkar M, Urayama K, Kawamura T and Kohjiya S: Swelling Behavior of Poly(butadiene) Gels in Liquid Crystal Solvents, *Liquid Crystals*, **27**, 795-800 (2000)

Kohjiya S, Urayama K and Takigawa T: Recent Progress in Polymeric Materials. Polymer Network Systems, *J. Soc. Mat. Sci. Jpn.*, **49**, 692-698 (2000) (in Japanese)

Kawamura T, Urayama K and Kohjiya S: Small Angle X-ray Scattering Study on Role of Trapped Entanglements in Structure of Swollen End-linked Poly(dimethylsiloxane) Networks, *J. Chem. Phys.*, **112**, 9105-9111 (2000)

Urayama K, Tsuji M and Neher D: Layer-Thinning Effects on Ferroelectricity and the Ferroelectric-to-paraelectric Phase Transition of Vinylidenefluoride Trifluoroethylene Copolymer Layers, *Macromolecules*, **33**, 8269-8279 (2000)

Ikeda Y, Wada Y, Matoba Y, Murakami S and Kohjiya S: Characterization of Comb-shaped High Molecular Weight Poly(oxyetylene) with Tri(oxyethylene) Side Chains for a Polymer Solid Electrolyte, *Electrochimica Acta*, **45**, 1167-1174 (2000)

Murakami S: Development of Heating / Drawing Device for in site X-Ray Diffraction Measurement of Polymer Films during Uniaxial Drawing, *NIPPON KAGAKU KAISHI*, 141-146 (2000) (in Japanese)

Kawaguchi A, Murakami S, Fujiwara M and Nishikawa Y: Dynamical Observation of Structure Transition of Polymers Using an X-ray Diffraction System with Imaging Plates. II. Crystalline Transition of Poly(butylene terephthalate), *J. Polym. Sci., Part B: Polym. Phys.*, **38**, 838-845 (2000)

Toasaka M, Hamada N, Yamakawa M, Tsuji M and Kohjiya S: Molecular Packing in the New Unit Cell of Poly (*p*-hydroxybenzoic acid) Whisker Crystal, *Comput. Theor. Polym. Sci.*, **10**, issue 3, 355-364 (2000)

Yamaguchi S, Tatemoto M and Tsuji M: Fine Structure in the Emulsion Particles of Fluoro Rubbers and Fluoro Resins, *Kobunshi Ronbunshu*, **57**, 59-66 (2000) (in Japanese)

Shimizu T, Tosaka M, Tsuji M and Kohjiya S: In situ TEM Observation of Natural Rubber Thin Films Crystallized under Molecular Orientation, *Nippon Gomu Kyokaishi*, **73**, 274-276 (2000) (in Japanese)

Tsuji M, Shimizu T and Kohjiya S: TEM Studies on Thin Films of Natural Rubber and Polychloroprene Crystallized under Molecular Orientation. II. Highly Prestretched Thin Films,

Polym. J., **32**, 505-512 (2000)

Kawahara Y, Ohara M, Tsuji M and Kikutani T: Surface Morphology of High-speed Spun Poly(ethylene terephthalate) Fibers, *J. Text. Mach. Soc. Jpn*. (*English Ed.*), **46**, 5-6 (2000)

Tsuji M and Fujita M: Analysis of Higher-Order Structures in Molded Plastics (3) - Morphological Observations: Electron Microscopy (SEM, TEM) -, *Seikei-Kakou*, **12**, 313-317 (2000) (in Japanese)

Kawahara Y, Tsuji M, Hananouchi T, Tamura H, Kimura T and Kohjiya S: Fibrillation Behavior of Silk Fibers from Japanese-oak-silkworm (*Antheraea yamamai*), *Sen'i Gakkaishi*, **56**, 462-465 (2000)

Kuwabara K, Kaji H, Tsuji M and Horii F: Crystalline-Noncrystalline Structure and Chain Diffusion Associated with the 180º Flip Motion for Polyethylene Single Crystals As Revealed by Solid-State ^{13}C NMR Analyses, *Macromolecules*, **33**, 7093-7100 (2000)

Senoo K, Endo K, Murakami S and Tosaka M: Crystallization of Newly Synthesized Syndiotactic Graft Copolymers, *Chem. Lett.*, **No. 3**, 278-279 (2000)

Tosaka M, Kamijo T, Tsuji M, Kohjiya S, Ogawa T, Isoda S and Kobayashi T: High-Resolution Transmission Electron Microscopy of Crystal Transformation in Solution-Grown Lamellae of Isotactic Polybutene-1, *Macromolecules*, **33**, 9666-9672 (2000)

INERFACE SCIENCE

I. Solutions and Interfaces

Wakai C, Saito H, Matubayasi N, and Nakahara M: Tumbling and Spinning Diffusions of Acetonitrile in Water and Organic Solvents, *J. Chem. Phys.*, **112**, 1462-1473 (2000).

Matubayasi N and Nakahara M: Super- and Subcritical Hydration of Nonpolar Solutes. I. Thermodynamics of hydration, *J. Chem. Phys.*, **112**, 8089-8109 (2000).

Sato H, Matubayasi N, Nakahara M, and Hirata F: Which Carbon Oxide is More Soluble? Ab Initio Study on Carbon Monoxide and Carbon Dioxide in Aqueous Solution, *Chem. Phys. Lett.*, **323**, 257-262 (2000).

Matubayasi N, Tsujino Y, and Nakahara M: Structure and Thermodynamics of Aqueous Solution of Nonpolar Solutes in Supercritical Conditions, *Proc. 13th International Conference of Water and Steam.*, **13**, 426-432 (2000).

Nakahara M, Wakai C, Tsujino Y, and Matubayasi N: *In-situ* NMR Study of Hydrothermal Reactions of Hazardous Chlorinated Organic Compounds: CH_2Cl_2, *Proc. 13th International Conference of Water and Steam.*, **13**, 456-463 (2000).

Matubayasi N and Nakahara M: Theory of Solutions in the Energetic Representation. I. Formulation, *J. Chem. Phys.*, **113**, 6070-6081 (2000).

Matubayasi N and Nakahara M: Association and Dissociation of Nonpolar Solutes in Super- and Subcritical Water, *J. Phys. Chem.* B, **104**, 10352-10358 (2000).

Matubayasi N, Nakao N, and Nakahara M: Dynamic Structural Analysis of Supercritical Water, *Koatsu-ryoku no Kagaku to Gijutsu* (*Rev. High Pressure Sci. Tech.*), **10**, 283-289 (2000) (in Japanese).

Tatsumi K, Conard J, Nakahara M, Menu S, Lauginie P, Sawada Y, and Ogumi Z: Low temperature ^{7}Li NMR investigations on Lithium inserted into carbon anodes for rechargeable Lithium-ion cells, *J. Power Sources*, **81-82**, 397-400 (1999).

Bossev DP, Matsumoto M, and Nakahara M: ^{19}F NMR Study of Molecular Aggregation of Lithium Perfluorooctylsulfonate in Water at Temperatures from 30 to 250 ºC, *J. Phys. Chem. B*, **104**, 155-158 (2000).

Ibuki K, Ueno M, and Nakahara M: Analysis of Concentration Dependences of Electrical Conductances for 1:1 Electrolytes in Sub- and Supercritical Water, *J. Phys. Chem. B*, **104**, 5139-5150 (2000).

Yonezawa T, Toshima N, Wakai C, Nakahara M, Nishinaka M, Tominaga T, Nomura H: Structure of monoalkyl-monocationic surfactants on the microscopic three-dimensional platinum surface in water, *Colloids and Surfaces A*, **169**, 35-45 (2000).

Shibata T, Matsuoka T, Koda S, Nomura H, Wakai C, and Nakahara M: Effects of the addition of a diluent on the translational and reorientational molecular motions in 4-cyano-4'-penthylbiphenyl, *J. Mol. Liquids*, **85**, 219-227 (2000).

Watanabe H, Sato T, Osaki K, Matsumoto M, Bossev DP, McNamee CE, and Nakahara M: Linear Viscoelestic Bahavior for Perfluorooctyl Sulfonate Micelles: Effects of Counterion, *Rheologica Acta*, **39**, 110-121 (2000).

Matsumoto M, McNamee CE, Bossev DP, Nakahara M, and Ogawa T: Structure of salted-out, solubilized micelles and microemulsions on the perfluorinated anionic surfactant tetraethylammonium perfluorooctyl sulfonate studied by cryogenic transmission electron microscopy, *Colloid. Polym. Sci.*, **278**, 619-628 (2000).

Yamasaki Y, Enomoto H, Yamasaki N, and Nakahara M: NMR Study of Hydrothermal Reactions of Dichloromethane with and without Alkali, *Bull. Chem. Soc. Jpn.*, **73**, 2687-2693 (2000).

Nakahara M: Twenty-sixth International Conference on Solution and Chemistry: Preface, *Pure Appl. Chem.*, **71**(9), vi (1999).

Nakahara M: In-situ NMR Observation of Supercritical Water as a Novel Reaction Medium, *Jasco Report, New Technology in Supercritical Conditions*, **4**, 57-62 (2000) (in Japanese).

Nakahara M: Solution Chemistry of the Twenty-first Century, *Denki Kagaku oyobi Kougyou Butsuri Kagaku*, **68**, 1028-1029 (2000) (in Japanese).

Yamamoto S, Ejaz M, Tsujii Y, Matsumoto M, and Fukuda T: Surface Interaction Forces of Well-Defined, High-Density polymer Brushes Studied by Atomic Force Microscopy. 1. Effect of Chain Length, *Macromolecules*, **33**, 5602-5607 (2000).

Imanishi Y, Miura, Y, Iwamoto, M, Kimura S and Umemura J: Surface Potential Generation by Helical Peptide Monolayers and Multilayers on Gold Surface, *Proc. Japan Acad.*, **75B**, 287-290 (1999).

Miura, Y, Kimura S, Kobayashi S, Iwamoto, M, Imanishi Y and Umemura J: Negative Surface Potential Produced by Self-assembled Monolayers of Helix Peptides Oriented Vertically to a Surface, *Chem. Phys. Lett.*, **315**, 1-6 (1999).

Umemura J and Sakai H: Hurdles in FT-IR External Reflection Measurements of Langmuir Monolayers on the Water Surface,

Fourier Transform Spectroscopy: Twelfth International Conference, Itoh K and Tasumi M, Eds., Waseda University Press, Tokyo, pp. 127-128 (1999).

Tano T and Umemura J: FT-IR Study of the Interaction of Cholesterol with Dimyristoyl-phosphatidylcholine in Black Films, *Fourier Transform Spectroscopy: Twelfth International Conference*, Itoh K and Tasumi M, Eds., Waseda University Press, Tokyo, pp. 391-392 (1999).

Hasegawa T, Hatada Y, Nishijo, J, Umemura J, Huo Q and Leblanc R M: Unique Hydrogen Bonding Network Structure Formed Between Two Langmuir-Blodgett Films Studied by Infrared Reflection-Absorption Spectrometry, *Fourier Transform Spectroscopy: Twelfth International Conference*, Itoh K and Tasumi M, Eds., Waseda University Press, Tokyo, pp. 401-402 (1999).

Hasegawa T, Nishijo, J and Umemura J: Separation of Raman Spectra from Fluorescence Emission Background by Principal Component Analysis, *Chem. Phys. Lett*., **317**, 642-646 (2000).

Huo Q, Russev S, Hasegawa T, Nishijo, J, Umemura J, Puccetti G, Russell K C and Leblanc R M: A Langmuir Monolayer with a Nontraditional Molecular Archictecture, *J. Am. Chem. Soc.* **122**, 7890 - 7897 (2000).

Hasegawa T, Nishijo, J and Umemura J: Analysis of Monolayer Formation of α-Mycolic Acid Derived from Mycobacterium bovis BCG Pasteur Strain by Infrared Reflection-Absorption Spectrometry with Two-dimensional Correlation Analysis, *Two-dimensional Correlation Spectroscopy* (*AIP CP503*), Ozaki Y and Noda I, Eds., American Institute of Physics, College Park, pp.265-268 (2000).

Okamura E, Kakitsubo R, and Nakahara M: NMR Determination of the Delivery Site of Local Anesthetics in Phospholipid Bilayer Membranes, *Prog. Anesth. Mech.*, **6**, 542-547 (2000).

Okamura E: NMR Study of Drug Deliveries from Water to Lipid Bilayer Membranes - Anesthetics and Endocrine Disruptors, *Maku* (*Membrane*), **25**, 174-176 (2000) (in Japanese).

Okamura E and Nakahara M: NMR Study on Delivery of Endocrine Disruptors from Water to Model Biomembranes, *Hyomen* (*Reviews and Topics on Surface Science & Technology Avant-garde*), **38**, 538-547 (2000) (in Japanese).

Kimura Y, Yamaguchi T and Hirota N: Photo-excitation dynamics of phenol blue, *Phys. Chem. Chem. Phys.*, **2**, 1415-1420 (2000).

Yamaguchi T: Vibrational overtone dephasing in liquids under the influence of non-Gaussian noise, *J. Chem. Phys.*, **112**, 8530-8533 (2000).

Yamaguchi T, Kimura Y and Hirota N: Vibrational energy relaxation of azulene in the S2 state I: Solvent species dependence, *J. Chem. Phys.*, **113**, 2772-2783 (2000).

Yamaguchi T, Kimura Y and Hirota N: Vibrational energy relaxation of azulene in the S_2 state II: Solvent density dependence" *J. Chem. Phys.*, **113**, 4340-4348 (2000).

Yamaguchi T and Kimura Y: Effects of the solute-solvent and solvent-solvent attractive interactions on solute Diffusion, *Mol. Phys.*, **98**, 1553-1563 (2000).

II. Molecular Aggregates

Sato N, Yoshida H. and Tsutsumi K: Unoccupied Electronic Structure in Organic Thin Films Studied by Inverse Photoemission Spectroscopy, *J. Mater. Chem.*, **10**, 85-89 (2000).

Yoshida K, Isoda S, Nemoto T, Kobayashi T, Sato N and Shirotani I: Dependence of Optical Absorption Spectra on Structures of Bis (1,2-benzoquinonedioximato) Pt (II) Thin Films, *Mol. Cryst. Liq. Cryst.*, **342**, 121-126 (2000).

Ashwell G J, N. Dyer A N, Green A, Sato N and Sakuma T: Monolayer Films of U-shaped Molecules: Suppression of the Aggregation-Induced Second-Harmonic Generation of Squaraine Dyes by Guest-Host Interactions, *J. Mater. Chem.*, **10**, 2473-2476 (2000).

Asami K and Irimajiri A: Dielectrospectroscopic Monitoring of Early Embryogenesis in Single Frog Embryos, *Phys. Med. Biol.*, **45**, 3285-3297 (2000).

Asami K, Takahahsi K and Shirahige K: Progression of Cell Cycle Monitored by Dielectric Spectroscopy and Flow-Cytometric Analysis of DNA Content, Yeast 16, 1359-1363 (2000).

Asami K: Perspective of Dielectric Spectroscopy in Biotechnology, *Seibutsu Kougaku Kaishi*, **78**, 1051 (2000) (in Japanese).

Asami K: Monitoring of Cell Division Cycle of Yeast by Dielectric Spectroscopy, *Seibutsu Kougaku Kaishi*, **78**, 1058-1062 (2000) (in Japanese).

Asami K, Okazaki T, Nagai Y and Nagaoka Y: Alamethicin Ion Channels Formed in Lipid Bilayers, *Maku*, **25**, 166-167 (2000) (in Japanese).

III. Separation Chemistry

Sohrin Y, Iwamoto S, Matsui M, Obata H, Nakayama E, Suzuki K, Handa N and Ishii M: The Distribution of Fe in the Australian Sector of the Southern Ocean, *Deep-Sea Res. I*, **47**, 55-84 (2000)

Umetani S, Kawase Y, Quyen L T H and Matsui M: Acylpyrazolone Derivatives of High Selectivity for Lanthanide Metal Ions: Effect of the Distance between the Two Donating Oxygens, *J. Chem. Soc., Dalton Trans.*, 2787-91 (2000)

Fujino O, Umetani S, Ueno E, Shigeta K and Matsuda T: Determination of Uranium and Thorium in Apatite Minerals by Inductively Coupled Plasma Atomic Emission Spectrometry with Solvent Extraction Separation into Diisobutyl Ketone, *Anal. Chim. Acta*, **420**, 65-71 (2000)

Fukuda R, Sohrin Y, Saotome N, Fukuda H, Nagata T and Koike I: East-West Gradient in Ectoenzyme Activities in the Subarctic Pacific: Possible Regulation by Zinc, *Limnol. Oceanogr.*, **45**, 930-39 (2000)

SOLID STATE CHEMISTRY

I. Artificial Lattice Alloys

Baczewski L T, Mibu K, Nagahama T and Shinjo T: Magnetic Anisotropy in Co/Nd Multilayers with Depth-Selectively Inserted ^{57}Fe Probe Layer, *Acta Physica Polonica A*, **97**, 439-442 (2000).

Shigeto K, Shinjo T and Ono T: Injection of a Magnetic Domain

Wall into a Submicron Magnetic Wire, *Appl. Phys. Lett.*, **75**, 2815-2817 (1999).

Mibu K, Tanaka S, Almokhtar M, Nakanishi A, Kobayashi T and Shinjo T: Magnetism of Ultrathin Cr Layers and Fe/Cr Multilayers Studied by ^{119}Sn Probes, *Hyper. Int.*, **126**, 367-370 (2000).

Yokoyama Y, Suzuki Y, Yuasa S, Ando K, Shigeto K, Shinjo T, Gogol P, Miltat J, Thiaville A, Ono T and Kawagoe T: Kerr Microscopy Observations of Magnetization Process in Microfabricated Ferromagnetic Wires, *J. Appl. Phys.*, **87**, 5618-5620 (2000).

Nagahama T, Mibu K and Shinjo T: Electric Resistance of Magnetic Domain Wall in NiFe Wires with CoSm Pinning Pads, *J. Appl. Phys.*, **87**, 5648-5650 (2000).

Shigeto K, Okuno T, Shinjo T, Suzuki Y and Ono T: Magnetization Switching of a Magnetic Wire with Trilayer Structure Using Giant Magnetoresistance Effect, *J. Appl. Phys.*, **88**, 6636-6644 (2000).

Almokhtar M, Mibu K, Nakanishi A, Kobayashi T and Shinjo T: Magnetism of Cr in V/Cr Multilayers Studied by ^{119}Sn Mössbauer Spectroscopy, *J. Phys. Condensed Matter*, **12**, 9247-9257 (2000).

Takeda M, Mibu K, Takanashi K, Himi K, Endoh Y, Shinjo T and Fujimori H: Spin Density Wave in Epitaxial Cr (001)/Sn and Cr (001)/Au Multilayers with Nonmagnetic Spacer Layers, *J. Phys. Soc. Jpn.*, **69**, 1590-1593 (2000).

Shinjo T, Shigeto K, Nagahama T, Mibu K and Ono T: Studies on Magnetization Reversal in Submicron Wires and Domain Wall Behaviors, *J. Phys. Soc. Jpn.*, **69**, Suppl. A, 91-98 (2000).

Yokoyama Y, Shigeto K, Gogol P, Miltat J, Thiaville A, Kawagoe T, Suzuki Y, Ono T, Shinjo T, Yuasa S and Ando K: Kerr Microscope Observation of Microfabricated NiFe Wires, *Nippon Oyo Jiki Gakkaishi*, **24**, 555-558 (2000) (in Japanese).

Ono T, Miyajima H, Shigeto K and Shinjo T: Study of Magnetic Domain Formation and Domain Wall Propagation Using the Giant Magnetoresistance Effect, *Nippon Oyo Jiki Gakkaishi*, **24**, 1136-1141 (2000) (in Japanese).

Mibu K, Almokhtar M, Tanaka S, Nakanishi A, Kobayashi T and Shinjo T: Reduction of Magnetic Moments in Very Thin Cr Layers of Fe/Cr Multilayers: Evidence from ^{119}Sn Mössbauer Spectroscopy, *Phys. Rev. Lett.*, **84**, 2243-2246 (2000).

Shinjo T and Mibu K: Magnetism in Thin Cr Layers Studied Using ^{119}Sn Mössbauer Probes, *Riken Review*, **27**, 3-6 (2000).

Shinjo T, Okuno T, Hassdorf R, Shigeto K and Ono T: Magnetic Vortex Core Observation in Circular Dots of Permalloy, *Science*, **289**, 930-932 (2000).

II. Quantum Spin Fluids

Wakimoto S, Ueki S, Endoh Y, Yamada K: Systematic study of short range antiferromagnetic order and the spin-glass state in lightly doped $La_{2-x}Sr_xCuO_4$, *Phys. Rev. B*, **62**, 3547-53 (2000)

Kimura H, Lee C H, Hirota K, Yamada K, Shirane G: Structural Instability Associated with the Tilting of CuO6 Octahedron in $La_{2-x}Sr_xCuO_4$, *J. Phys. Soc. Jpn.*, **69**, 851-57 (2000)

Lee C H, Yamada K, Endoh Y, Shirane G, Birgeneau R J, Kastner M A, Greven M, Greven, Kim Y J: Energy Spectrum of Spin Fluctuations in the Superconducting $La_{2-x}Sr_xCuO_4$ (x=0.10,0.15,0.18 and 0.25), *J. Phys. Soc. Jpn.* **69**, 1170-76 (2000)

Matsuda M, Lee Y S, Greven M, Kastner M A, Birgeneau R J, Yamada K, Endoh Y, Bonni P, Lee S-H, Wakimoto S, Shirane G: Freezing of anisotropic spin clusters in $La_{1.98}Sr_{0.02}CuO_4$, *Phys. Rev. B*, **61**, 4326-33 (2000)

Hamada K, Takagi S, Murata D, Matsuura M, Hiraka H, Yamada K., Endoh Y: Development of itinerant-electron antiferromagnetism in the approach to metal-insulator transition in metallic $NiS_{2-x}Se_x$ as studied by ^{77}Se NMR, *Physica B*, **281&282**, 641-643 (2000)

Matsuura M, Hiraka H, Yamada K, Endoh Y: Magnetic phase diagram and metal-insulator transition of $NiS_{2-x}Se_x$, *J. Phys. Soc. Jpn*. **69**, 1503-08 (2000)

Kimura H, Matsushita H, Hirota K, Endoh Y, Yamada K, Shirane G, Lee Y S, Kastner M A, Birgeneau R J: Incommensurate geometry of the elastic peaks in supercondcuting $La_{1.88}Sr_{0.12}CuO_4$, *Phys. Rev.B*, **61**, 14366-69 (2000)

Matsuda M, Fujita M, Yamada K, Birgeneau R J, Kastner M A, Hiraka H, Endoh Y, Wakimoto S, Shirane G: Static and dynamical spin correlations in the spin-glass phase of slightly doped $La_{2-x}Sr_xCuO_4$, *Phys. Rev.B*, **62**, 9148-54 (2000)

Katano S, Sato M, Yamada K, Suzuki T, Fukase T: Enhancement of static antiferromanetic correlations by magnetic field in a superconductor $La_{2-x}Sr_xCuO_4$ with x=0.12, *Phys. Rev. B*, **62**, R14677-R147680 (2000)

Suzuki T, Fukase T, Wakimoto S, Yamada K: Anomalous change of the sound velocity in La_2CuO_{4+d}, *Physica B*, **479-480**, 284-88 (2000)

Fukase T, Shinoda T, Oshima Y, Suzuki T, Chiba K, Goto T, Yamada K.: Elastic anomalies induced by spin-flop in $La_{1.88}Sr_{0.12}CuO_4$, *Physica B*, **483-484**, 284-88 (2000)

Endoh Y, Fukuda T, Wakimoto S, Arai M, Yamada K, Bennington S M: Dynamical magnetic susceptibility in the optimum doped LSCO with Tc=37K, *J. Phys. Soc. Jpn.*, **69**, Suppl. B. 16-21 (2000)

Fujita M: Spin dynamics of the spin-Peierls system $CuGeO_3$ using pulsed neutron scattering, *J. Phys. Soc. Jpn.*, **69**. Suppl. B. 59-64 (2000)

III. Multicomponent Materials

Okamoto J, Miyauchi H, Sekine T, Shidara T, Koide T, Amemiya K, Fujimori A, Saitoh T, Tanaka A, Takeda Y and Takano M: Magnetic Circular X-Ray Dichroism Study of $La_{1-x}Sr_xCoO_3$, *Phys. Rev. B*, **62**, 4455-4458 (2000).

Furubayashi Y, Terashima T, Takano M, Yagi K, Shima S and Terauchi H: Epitaxial Growth of Single-Crystalline Thin Film of Two-Legged Spin Ladder Compound $Ca_{14}Cu_{24}O_{41}$, *Advances in Superconductivity XII: Proceedings of the 12th International Symposium on Superconductivity (ISS'99), Oct. 17-19, 1999, Morioka, Japan (ed. Yamashita T and Tanabe K), Springer-Verlag, Tokyo*, 104-106 (2000).

Kojima K M, Someya M, Motoyama N, Eisaki H, Uchida S, Furubayashi Y, Terashima T and Takano M: Charge Dynamics of $A_{14}Cu_{24}O_{41}$ Ladder Compounds in Two Ends: Sr_{14} and Ca_{14},

Advances in Superconductivity XII: Proceedings of the 12th International Symposium on Superconductivity (ISS'99), Oct. 17-19, 1999, Morioka, Japan (ed. Yamashita T and Tanabe K), Springer-Verlag, Tokyo, 179-181 (2000).

Saito T, Terashima T, Azuma M, Takano M, Goto T, Ohta H, Utsumi W, Bordet P and Johnston D C: Single Crystal Growth of the High Pressure Phase of $(VO)_2P_2O_7$ at 3 GPa, *J. Solid State Chem.*, **153**, 124-131 (2000).

Larkin M I, Fudamoto Y, Gat I M, Kinkhabwala A, Kojima K M, Luke G M, Merrin M, Nachumi B, Uemura Y J, Azuma M, Saito T and Takano M: Crossover from Dilute to Majority Spin Freezing in Two Leg Ladder System $Sr(Cu, Zn)_2O_3$, *Phys. Rev. Lett.*, **85**, 1982-1985 (2000).

Fujiwara N, Azuma M and Takano M: NMR Study of Zn-Doped $SrCu_2O_3$ near the Ordering Point, *Physica B*, **284-288**, 1392-1393 (2000).

Ishii K, Yamashita A, Ohishi K, Akimitsu J, Kadono R, Kobayashi N, Takano M and Hiroi Z: Appearance of Magnetic Long-Range Order in the Spin Ladder Compound $La_{1-x}Sr_xCuO_{2.5}$, *Physica B*, **289-290**, 165-167 (2000).

Fujiwara N, Saito T, Azuma M and Takano M: NMR Study of the Critical Behavior near the Ordering Point in a Zn-Doped Spin Ladder $SrCu_2O_3$, *Phys. Rev. B*, **61**, 12196-12199 (2000).

Thurber K R, Imai T, Saitoh T, Azuma M, Takano M and Chou F C: 63Cu NQR Evidence of Dimensional Crossover to Anisotropic 2D Regime in S=1/2 Three-Leg Ladder $Sr_2Cu_3O_5$, *Phys. Rev. Lett.*, **84**, 558-561 (2000).

Azuma M, Saito T, Hiroi Z, Takano M, Narumi Y and Kindo K: New S=1/2 Alternating Chain Compound - High Pressure Form of $(VO)_2P_2O_{7-}$, *ACTA Physica Polonica A*, **97**, 205-208 (2000).

Utsumi W, Katayama Y, Mizutani T, Shimomura O, Yamakata M, Azuma M and Saito T: In situ X-Ray Diffraction Experiments under High Pressures and High Temperatures at BL14B1 Beamline, *Nihon Kessyo Gakkaishi*, **42**, 59-67 (2000) (in Japanese).

Hiroi Z, Okumura M, Yamada T and Takano M: Coexistence of S=1/2 Antiferromagnetic Chains and Dimers on Hole-Doped CuO2 Chains in $Ca_{1-x}CuO_2$, *J. Phys. Soc. Jpn.*, **69**, 1824-1833 (2000).

Ohsugi S, Kitaoka Y, Azuma M, Fujishiro Y and Takano M: Antiferoomagnetic Long-Range Order in Ni-Doped Spin-Ladder Compound $SrCu_2O_3$, *Physica B*, **281&282**, 665-666 (2000).

Ohtani T, Kawasaki S, Takano M, Harima Y, Chika T and Kirino S: Magnetic Susceptibility of Deintercalated Tunnel Compound of KxCr5Se8 and Mossbauer Spectra of $Kx(Cr_{0.9557}Fe_{0.05})_5Se_8$, *Mol. Cryst. and Liq. Cryst.*, **341**, 39-44 (2000).

Azuma M, Saito T and Takano M: Two New Quantum Spin Compounds: S=1/2 Alternating Chain System, High Pressure Form of $(VO)_2P_2O_7$ and 2D Spin Trimer Compound $La_4Cu_3MoO_{12}$, *J. Phys. Soc. Jpn.*, **69**, 108-113 (2000).

Azuma M, Odaka T, Takano M, Griend D A V, Poeppelmeier K R, Narumi Y, Kindo K, Mizuno Y and Maekawa S: Antiferromagnetic Ordering of S=1/2 Triangles in $La_4Cu_3MoO_{12}$, *Phys. Rev. B*, **62**, R3588-R3591 (2000).

Yamada T, Hiroi Z, Takano M, Nohara M and Takagi H: Spin-1/2 Heisenberg Antiferromagnetic Chains in the Frustrated Spinel Lattice of $GeCu_2O_4$, *J. Phys. Soc. Jpn.*, **69**, 1477-1483 (2000).

IV. Amorphous Materials

Takaishi D, Jin J, Uchino T and Yoko T: Structural Study of $PbO-B_2O_3$ Glasses by X-ray Diffraction and ^{11}B MAS NMR Techniques, *J. Am. Ceram. Soc.*, **83**, 2543-48 (2000)

Jin J, Sakida S, Yoko T and Nogami M: The local structure of Sm-doped aluminosilicate glasses prepared by sol-gel method, *J. Non-Cryst. Solids*, **262**, 183-190 (2000)

Uchino T, Kitagawa Y and Yoko T : Structure, Energies, and Vibrational Properties of Silica Rings in SiO_2 Glass, *Phys. Rev. B*, **61**(1), 234-240 (2000).

Uchino T, Nakaguchi K, Nagashima Y and Kondo T: Prediction of Optical Properties of Commercial Soda-Lime-Silicate Glasses Containing Iron, *J. Non-Cryst. Solids*, **261**, 72-78 (2000).

Uchino T and Yoko T, Structure and Vibrational Properties of Alkali Phosphate Glasses from ab Initio Molecular Orbital Calculations, *J. Non-Cryst. Solids*, **263&264**, 180-188 (2000).

Uchino T, Takahashi M and Yoko T: Structure and Formation Mechanism of Ge E' Center from Divalent Defects in Ge-doped SiO_2 Glass, *Phys. Rev. Lett.*, **84**(7), 1475-1478 (2000).

Uchino T, Takahashi M and Yoko T: Model of Oxygen-Deficiency-Related Defects in SiO_2 Glass, *Phys. Rev. B*, **62**(5), 2983-2986 (2000).

Uchino T, Clary D C and Elliott S R: Mechanism of Photo-induced Changes in the Structure and Optical Properties of Amorphous As_2S_3 *Phys. Rev. Lett.*, **85**(15), 3305-3308 (2000).

Uchino T, Takahashi M and Yoko T: Structure and Paramagnetic Properties of Defect Centers in Ge-doped SiO_2 glass: Localized and Delocalized Ge E' centers *Phys. Rev. B*, **62**(23), 15303-15306 (2000).

Takahashi M and Yoko T: The films prepared by Sol-Gel Method, *J. Cryst. Grow.*, **29**, 2000, 29 (In Japanese)

Monde T, Fukube H, Nemoto F, Yoko T and Konakahara T: Preparation and Surface Properties of Silica-Gel Coating Films Containing Branched-Polyfluoroalkylsilane, *J. Non-Cryst. Solids*, **246**, 54-64 (1999)

Kamiusuki T, Monde T, K. Yano, Yoko T and Konakahara T: Preparation of Branched-Polyfluoroalkylsilane-Coated Silica-Gel Columns and their HPLC Separation Characteristics, *Chromatographia*, **49**, 649-656 (1999)

Kamiusuki T, Monde T, K. Yano, Yoko T and Konakahara T: Interaction between a Solute Molecule and a Fluorocarbon Bonded Layer in Reversed-Phase High-Performance Liquid Chromatography, *J. Colloid and Interface Science*, **220**, 123-127 (1999)

Kamiusuki T, Monde T, Nakayama N, Yano K, Yoko T and Konakahara T: Separation Behavior of Various Organic Compounds on Branched-Polyfuluoroalkylsilane Coated Silica Gel Columns, *J. Chromat. Sci.*, **37**, 388-394 (1999)

Kozuka H, Takahashi Y, Zhao G and Yoko T: Preparation and Photoelectrochemical Properties of Porous Thin Films Composed of Submicron TiO_2 Particles, *Thin Solid Films.*, **358**, 172-79 (2000)

Kondo Y, Kuroiwa Y, Sugimoto N, Manabe T, Ito S, Yoko T and Nakamura A: Ultraviolet Irradiation Effect on the Third-Order Optical Nonlinearlity of CuCl microcrystallite-Doped Glass, *J,*

Opt. Soc. Am. B, **17**, 548-554 (2000)

Narushima S, H. Hosono, Jin J, Yoko T and Shimakawa K: Electronic Transport and Optical Properties of Proton-Implanted Amorphous 2CdO · GeO_2 Films, *J. Non-Cryst. Solids*, **274**, 313-8 (2000)

Sakida S, Jin J and Yoko T: X-Ray Diffraction Study of MO-TeO_2 (M= Zn and Ba) Glasses", *Phys. Chem. Glasses*, **41**, 65-70 (2000)

Sakida S, Hayakawa S and Yoko T: ^{125}Te and ^{51}V Static NMR Study of V_2O_5-TeO_2 Glasses, *J. Phys. Condensed Matter*, **12**, 2579-95 (2000)

FUNDAMENTAL MATERIAL PROPERTIES

I. Molecular Rheology

Watanabe H: Viscoelasticity and Dynamics of Entangled Polymers, *Prog. Polym. Sci.*, **24**, 1253-1403 (1999).

Matsumiya Y, Watanabe H, and Osaki K: Comparison of Dielectric and Viscoelastic Relaxation Functions of cis-Polyisoprenes: Test of Tube Dilation Molecular Picture, *Macromolecules*, **33**, 499-506 (2000).

Karatasos K, Anastasiadis SH, Pakula T, and Watanabe H: On the Loops to Bridges Ratio in Ordered Triblock Copolymers: An Investigation by Dielectric Relaxation Spectroscopy and Computer Simulations", *Macromolecules*, **33**, 523-541 (2000).

Sato T, Watanabe H, and Osaki K: Thermoreversible Physical Gelation of Block Copolymers in a Selective Solvent", *Macromolecules*, **33**, 1686-1691 (2000).

Watanabe H, Sato T, and Osaki K: Concentration Dependence of Loop Fraction in Styrene-Isoprene-Styrene Triblock Copolymer Solutions and Corresponding Changes in Equilibrium Elasticity, *Macromolecules*, **33**, 2545-2550 (2000).

Watanabe H, Kilbey SM, and Tirrell M.: A Scaling Model for Osmotic Energy of Polymer Brushes, *Macromolecules*, **33**, 9146-9151 (2000).

Watanabe H, Sato T, Osaki K, Matsumoto M, Bossev DP, McNamee CE, and Nakahara M: Linear Viscoelastic Behavior of Perfluorooctyl Sulfonate Micelles: Effects of Counter-Ion", *Rheol. Acta*, **39**, 110-121 (2000).

Watanabe H, Matsumiya Y, and Osaki K: Tube Dilation Process in Star-Branched cis-Polyisoprenes, *J. Polym. Sci. Part B: Polym. Phys.*, **38**, 1024-1036 (2000).

Matsumiya Y. and Watanabe H: Entanglement Relaxation of Branched Polymers: Constraint Release and Dynamic Tube Dilation.", Kobunnshi Ronbunshu, **57**, 618-628 (2000) (in Japanese)

Kakiuchi M, Aoki Y, Watanabe H, and Osaki K: Dielectric Behavior of PVC Gels and Sols in Dioctyl Phthalate.", *J. Soc. Rheol. Japan*, **28**, 197-198 (2000).

Y. Takahashi, M. Noda, M. Naruse, T. Kanaya, H. Watanabe, T. Kato, M. Imai, and Y. Matsushita: Apparatus for Small-Angle Neutron Scattering and Rheological Measurements under Sheared Conditions, *J. Soc. Rheol. Japan*, **28**, 187-191 (2000).

Osaki K, Inoue T and Isomura T: Stress Overshoot of Polymer Solutions at High Rates of Shear, *Journal of Polymer Science: Part B: Polymer Physics*, **38**, 1917-1925 (2000).

Osaki K, Inoue T and Isomura T: Stress Overshoot of Polymer Solutions at High Rates of Shear; Polystyrene with Bimodal Molecular Weight Distribution, *Journal of Polymer Science: Part B: Polymer Physics*, **38**, 2043-2050 (2000).

Osaki K, Inoue T and Isomura T: Stress Overshoot of Polymer Solutions at High Rates of Shear: Semidilute Polystyrene Solutions with and without Chain Entanglement, *Journal of Polymer Science: Part B: Polymer Physics*, **38**, 3271-3276 (2000).

Inoue T: Viscoelasticity and Birefrigence of Amorphous Polymers in the Glass Transition Zone, *J. Soc. Rheol. Japan*, **28**, 167-175 (2000).

Inoue T, Fujiwara K, Ryu D-S, Osaki K, Fuji M and Sakurai K: Viscoelasticity and Birefringence of Low Birefringent Polyesters, *Polymer J.*, **32**, 411-414 (2000).

Inoue T, Onogi T and Osaki K: Dynamic Birefringence of Oligostyrene Polystyrene, *Journal of Polymer Science: Part B: Polymer Physics*, **38**, 954-964 (2000).

Inoue T, Osaki K, Morishita H, Tamura H and Sakamoto S: Viscoelasticity and Morphology of Soft Polycarbonate as a Substitute for Poly (vinyl Chloride), *Zairyo*, **49**, 1291-1297 (2000).

Inoue T, Nomura S, Ogawa T and Osaki K: Sub-Relaxation of Bisphenol A Polycarbonate Studied with Dynamic Birefringence, *Zairyou*, **49**, 1298-1301 (2000).

II. Polymer Materials Science

Matsuba G, Kaji K, Nishida K, Kanaya T and Imai M: Conformational Change and Orientational Fluctuations Prior to the Crystallization of Syndiotactic Polystyrene, *Macromolecules*, **32**, 8932-8937 (1999).

Nishida K, Shibata M, Kanaya T and K. Kaji: Imcompatibility of Polyelectrolyte Solutions - Mixed Solutions of PSSNa and PVSNa, *Polymer*, **42**, 1501-1505 (2000).

Kanaya T, Buchenau U, Koizumi S, Tsukushi I and K. Kaji: Non-Gaussian Behavior of Crystalline and Amorphous Phases of Polyethylene, *Phys. Rev.*, **B61**, R6451-R6454 (2000).

Kanaya T, Tsukushi I, Kaji K, Bartos J and Kristiac J: Heterogeneity of Amorphous Polymers as Studied by Quasielastic Neutron Scattering and Positron Annihilation Spectroscopy, *J. Phys. IV France*, **10**, 317-320 (2000).

Yamamuro O, Harabe K, Matsuo T, Takeda K, Tsukushi I and Kanaya T: Boson Peaks of Glassy Mono- and Polyalcohols Studied by Inelastic Neutron Scattering, *J. Phys.: Condens. Matter*, **12**, 5143-5154 (2000).

Takeshita H, Kanaya T, Nishida K and Kaji K: Ultra-small-angle Neutron Scattering Studies on Phase Separation of Poly(vinyl alcohol) Gels, *Phys. Rev.*, **E61**, 2125-2128 (2000).

Matsuba G, Kanaya T, Saito M, Kaji K and Nishida K: Further Evidence of Spinodal Decomposition during the Induction Period of Polymer Crystallization: Time-resolved Small-angle X-ray Scattering Prior to Crystallization of Poly (ethylene naphthalate), *Phys. Rev.*, **E62**, R1496-R1500 (2000).

Kaji K: Crystalline and Amorphous Polymers, Applications of Neutron Scattering to Soft Condensed Matter, ed by B. J. Gabrys, Gordon and Breach Science Publishers, Australia, Chapter 5, 107-161 (2000).

III. Molecular Motion Analysis

Kuwabara K, Kaji H, Tsuji M, Horii F: Crystalline-Noncrystalline Structure and Chain Diffusion Associated with the 180º Flip Motion for Polyethylene Single Crystals As Revealed by Solid-State ^{13}C NMR Analyses, *Macromolecules*, **33**, 7093-7100 (2000)

Ohira Y, Horii F, Nakaoki T: Crystal Transformation Behavior and Structural Changes of the Planar Zigzag Form for Syndiotactic Polypropylene, *Macromolecules*, **33**, 5566-5573 (2000)

Kuwabara K, Kaji H, Horii F: Solid-State ^{13}C NMR Analyses for the Structure and Molecular Motion in the Relaxation Temperature Region for Metallocene-Catalyzed Linear Low-Density Polyethylene, *Macromolecules*, **33**, 4453-4462 (2000)

Nakaoki T, Yamanaka T, Ohira Y, Horii F: Dynamic FT-IR Analysis of the Crystallization to the Planar Zigzag Form for Syndiotactic polypropylene, *Macromolecules*, **33**, 2718-2721 (2000).

Ohira Y, Horii F, Nakaoki T: Spontaneous Crystallization Process of the Planar Zigzag Form at 0 ºC from the Melt for Syndiotactic Polypropylene, *Macromolecules*, **33**, 1801-1806 (2000)

Schacht J, Zugenmaier P, Buivydas M, Komitov L, Stebler B, Largerwall S T, Gouda F, Horii F: Intermolecular and Intramolecular Reorientations in Nonchiral Smectic Liquid-Crystalline Phases Studied by Broadband Dielectric Spectroscopy, *Phys. Rev. E*, **61**, 3926-3935 (2000)

Kuwabara K, Horii F, Ogawa Y: Solid-State NMR Analyses of the Crystalline Phase Transitions for 1, 20-eicosanediol Crystals, *J. Mol. Struct.*, **525**, 163-171 (2000)

Masuda K, Kaji H, Horii F: CP/MAS ^{13}C NMR Analyses of Hydrogen Bonding and the Chain Conformation in the Crystalline and Noncrystalline Regions for Poly (vinyl alcohol) Films. *J. Polym. Sci. Polym. Phys. Ed.*, **38**, No.1, 1-10 (2000)

Horii F: Analyses by Spectroscopic Methods, *Encyclopedia of Cellulose*, Asakura, Tokyo, 2000, p.87-92 (in Japanese)

Horii, F: New Cellulosic Materials, *Comvertech*, **28**, No.2, 54-56 (2000) (in Japanese)

Kawanishi H, Tsunashima T, Horii F: Dynamic Light Scattering Study of Structural Changes of Cellulose Diacetate in Solution under Couette Flow, *Macromolecules*, **33**, No.6, 2092-2097 (2000)

Tsunashima Y: Polymer Chain Dynamics in Solution in Couette Flow, *Statistical Physics*, Tokuyama M and Stanley H E, Eds., Amer. Inst. Phys. New York, 2000, pp.326-328

Tsunashima, Y: Dilute Solution Properties of Cellulose Derivatives, *Encyclopedia of Cellulose*, Asakura, Tokyo, 2000, p.253-257 (in Japanese)

Kaji H, Schmidt-Rohr K: Conformation and Dynamics of Atactic Poly(acrylonitrile). 1. Trans/Gauche Ratio from Double-Quantum Solid-State ^{13}C NMR of the Methylene Groups, *Macromolecules*, **33**, 5169-5180 (2000).

Tsunashima Y, Suzuki S: Dynamics of a High-Molecular-Weight PS-PMMA Diblock Copolymer in Mixed Selective Solvents: 1. Unimer-Micelle Coexistence, *J. Phys. Chem., B*. **103**, No.41, 8675-8685 (1999)

Kurata M and Tsunashima Y: *Viscosity-Molecular Weight Relationships and Unperturbed Dimensions of Linear Chain Molecules, Polymer Handbook, 4th ed.*; Brandrup J and Immergut E H, Eds., John Wiley & Sons, New York, 1999, **Chapter VII**, pp. 1-83

ORGANIC MATERIALS CHEMISTRY

I. Polymeric Materials

Fukuda T, Goto A and Ohno K: (Feature Article) Mechanisms and Kinetics of Controlled Radical Polymerizations, *Macromol. Rapid Commun.*, **21**, 151-165 (2000).

Fukuda T and Goto A: Kinetics of Living Radical Polymerization, *ACS Symp. Ser.*, **768**, 27-38 (2000).

Goto A and Fukuda T: Comparative Study on Activation Rate Constants for Some Styrene/Nitroxide Systems, *Macromol. Chem. Phys.*, **201**, 2138-2142 (2000).

Goto A, Tsujii Y and Fukuda T: Effects of Acetic Anhydride on the Activation and Polymerization Rates in Nitroxide-Mediated Polymerization of Styrene, *Chem. Lett.*, 788-789 (2000).

Ejaz M, Ohno K, Tsujii Y and Fukuda T: Controlled Grafting of a Well-Defined Glycopolymer on a Solid Surface by Surface-Initiated Atom Transfer Radical Polymerization, *Macromolecules*, **33**, 2870-2874 (2000).

Yamamoto S, Ejaz M, Tsujii Y, Matsumoto M and Fukuda T: Surface Interaction Forces of Well-Defined, High-Density Polymer Brushes Studied by Atomic Force Microscopy. 1. Effect of Chain Length, *Macromolecules*, **33**, 5602-5607 (2000).

Yamamoto S, Ejaz M, Tsujii Y and Fukuda T: Surface Interaction Forces of Well-Defined, High-Density Polymer Brushes Studied by Atomic Force Microscopy. 2. Effect of Graft Density, *Macromolecules*, **33**, 5608-5612 (2000).

Yamamoto S, Tsujii Y and Fukuda T: Atomic Force Microscopic Study of Stretching Single Polymer Chain in Polymer Brush, *Macromolecules*, **33**, 5995-5998 (2000).

Okamura H, Miyazono K, Minoda M, Komatsu K, Fukuda T and Miyamoto T: Synthesis of Highly Water-Soluble C_{60} End-Capped Vinyl Ether Oligomers with Well-Defined Structure, *J. Polym. Sci., Polym. Chem. Ed.*, **38**, 3578-3585 (2000).

Minoda M, Wataoka I, Fukuda T and Miyamoto T: Controlled Synthesis of Poly(macromonomer)s and their Properties, *Kasen-Kouenshu*, **57**, 81-88 (2000) (in Japanese).

Fukuda T: Comments on 'Living Polymerization: Rationale for Uniform Terminology'by Darling et al., *J. Polym. Sci., Polym. Chem. Ed.*, **38**, 1719-1720 (2000).

II. High-Pressure Organic Chemistry

Ohtsuki T, Masumoto K, Shikano K, Sueki K, Tanaka T, Komatsu K: Direct Preparation of Radioactive Fullerenes as a Tracer for Applications, *Biological Trace Element Research*, **71-72**, 489-498 (1999).

Nagel P, Pasler V, Lebedkin S, Soldatov A, Meingast C, Sundqvist B, Persson P-A, Tanaka T, Komatsu K, Buga S, Inaba A: C_{60} One- and Two-dimensional Polymers, Dimers, and Hard Fullerite: Thermal Expansion, Anharmonicity, and Kinetics of Depolymerization, *Chem. Rev. B.*, **60**, 16920-16927 (1999).

Komatsu K, Fujiwara K, Tanaka T, Murata Y: The Fullerene Dimer C_{120} and Related Carbon Allotropes, *Carbon*, **38**, 1529-1534 (2000).

Komatsu K, Fujiwara K, Murata Y: The Fullerene Cross-Dimer C_{130}: Synthesis and Properties, *Chem. Commun.*, **2000**, 1583-1584.

Komatsu K, Fujiwara K, Murata Y: The Mechanochemical Synthesis and Properties of the Fullerene Trimer C_{180}, *Chem. Lett.*, **2000**, 1016-1017.

Nishinaga T, Izukawa Y, Komatsu K: The First Cyclic π-Conjugated Silylium Ion: The Silatropylium Ion Annelated with Rigid σ-Frameworks, *J. Am. Chem. Soc.*, **122**, 9312-9313 (2000).

Matsuura A, Nishinaga T, Komatsu K: The Structural Studies on the Radical Cations of Benzene, Naphthalene, Biphenylene, and Anthracene Fully Annelated with Bicyclo[2.2.2]octene Frameworks, *J. Am. Chem. Soc.*, **122**, 10007-10016 (2000).

Komatsu K, Murata Y, Kato N: Solid-State Reaction of C_{60} with N-Containing Aromatics to Give Novel Addition Products, *Fullerenes 2000: Functionalized Fullerenes*, **9**, 20-27 (2000).

Cho HS, Kim SK, Kim D, Fujiwara K, Komatsu K: Ultrafast Energy Relaxation Dynamics of C_{120}, a [2+2]-bridged C_{60} Dimer, *J. Phys. Chem. A*, **104**, 9666-9669 (2000).

Murata Y, Komatsu K: Mechanochemistry: Application to the Chemistry of Fullerenes, *Kikan Fullerene*, **8** (No.2), 137-151 (2000) (in Japanese).

Komatsu K, Murata Y: Organic Chemistry of Fullerenes: A Fascinating Molecule, C_{60}, *Gendai-Kagaku*, **2000**, No. 351, 46-53 (in Japanese).

Komatsu K: Organic Reactions without Solvent, New Trends in Organic Synthesis, *Kikan Kagaku Sosetsu*, **2000**, 163-175 (in Japanese).

SYNTHETIC ORGANIC CHEMISTRY

I. Synthetic Design

Yamaguchi S, Jin R-Z, Itami Y, Goto T and Tamao K: The First Synthesis of Well-Defined Poly(2,5-silole), *J. Am. Chem. Soc.*, **121**, 10420-10421 (1999).

Kawachi A and Tamao K: Structures of [(Amino)phenylsilyl] lithiums and Related Compounds in Solution and in the Solid State, *J. Am. Chem. Soc.*, **122**, 1919-1926 (2000).

Yamaguchi S, Akiyama S and Tamao K: Tri-9-anthrylborane and Its Derivatives: New Boron-Containing-Electron Systems with Divergently Extended-Conjugation through Boron, *J. Am. Chem. Soc.*, **122**, 6335-6336 (2000).

Yamaguchi S, Akiyama S and Tamao K: Photophysical Properties Changes Caused by Hypercoordination of Organosilicon Compounds: From Trianthrylfluorosilane to Trianthryldifluorosilicate, *J. Am. Chem. Soc.*, **122**, 6793-6794 (2000).

Tamao K, Asahara M, Saeki T and Toshimitsu A: Enhanced Nucleophilicity of Ambiphilic Silylene and Silylenoid Bearing 8-(Dimethylamino)-1-naphthyl Group, *J. Organomet. Chem.*, **600**, 118-123 (2000).

Kawachi A and Tamao K: Mixed Reagent (Aminosilyl)lithium/i-PrMgBr for the Synthesis of Functionalized Oligosilanes, *J. Organomet. Chem.*, **601**, 259-266 (2000).

Tamao K and Yamaguchi S: Introduction to the Chemistry of Interelement Linkage, *J. Organomet. Chem.*, **611**, 3-4 (2000).

Tamao K and Yamaguchi S: New Type of Polysilanes: Poly(1,1-silole)s, *J. Organomet. Chem.*, **611**, 5-11 (2000).

Tamao K, Asahara M and Toshimitsu A: Trimerization of a Divalent Silicon Species Bearing the 8-Dimethylamino-1-naphthyl Group Accompanied by the Migration of Methyl and Dimethylamino Groups, *Chem. Lett.*, 658-659 (2000).

Tamao K, Asahara M, Saeki T, Feng S-G, Kawachi A and Toshimitsu A: Nucleophilic Addition of a Divalent Silicon Species Bearing the 8-Dimethylamino-1-naphthyl Group to Diphenylacetylenes to Form the 1-Amino-1-silaphenalene Skeleton, *Chem. Lett.*, 660-661 (2000).

Kawachi A, Maeda H and Tamao K: Stereoselective Formation of Cyclopropylsilane through Intramolecular Rearrangement of [(Allyloxy)dimesitylsilyl]lithiums, *Chem. Lett.*, 1216-1217 (2000).

Yamaguchi S, Endo T, Uchida M, Izumizawa T, Furukawa K and Tamao K: Toward New Materials for Organic Electroluminescent Devices: Synthesis, Structures, and Properties of a Series of 2,5-Diaryl-3,4-diphenylsiloes, *Chem. Eur. J.*, **6**, 1683-1692 (2000).

Tamao K, Tsuji H, Terada M, Asahara M, Yamaguchi S and Toshimitsu A: Conformation Control of Oligosilanes Based on Configurationally Constrained Bicyclic Disilane Units, *Angew. Chem. Int. Ed.*, **39**, 3287-3290 (2000).

Yamaguchi S, Goto T and Tamao K: Silole-Thiophene Alternating Copolymers with Narrow Band Gaps, *Angew. Chem. Int. Ed.*, **39**, 1695-1697 (2000).

Tamao K: New Aspects of Pentacoordinate Organosilicon Compounds Based on the X-ray Structure Determination, *The Rigaku-Denki Journal*, **31**, 32-37 (2000) (in Japanese).

Tamao K: New Discoveries Impossible with a Sole Chemist, *Journal of Synthetic Organic Chemistry, Japan*, **58**, 450-452 (2000) (in Japanese).

II. Fine Organic Synthesis

Kawabata T, Suzuki H, Nagae Y, Fuji K: A Chiral Nonracemic Enolate with Dynamic Axial Chirality: Direct Asymmetric α-Methylation of α-Amino Acid Derivatives, *Angew. Chem. Int. Ed.*, **39**, 2155-2157 (2000)

Kawabata T, Fuji K: Memory of Chirality: Alkylation of Amino Acid Derivatives, *J. Syn. Org. Chem. Jpn.*, **58**, 1095-1099 (2000)

Kawabata T, Chen J, Suzuki H, Nagae Y, Kinoshita T, Chancharunee S, Fuji K: Memory of Chirality in Diastereoselective Alkylation of Isoleucine and *allo*-Isoleucine Derivatives, *Org. Lett.*, **2**, 3883-3885 (2000)

Tsubaki K, Tanaka H, Furuta T, Kinoshita T, Fuji K: Recognition

of the Chain Length of Diamines by a *meso*-Ternaphthalene Derivative with Two Crown Ethers, *Tetrahedron Lett.*, **41**, 6089-6093 (2000)

Tsubaki K, Mukoyoshi K, Ohtsubo T, Fuji K: The '2+1' Construction of Homooxacalix[3]arenes Possessing Different Substituents on Threir Upper Rims, *Chem. Pharm. Bull.*, **48**, 882-884 (2000)

Fuji K, Ohnishi H, Moriyama S, Tanaka K, Kawabata T, Tsubaki K: Palladium-Catalyzed Asymmetric Allylic Alkylation with a Chiral Monodentate Phosphine Ligand: 8-Diphenylphosphino-8'-methoxy-1,1'-binaphthyl, *Synlett*, **2000**, 351-352

Takasu, K, Miyamoto H, Tanaka K, Taga T, Bando M, Fuji K: Conformational Difference between Mono- and Diprotonated cis-2,5-Diphenylpiperazinium Salts in the Solid State, *Chem. Pharm. Bull.*, **48**, 2014-2016 (2000)

Fuji K: Asymmetric Synthesis beyond Common Knowledge of Chemistry, *Kagaku to Kogyo*, **74**, 515-519 (2000) (in Japanese)

BIOORGANIC CHEMISTRY

I. Bioorganic Reaction Theory

Tokitoh N, Ito M and Okazaki R: New Aspects of Boron-containing Low-Coordinate Compounds, *Main Group Chemistry News*, **7**, 27-36 (2000).

Wakita K, Tokitoh N, Okazaki R and Nagase S: Synthesis and Properties of an Overcrowded Silabenzene Stable at Ambient Temperature, *Angew. Chem. Int. Ed.*, **39**, 636-638 (2000).

Takeda N, Tokitoh N and Okazaki R: Reaction of a Stable Silylene-Isocyanide Complex with Nitrile Oxides: A New Approach to the Generation of a Silanone, *Chem. Lett.*, 244-245 (2000).

Takeda N, Tokitoh N and Okazaki R: A Novel Reaction Mode in the Cycloaddition of Thermally Generated Silylenes with Conjugated Dienes, *Chem. Lett.*, 622-623 (2000).

Hatano K, Tokitoh N, Takagi N and Nagase S: The First Stable Heteracyclopropabenzene: Synthesis and Crystal Structure of a Silacyclopropabenzene, *J. Am. Chem. Soc.*, **122**, 4829-4830 (2000).

Wakita K, Tokitoh N, Okazaki R, Takagi N and Nagase S: Crystal Structure of a Stable Silabenzene and Its Photochemical Valence Isomerization into the Corresponding Silabenzvalene, *J. Am. Chem. Soc.*, **122**, 5648-5649 (2000).

Sasamori T, Takeda N and Tokitoh N: Synthesis of a Stable Stibabismuthene; The First Compound with an Antimony-Bismuth Double Bond, *Chem. Commun.*, 1353-1354 (2000).

Saiki T, Akine S, Goto K, Tokitoh N, Kawashima T and Okazaki R: Structural Elucidation of *m*-Xylylene-Bridged Calix[6]arenes with Four Uncapped Hydroxy Groups, *Bull. Chem. Soc. Jpn.*, **73**, 1893-1902 (2000).

Wakita K, Tokitoh N and Okazaki R: Separation of Orientational Disorder in the X-Ray Analysis of the Kinetically Stabilized 2-Silanaphthalene, *Bull. Chem. Soc. Jpn.*, **73**, 2157-2158 (2000).

Okazaki R and Tokitoh N: Heavy Ketones, the Heavier Element Congeners of a Ketone, *Acc. Chem. Res.*, **33**, 625-630 (2000).

Saiki T, Goto K, Tokitoh N, Goto M and Okazaki R: Syntheses and Structures of Novel *m*-Xylylene-Bridged Calix[6]arenes: Stabilization of a Sulfenic Acid in the Cavity of Calix[6]arene, *J. Organomet. Chem.*, **611**, 146-157 (2000).

Tokitoh N: New Aspects in the Chemistry of Low-coordinated Interelement Compounds of Heavier Group 15 Elements, *J. Organomet. Chem.*, **611**, 217-227 (2000).

Tokitoh N and Okazaki R: Recent Topics in the Chemistry of Heavier Congeners of Carbenes, *Coord. Chem. Rev.*, **210**, 251-277 (2000).

Tokitoh N and Ando W: Thiirenes and Their Derivatives, Selenirenes, and Tellurirenes., In *Science of Synthesis*, Vol. 9, Eds. Belllus D, Ley S V, Noyori R, Regitz M, Reider P J, Schaumann E, Shinkai I, Thomas E J and Trost B M, Vol. Ed. Maas G, George Thieme Velag, Stuttgart, New York, 43-65 (2000)

Matsuda T, Harada T, Nakajima N, Itoh T, and Nakamura K: Two Classes of Enzymes of Oposite Stereochemistry in an Organism: One for Fluorinated and Another for Non-fluorinated Substrate, *J. Org. Chem.*, **65**, 157-163 (2000).

Matsuda T, Harada T, Nakajima N, and Nakamura K: Mechanism for Improving Stereoselectivity for Asymmetric Reduction Using Acetone Powder of Microorganism, *Tetrahedron Lett.*, **41**, 4135-4138 (2000).

Matsuda T, Harada T, and Nakamura K: Alcohol Dehydrogenase is Active in Supurcritical Carbon Dioxide, *J. Chem. Soc. Chem. Commun.*, 1367-1368 (2000).

Nakamura K, Yamanaka R, Tohi K, and Hamada H: Cyanobacterium-Catalyzed Asymmetric Reduction of Ketones, *Tetrahedron Lett.*, **41**, 6799-6802 (2000).

Nakamura K, Fujii M, and Ida Y: Asymmetric Reduction of Ketones by Geotrichum candidum in the Presence of Amberlite XAD, a Solid Organic Solvent, *J. Chem. Soc. Perkin I*, 3205-3211 (2000).

Ishihara K, Yamaguchi H, Hamada H, Nakamura K, Nakajima N: Asymmetric Reduction of α-Keto Esters with Thermophilic Actinomycete: Purification and Chacterization of α-Keto Ester Reductase from Streptomyces Thermocyaneoviolaceus IFO 14271, *J. Mol. Cat. B: Enzymatic*, **10**, 419-428 (2000).

Ishihara K, Yamaguchi H, Hamada H, Nakajima N, Nakamura K: Stereocontrolled Reduction of α-Keto Esters with Thermophilic Actinomycete, Streptomyces Thermocyaneoviolaceus IFO 14271, *J. Mol. Cat. B: Enzymatic*, **10**, 429-434 (2000).

Shioji K, Matsuo A, Okuma K, Nakamura K, Ohno A: Lipase-catalyzed Kinetic Resolution of Racemic Seven-membered Substituted Lactones, *Tetrahedron Lett.*, **41**, 8799 -8802 (2000).

Kawai Y, Matsuo T and Ohno A: Kinetic Study on Conformational Effect in Hydrolysis of *p*-Nitroanilides Catalyzed by α-Chymotrypsin, *J. Chem. Soc., Perkin Trans. 2*, 887-891 (2000).

Kimura T, Tsujimura K, Mizusawa S, Ito S, Kawai Y, Ogawa S and Sato R: Photolytic Preparation, Structure, and Electrochemical Properties of Thianthrene Derivatives Bearing Trithiole and Dithian Rings, *Tetrahedron Lett.*, **41**, 1801-1805 (2000).

Ohno A, Oda S, Ishikawa Y and Yamazaki N: $NAD(P)^+$-NAD(P)H Models. 90. Stereoselection Controlled by Electronic Effect of a Carbonyl Group in Oxidation of NAD(P)H Analog, *J. Org. Chem.*, **65**, 6381-6387 (2000).

II. Bioactive Chemistry

Imanishi M, Hori Y, Nagaoka M and Sugiura Y: DNA-Bending Finger. Artificial Design of 6-Zinc Finger Peptides with Polyglycine Linker and Induction of DNA Bending. *Biochemistry*, **39**, 4383-4390 (2000).

Okuno Y, Iwashita T and Sugiura Y: Structural Basis for Reaction Mechanism and Drug Delivery System of Chromoprotein Antitumor Antibiotic C-1027. *J.Am.Chem.Soc.*, **122**, 6848-6854 (2000).

Hori Y, Suzuki K, Okuno Y, Nagaoka M, Futaki S and Sugiura Y: Artificial Zinc Finger Peptide Containing a Novel His_4 Domain. *J.Am.Chem.Soc.*, **122**, 7648-7653 (2000).

Araki M, Okuno Y and Sugiura Y: Expression Mechanism of the Allosteric Interactions in a Ribozyme Catalysis. *Nucleic Acids Sym.Ser.*, **44**, 205-206 (2000).

Hori Y, Suzuki K, Okuno Y, Nagaoka M, Futaki S and Sugiura Y: The Engineering, Structure, and DNA Binding Properties of a Novel His4-Type Zinc Finger Peptide. *Nucleic Acids Sym.Ser.*, **44**, 295-296 (2000).

Sugiura Y: Molecular Mechanisms of DNA Recognition and Function by Bioactive Compounds. *Yakugaku Zasshi*, **120**, 1409-1418 (2000) (in Japanese).

Nagaoka M and Sugiura Y: Artificial Zinc Finger Peptides: Creation, DNA Recognition, and Gene Regulation. *J. Inorg. Biochem.*, **82**, 57-63 (2000).

Futaki S, Suzuki T, Ohashi W, Yagami T, Tanaka S, Ueda K and Sugiura Y: Intracellular Delivery of Synthetic Peptides Mediated by Tat-Related Peptides. Peptide Science 1999, ed by N Fujii, Protein Research Foundation, 241-244 (2000).

Monoi H, Futaki S, Kugimiya S, Minakata H and Yoshihara K: Poly-L-Glutamine Forms Cation Channels. Relevance to the Pathogernesis of the Polyglutamine Diseases. *Biophysical J.*, **78**, 2892-2899 (2000).

Yagami T, Kitagawa K, Aida C, Fujiwara H and Futaki S: Stabilization of a Tyrosine O-Sulfate Residue by a Cationic Functional Group. Formation of a Conjugate Acid-Base Pair. *J.Peptide Res.*, **56**, 239-249 (2000).

Sugiura Y and Nagaoka M: Design and Development of New Reaction Systems Based on Nucleic Acid Recognition. *Kikan Kagaku Sosetsu*, **47**, 231-240 (2000) (in Japanese).

III.Molecular Clinical Chemistry

Tanaka S, Takehashi M, Matoh N and Ueda K: α-Synuclein / NACP and neurodegeneration. In "*Neuroscientific Basis of Dementia*" (*C. Tanaka, P. L. McGeer, and Y. Ihara, eds.*), *Birkhäuser Verlag, Basel*, 137-141 (2000)

Tanaka S, Takehashi M, Matoh N, Masliah E and Ueda K: Interaction of NAC with Aβ protein in neuronal cell injury in Alzheimer's disease, *Neurobiol Aging*, **21**, S111 (2000)

Ueda K: Advanced technology in gene diagnosis, *46th Scientific Congress* "*International Meeting*", *Egyptian Society of Clinical Chemistry* Program & Abstracts, 8 (2000)

Ueda K: Expanding molecular technology, *2nd IFCC-Roche Conference* "*Human Genomics*; *The Basis of the Medicine of Tomorrow*" Abstracts 70 (2000)

Tanaka S, Matoh N, Masliah E and Ueda K: Microsatellite polymorphisms in the *CYP2D* locus in Lewy body diseases, *2nd IFCC-Roche Conference* "*Human Genomics*; *The Basis of the Medicine of Tomorrow*", Abstracts 110 (2000)

Ueda K: Diagnosis of hereditary diseases and bioethics, In "*Basics of modern medicine*" (*Kagawa Y and K Sasazuki, eds*), *Iwanamishoten*, 179-199 (2000) (in Japanese)

Takehashi M, Tanaka S and Ueda K: A pathological role of α-synuclein in neurodegenerative diseases, *Saishin Igaku*, **55**, 2240-2249 (2000) (in Japanese)

Tanaka S: Gene diagnosis of Alzheimer's disease and related disorders, *Rinsho Byouri*, **48**, 621-624 (2000) (in Japanese)

MOLECULAR BIOFUNCTION

I. Molecular Biocatalyst

Sakata K: β-Primeverosidase relationship with floral tea aroma formation during processing of oolong tea and black tea. In "Caffeinated Beverages. Health Benefits, Physiological Effects, and Chemistry, ACS Symposium Series 754," ed. by Parliament, T. H., Ho, C. and Schieberie, P., American Chemical Society, Washington, DC, 2000, pp. 327-335.

Lu Y, Umeda T, Yagi A, Sakata K, Chaudhuri T, Ganguly D K and Sarma S: Triterpenoid saponins from the roots of tea plant (*Camellia sinensis* var. *assamica*). *Phytochemistry*, **53** (8), 941-946 (2000).

Moon J-H, Ma S-J., Lee H-H, Watanabe N, Yagi A, Sakata K and Park K-H: Isolation and structural determination of a novel antimicrobial compound from the root of *Pulsatilla koreana. Natural Product Letters*, **14** (4), 311-317 (2000).

Inoue M, Hiratake J, Suzuki H, Kumagai H and Sakata K: Identification of Catalytic Nucleophile of E. coli γ-Glutamyltranspeptidase by γ-Monofluorophosphono Derivative of Glutamic Acid: N-Terminal Thr-391 in Small Subunit is the Nucleophile, *Biochemistry*, **39**, 7764-7771 (2000).

Mano J, Babiychuk E, Belles-Boix E, Hiratake J, Kimura A, Inze D, Kushnir S and Asada K: A Novel NADH:diamide Oxidoreductase Activity in Arabidopsis thaliana P1 ζ-crystallin, *Eur. J. Biochem*. **267**, 3661-3671 (2000).

Fujii R, Hiratake J: Evolution of Enzymes -Artificial Alteration of Enzymes by Directed Evolution, *Chemistry Today*, **354**, 36-43 (2000) (in Japanese).

Hiratake J: Catalytic Antibodies and Enzymes: How do they look alike?, *BIOClinica*, **15**, 1162-1167 (2000) (in Japanese)

Ohta D, Fujimori K, Mizutani M, Nakayama Y, Kunpaisal-Hashimoto R, Munzer S, Kozaki A: Molecular cloning and characterization of ATP-phosphoribosyl transferase from Arabidopsis, a key enzyme in the histidine biosynthetic pathway, *Plant Physiol.*, **122**, 907-14 (2000)

Shimizu B, Fujimori A, Miyagawa H, Ueno T, Watanabe K, Ogawa K: Resistance against fusarium wilt induced by non-pathogenic Fusarium in *Ipomoea tricolor, J. Pestic. Sci.*, **25**, 365-372 (2000)

II. Molecular Microbial Science

Ichiyama S, Kurihara T, Li Y-F, Kogure Y, Tsunasawa S, Esaki N: Novel Catalytic Mechanism of Nucleophilic Substitution by Asparagine Residue Involving Cyanoalanine Intermediate Revealed by Mass Spectrometric Monitoring of an Enzyme Reaction, *J. Biol. Chem.*, **275**, 40804-40809 (2000).

Gutierrez A, Yoshimura T, Fuchikami Y, Esaki N: Modulation of Activity and Substrate Specificity by Modifying the Backbone Length of the Distant Interdomain Loop of D-amino Acid Aminotransferase, *Eur. J. Biochem.*, **267**, 7218-7223 (2000).

Kato S, Mihara H, Kurihara T, Yoshimura T, Esaki N: Gene Cloning, Purification, and Characterization of Two Cyanobacterial NifS Homologs Driving Iron-Sulfur Cluster Formation, *Biosci. Biotechnol. Biochem.*, **64**, 2412-2419 (2000).

Okubo Y, Yokoigawa K, Esaki N, Soda K, Misono H: High Catalytic Activity of Alanine Racemase from Psychrophilic *Bacillus Psychrosaccharolyticus* at High temperatures in the Presence of Pyridoxal 5'-phosphate, *FEMS Microbiol. Lett.*, **192**, 169-173 (2000).

Inoue H, Inagaki K, Adachi N, Tamura T, Esaki N, Soda K: Role of Tyrosine 114 of L-Methionine γ-lyase from *Pseudomonas putida, Biosci. Biotechnol. Biochem.*, **64**, 2336-2343 (2000).

Kurihara T, Esaki N: Biogenesis of Iron-sulfur Clusters, Seikagaku (in Japanese), **72**, 1266-1269 (2000).

Jhee K-H, Yoshimura T, Miles EW, Takeda S, Miyahara I, Hirotsu K, Soda K, Kawata Y, Esaki N: Stereochemistry of the Transamination Reaction Catalyzed by Aminodeoxychorismate Lyase from *Escherichia coli*: Close Relationship between Fold Type and Stereochemistry, *J. Biochem.*, **128**, 679-686 (2000).

Motoshima H, Inagaki K, Kumasaka T, Furuchi M, Inoue H, Tamura T, Esaki N, Soda K, Tanaka N, Yamamoto M, Tanaka H: Crystal Structure of the Pyridoxal 5'-phosphate Dependent L-Methionine γ-Lyase from *Pseudomonas putida, J. Biochem.*, **128**, 349-354 (2000).

Kurihara T, Esaki N, Soda K: Bacterial 2-haloacid Dehalogenases: Structures and Reaction Mechanisms, *J. Mol. catal. B*: *Enzymatic.*, **10**, 57-65 (2000).

Nakai T, Mizutani H, Miyahara I, Hirotsu K, Takeda S, Jhee K-H, Yoshimura T, Esaki N: Three-Dimensional Structure of 4-Amino-4-Deoxychorismate Lyase from *Escherichia coli., J. Biochem.*, **128**, 29-38 (2000).

Lacourciere GM, Mihara H, Kurihara T, Esaki N, Stadtman TC: *Escherichia coli* Nifs-like proteins provide selenium in the pathway for the biosynthesis of selenophosphate, *J. Biol. Chem.*, **275**, 23769-23773 (2000).

Mihara H, Kurihara T, Yoshimura T, Esaki N: Kinetic and mutational studies of three NifS homologs from *Escherichia coli*: mechanistic difference between L-cysteine desulfurase and L-selenocysteine lyase reactions, *J. Biochem.*, **127**, 559-567 (2000).

Takita T, Shimizu N, Sukata T, Hashimoto S, Akita E, Yokota T, Esaki N, Soda K, Inoue K, Tonomura B: Lysyl-tRNA Synthetase of *Bacillus stearothermophilus* Molecular Cloning and Expression of the Gene, *Biosci. Biotechnol. Biochem.*, **64**, 432-437 (2000).

Mihara H, Kurihara T, Watanabe T, Yoshimura T, Esaki N: cDNA Cloning, Purification, and Characterization of Mouse Liver Selenocysteine Lyase. Candidate for selenium delivery protein in selenoprotein synthesis, *J. Biol. Chem.*, **275**, 6195-200 (2000)

Fujii T, Maeda M, Mihara H, Kurihara T, Esaki N, Hata Y: Structure of a NifS Homologue: X-ray Structure Analysis of CsdB, an *Escherichia coli* Counterpart of Mammalian Selenocysteine Lyase. *Biochemistry*, **39**, 1263-1273 (2000).

Shimoni Y, Kurihara T, Ravazzola M, Amherdt M, Orci L, Schekman R: Lst1p and Sec24p cooperate in sorting of the plasma membrane ATPase into COPII vesicles in *Saccharomyces cerevisiae*, *J. Cell Biol.*, **151**, 973-984 (2000).

Kurihara T, Hamamoto S, Gimeno RE, Kaiser CA, Schekman R, and Yoshihisa T: Sec24p and Iss1p function interchangeably in transport vesicle formation from the endoplasmic reticulum in *Saccharomyces cerevisiae, Mol. Biol. Cell*, **11**, 983-998 (2000).

MOLECULAR BIOLOGY AND INFORMATION

I. Biopolymer Structure

Fujii T, Maeda M, Mihara H, Kurihara T, Esaki N and Hata Y: Structure of a NifS Homologue: X-ray Structure Analysis of CsdB, an *Escherichia coli* Counterpart of Mammalian Selenocysteine Lyase, *Biochemistry*, **39**, 1263-1273 (2000).

Hata Y: Three-dimensional structures of cellulases and xylanases, *Serurosu no Jiten*, Asakura-shoten, 350-359 (2000) (in Japanese).

Hata Y: Crystallographic Analysis of the Catalytic Mechanism of L-2-Haloacid Dehalogenase, *4th ICRS International Symposium*, Abstracts, 5 (2000).

Hata Y, Fujii T, Mihara H, Kurihara T and Esaki N: Crystal structure of a NifS homologue *E. coli* CsdB and implications for catalytic mechanism, *2000 International Chemical Congress of Pacific Basin Societies*, Abstracts, 387 (2000).

Hata Y, Fujii T, Maeda M, Mihara H, Kurihara T and Esaki N: Crystal structure of a NifS homolog CsdB from *Escherichia coli, Third East Asian Biophysics Symposium*, Abstracts, 55 (2000).

Higurashi T, Hiragi Y, Ichiyama K, Mizobata T, Nagai J and Kawata Y: Unfolding and refolding of chaperonin GroES studies by small-angle X-ray scattering, *Third East Asian Biophysics Symposium*, Abstracts, 111 (2000).

Ichimura K, Hiragi Y and Matsuzaki S: Solution X-ray Scattering Study on Structural Stability of GroEL Coordinated with Nucleotides and Magnesium Ion, *Third East Asian Biophysics Symposium*, Abstracts, 60 (2000).

Morihara K, Hata Y and Okuda K: Serralysin Zn-metalloproteases -Structure, function, secretion pathway, and pathogenicity-, *Seikagaku*, **72**, 16-25 (2000) (in Japanese).

Muroga Y, Sano Y, Inoue H, Suzuki K, Miyata T, Hiyoshi T, Yokota K, Watanabe Y, Liu X, Ichikawa S, Tagsawa H and Hiragi Y: Small-Angle X-ray Scattering Studies on Local structure of Tobacco Mosaic Virus RNA in Solution, *Biophysical Chem*. **83**, 197-209 (1999).

Sano Y, Inoue H and Hiragi Y: Differences of Reconstitution

Process between Tobacco Mosaic Virus and Cucumber Green Mottle Mosaic Virus by Synchrotron Small Angle X-ray Scattering Using Low-Temperature Quenching, *J. Protein Chem*. **18**, 801-805 (1999).

Seki Y, Hiragi Y, Ichimura K and Soda K: Analysis of the solution X-ray scattering profile of chaperonin GroEL, *Third East Asian Biophysics Symposium*, Abstracts, 127 (2000).

II. Molecular Biology

Kojima S, Banno H, Yoshioka Y, Oka A, Machida C and Machida Y: A binary vector plasmid for gene expression in plant cells that is stably maintained in *Agrobacterium* cells, *DNA Research*, **6**, 407-410 (1999).

Sakai H, Aoyama T, and Oka A: *Arabidopsis* ARR1 and ARR2 response regulators operate as transcriptional activators, *Plant J.*, **24**, 715-723 (2000).

Honma T and Goto K: The *Arabidopsis* floral homeotic gene *PISTILLATA* is regulated by discrete *cis*-elements responsive to induction and maintenance signals, *Development*, **127**, 2021-2030 (2000).

Muramoto T and Aoyama T: Application of reporter genes, In, *A laboratory manual of model plants* (M. Iwabuchi, K. Okada and K. Shimamoto, eds. Springer-Verlag Tokyo) , pp 194-203 (2000) (in Japanese).

Aoyama T: Procedures for use of DNA-processing enzymes in recombinant DNA experiments, In, *Experimental procedures for basic biochemistry* (The Japanese Biochemical Society, ed. Tokyo Kagakudoujin), vol. 4, pp 133-147 (2000) (in Japanese).

III. Biological Information Science

Kanehisa M.: Post-genome Informatics, Oxford University Press (2000)

Kihara D. and Kanehisa M.: Tandem clusters of membrane proteins in complete genome sequences., *Genome Res*. **10**, 731-743 (2000).

Kanehisa M.: Pathway databases and higher order function. *Adv. Protein Chem.*, **54**, 381-408 (2000).

Kawashima S. and Kanehisa M.: AAindex: amino acid index database. *Nucleic Acids Res.*, **27**, 368-369 (2000).

Goto S., Nishioka T., and Kanehisa M.: LIGAND: chemical database of enzyme reactions. *Nucleic Acids Res.*, **28**, 380-382 (2000).

Kanehisa M., and Goto S.: KEGG: Kyoto Encyclopedia of Genes and Genomes. *Nucleic Acids Res.*, **28**, 29-34 (2000).

Ogata H., Fujibuchi W., Goto S., and Kanehisa M.: A heuristic graph comparison algorithm and its application to detect functionally related enzyme clusters. *Nucleic Acids Res.*, **28**, 4021-4028 (2000).

Fujibuchi W., Ogata H., Matsuda H., and Kanehisa M.: Automatic detection of conserved gene clusters in multiple genomes by graph comparison and P-quasi grouping. *Nucleic Acids Res.*, **28**, 4029-4036 (2000).

Goto S., Kawashima S., Okuji Y., Kamiya T., Miyazaki S., Numata Y., Kanehisa M.: KEGG/EXPRESSION: A Database for Browsing and Analysing Microarray Expression Data. *Genome Informatics*, **11**, 222-223 (2000).

Nakao M., Okuji K. Y., Kanehisa M.: Quantitative Estimation of Cross-Hybridization in DNA Microarrays Based on a Linear Model. *Genome Informatics*, **11**, 231-232 (2000).

Okuji K. Y. Hihara Y., Kamei A., Ikeuchi M., Suzuki I., Murata N., Kanehisa M.: Gene Expression Analysis of Orthologs in *Synechocystis* sp. with Operons in *Escherichia coli*. *Genome Informatics*, **11**, 233-234 (2000).

Katayama T., Kanehisa M.: The Role of Gene Expression Regulation in Yeast Cell Cycle Pathway. *Genome Informatics*, **11**, 268-269 (2000).

Nakaya A., Goto S., Kanehisa M.: Extraction of Correlated Gene Clusters from Multiple Graph Structures: Theory. *Genome Informactis*, **11**, 270-271 (2000).

Kawashima S., Nakaya A., Okuji Y., Goto S., Kanehisa M.: Extraction of Correlated Gene Clusters from Multiple Graph Structures: Application. *Genome Informatics*, **11**, 272-273 (2000).

Igarashi Y., Kihara D., Kanehisa M.: Classification and Analysis of Eukaryotic ABC Transporters in Complete Eukarya Genomes. *Genome Informatics*, **11**, 274-275 (2000).

Yoshizawa C. A., Kawashima S., Kanihisa M.: The Construction of a Database on the Intracellular Vesicular Transport. *Genome Informatics*, **11**, 276-277 (2000).

Itoh M., Katayama T., Okuji K. Y., Kanehisa M.: Sequence Analysis of Redundant Usage of DNA fragments in Complete Genomes. *Genome Informatics*, **11**, 321-322 (2000).

Kawashima T, Kawashima S, Kanehisa M, Nishida H and Makabe WK: MAGEST: Maboya Gene expression patterns and Expression Sequence Tags, *Nucleic Acids Res.*, **28**, 133-135 (2000)

Kawashima S and Kanehisa M: DNA chips and bioinformatics, *idenshiigaku*, **4** (1), 129-133 (2000) (in Japanese)

Kawashima S and Kanehisa M: From genomes to molecular interaction networks, *seibutsubutsuri*, **40** (5), 315-316 (2000) (in Japanese)

Nakaya A and Kanehisa M: Homology search, *Bulletin of the Japan Society for Industrial and Applied Mathematics*, **10**, 61-70 (2000) (in Japanese)

Nakaya A: Data mining for QTL analysis, *Gene and Medicine*, **4**, 415-420 (2000) (in Japanese)

Katayama T, Kanehisa M: Reconstruction of life systems in silico, *Kagaku*, **55**, 19-22 (2000) (in Japanese)

Katayama T, Kanehisa M: Analysis of life systems by genome informatics, *Kagaku Kougyou*, **51**, 25-30 (2000) (in Japanese)

NUCLEAR SCIENCE RESEARCH FACILITY

I. Particle and Photon Beams

II. Beams and Fundamental Reaction

Ao H, Inoue M, Iwashita Y, Shirai T and Noda A: Model Test of Biperiodic L-support Disk-and-Washer Linac Structure, *Jpn. J. Appl. Phys*. **39**, 651-6 (2000)

Noda A: Accelerator complex of ion and electron storage rings, *Nucl. Instr. and Meth*. **A441**, 154-8 (2000)

Iwashita Y: PARMSOL - PARticle Motion in SOLenoid field, *Beam Science and Technology, NSRF ICR Kyoto Univ.*, **5**, 6-8 (2000)

Noda A: Accelerator Complex based on Combination of TARN II with KSR, *Beam Science and Technology, NSRF ICR Kyoto Univ.*, **5**, 13-16 (2000)

Ao H: Fast Tuner Design of Superconducting RFQ for the New LNL Injector Piave, *Beam Science and Technology, NSRF ICR Kyoto Univ.*, **5**, 20-24 (2000)

Morita A and Iwashita Y: Kilpatrick's Sparking Limit for Geaneral RF Wave Forms, *Beam Science and Technology, NSRF ICR Kyoto Univ.*, **5**, 25-27 (2000)

Kapin V: A PIC Code Development for Space-Charge Dominated Beams, *Beam Science and Technology, NSRF ICR Kyoto Univ.*, **5**, 28-34 (2000)

Bisoffi G, Andreev V, Bezzon G.P, Chiurlotto F, Comunian M, Lombardi A, Palmieri V, Pisent A, Porcellato A.M, Stark S, Shirai T, Singer W, Chiaveri E: First Results with the Full Niobium Superconducting RFQ Resonator at INFN-LNL, *Proc. of the 2000 European Particle Accelerator Conference, Vienna, Austria*, 324-326 (2000)

Shirai T, Iwashita Y, Tonguu H, Sugimura T, Fujita H, Noda A and Lee T-Y: Beam Commissioning of the Electron Storage/ Stretcher Ring (KSR), *Proc. of the Seventh European Accelerator Conference, Vienna, Jun. 26-30, 2000*, 442-4 (2000)

Noda A, Iwashita Y, Kihara T, Morita A, Shirai T, Sugimura T, Tonguu H, Imai K, Nakamura M, Okamoto H., Tanabe T and Noda K: Beam Science Facility with Combination of Ion and Electron Storage Rings, *Proc. of the 7th European Paerticle Accelerator Conference, Wien* 563-565 (2000)

Iwashita Y and Morita A: Superposition of Multiple Higher Order Modes in a Cavity, *Proc. of the Seventh European Accelerator Conference, Vienna, Jun. 26-30, 2000*, 818-820 (2000)

Sugimura T, Morita A, Tongu H, Shirai T, Iwashita Y and Noda A: Stretcher Mode Operation of KSR, *Proc. EPAC2000*, 1002-4 (2000)

Tongu H, Shirai T, Fujita H, Sugimura T, Iwashita Y and Noda A: Development of Evacuation System for Electron Storage Ring, KSR, *Proc. EPAC2000*, 2307-9 (2000)

Morita A, Noda A, Tonguu H, Shirai T and Iwashita Y: Field Measurement of Combined Function Magnet for Medical Proton Synchrotron, *Proc. of the 7th European Particle Accelerator Conference, EPAC-2000, Vienna, Austria*, 2110-2112 (2000)

Morita A and Iwashita Y: Analysis of Herical Quadrupole Focusing Channel, *Proc of the 25th Linear Accelerator Meeting in Japan, July 12-14 Himeji, Japan*, 270-2 (2000) (in Japanese)

Ao H, Iwashita Y, Shirai T, Noda A, Inoue M, Kawakita T and Nakanisi K: High Power Model Fabrication of Disk-and-Washer Cavity, *Proc of the 25th Linear Accelerator Meeting in Japan, July 12-14 Himeji, Japan*, 285-7 (2000) (in Japanese)

Iwashita Y and Morita A: High Gradient Air Core Cavity for Energy Compression of Long Bunch, *Proc of the 25th Linear Accelerator Meeting in Japan, July 12-14 Himeji, Japan*, 288-90 (2000) (in Japanese)

Nakanishi K, Ao H, Iwashita Y, Kawakita T, Okubo K and Matsuoka M: Fabrication of a Disk-and-Washer Linac, *Proc of the 25th Linear Accelerator Meeting in Japan, July 12-14 Himeji, Japan*, 303-5 (2000) (in Japanese)

Morita A, Noda A, Tonguu H, Shirai T and Iwashita Y: Magnetic Field Measurement of Combined Function Magnet, *Proc. of the 6th Symposium on Power Supply Technology for Accelerators, Nov 21-22 SPring-8, Japan*, 137-148 (2000) (in Japanese)

Shirai T, Iwashita Y, Tonguu H, Sugimura T, Fujita H, Noda A: Commissioning of the Electron Ring,KSR, *Proc. of the First Symposium on Advanced Photon Research*, 234-237 (1999) (in Japanese)

SEMINARS

Professor Fred Wudl
Department of Chemistry and Biochemistry, University of California, Los Angeles, U.S.A.
"Recent Advances in Heterocycles for Organic Materials"
Tuesday 11 January 2000

Professor Rajeshwar N. Sharan
Department of Biochemistry, North-Eastern Hill University, India
"Non-random, sequence dependent interaction of radiation with plasmid DNA"
Monday 17 January 2000

Dr. Koichi Fukase
Graduate School of Science, Osaka University
Towards Efficient Synthesis of Glyco Chains: Development of New Glycosylation Reactions and Rapid Glyco Synthesis
Tuesday 18 January 2000

Professor Uwe H. F. Bunz
Department of Chemistry and Biochemistry, The University of South Carolina, U.S.A.
"Cyclobutadiene Complexes as Scaffold for Organometallic Materials"
Wednesday 26 January 2000

Professor Yosho Hirai
Toyama University, Japan
"Development of Stereoselective Cyclization using Palladium(II) Catalysts and its Application to Natural Products Synthesis"
Wednesday 26 January 2000

Professor Susumu Okazaki
Tokyo Institute of Technology, Japan
"Computer simuations of phospholipid bilayers"
Wednesday 26 January 2000

Professor Robert A. Pascal, Jr.
Department of Chemistry, Princeton University, U.S.A.
"Polyphenyl Polycyclic Aromatic Compounds"
Wednesday 26 January 2000

Professor Junji Watanabe
Tokyo Institute of Technology
"Polymer Liquid Crystals with Large Dipole Moments"
Wednesday 26 January 2000

Dr. Marie-Emmanuelle Couprie
CEA/LURE, France
"The interplay between the FEL and the electron beam in the case of the storage ring FEL Super-ACO"
Monday 31 January 2000

Professor Kazukiyo Kobayashi
Nagoya University
"Developments of Artificial Complex Carbohydrate Polymers to Material Life Technology"
Tuesday 1 February 2000

Dr. Marie-Emmanuelle Couprie
CEA/LURE, France
"The Super-ACO FEL source"
Thursday 3 February 2000

Professor Masayasu Inoue
1st Department of Biochemistry, Osaka City University Medical School
"Supersystem of Oxgen Metabolism and Life-sustaining Mechanism"
Thursday 3 February 2000

Doctor Miroslav Nývlt
Institute of Physics, Charles University, Czech Republic
"Some Remarks about Recent Understanding of Antiferromagnetic-Ferromagnetic Exchange Interaction"
Thursday 10 February 2000

Professor Hisanori Suzuki
Institute of Biochemistry, Faculty of Medicine, University of Verona, Itary
"A Cross-talk between Different NO Synthases"
Thursday 10 February 2000

Professor Parthasarathy Ganguly
National Chemical Laboratory, Pune, India
"ATOMIC SIZE : A NEW APPROACH"
Wednesday 1 March 2000

Professor Gernot Güntherodt
II. Physikalisches Institut, RWTH Aachen, Germany
"Microscopic Origin of Exchange Bias at Ferro/Antiferromagnetic Interfaces"
Monday 6 March 2000

Doctor Daniel T. Pierce
National Institute of Standards and Technology, U.S.A.
"Magnetic Order in Fe/Cr Multilayers"
Monday 6 March 2000

Dr. Eiji Kikutani
High Energy Accelerator Research Organization (KEK), Japan
"Comissioning of KEKB and Bunch Selection System"
Wednesday 15 March 2000

Dr. Joerg Lohmar
Degussa Hüls AG, Marl, Germany
"Polyetherblockamides - High Performance TPE for High Performance Applications"
Tuesday 21 March 2000

Dr Yuich Shimakawa
NEC Corporation
"Recent Topics in Crystal Structure Analysis"
23 March 2000

Dr. Han Young Hwan
Korea Atomic Energy Research Institute (KAERI) , Korea
"Investigation of Cesium Telluride Photocathode for Free Electron Laser"
Monday 27 March 2000

Professor Naoto Nagaosa
School of Engineering, University of Tokyo
"Anomalous Hall Effect in the Frustrated Ferromagnet"
Tuesday 28 March 2000

Professor Tsuneo Okubo
Faculty of Engineering, Gifu University, Gifu, Japan
"Beautiful World of Colloid Crystals"
Friday 21 April 2000

Professor Jin Q Kim
Department of Clinical Pathology, Seoul National University College of Medicine, Korea
"The Genetic Basis of Atherosclerosis among Koreans"
Monday 24 April 2000

Doctor Ralf Haβdorf
Center of Advanced European Studies and Research, Germany
"Smart Materials"
Thursday 11 May 2000

Dr. Tae-Yeon Lee
Pohang Accelerator Laboratory, Korea
"The operational status of PLS"
Wednesday 24 May 2000

Professor Takeshi Kawase
Graduate School of Science, Osaka University, Japan
"Supramolecular Chemistry of Curved Conjugated System - Complex Formation between the Belt-shaped Conjugated Molecule and Fullerenes"
Thursday 25 May 2000

Professor F. Brochard Wyart
University Pierre et Marie Curie, Paris, France
"Dynamics of Wetting"
Friday 26 May 2000

Professor P. G. de Gennes
College of France, Paris, France
"Strange Glass Transitions of Polymer Films"
Friday 26 May 2000

Professor Thomas B. Jones
University of Rochester
"Liquid Microdielectrophoresis"
Friday 26 May 2000

Doctor Wolfgang Kuch
Max-Planck-Institut für Mikrostrukturphysik, Germany
"Magnetic Domain Imaging by Photoelectron Emission Microscopy"
Thursday 1 June 2000

Professor Giuseppe Marrucci
Universita degli Studi di Napoli
"Molecular Modeling of Polymer Rheology in Fast Flows"
Wednesday 7 Jun 2000

Dr. Hans-Peter Fleischmann
Department of Applied Biological Chemistry, Shizuoka University
Carotenoid Derived Aroma Formation in Quince, Starfruit and Rose Flowers
Thursday 8 June 2000

Professor Hirobumi Teraoka
Medical Research Institute, Tokyo Medical and Dental University
"Current Research of DNA-department Protein Kinase"
Monday 12 June 2000

Professor Tomiki Ikeda
Tokyo Institute of Technology, Tokyo, Japan
"Application of Refractive Index Modulation on the Basis of Optically-Controlled Liquid Crystal Orientation to Optical Devices"
Friday 16 June 2000

Professor Alastair N. Cormack
School of Ceramic Engineering & Material Science, The New York State College of Ceramics at Alfred University, USA
"The Computer simulation of silicate glass and melt at atomic scale"
Thursday 6 July 2000

Dr. Mark Johnson
Institut Laue-Langevin, Grenoble, France
"Proton Tunnelling in the Solid State - from Molecular Rotors to Hydrogen Bonds"
Wednesday 12 July 2000

Professor David I. Schuster
Department of Chemistry, New York University, U.S.A.
"Synthesis, Photochemistry and Biological Activity of Fullerene Derivatives"
Thursday 13 July 2000

Professor Shigetaka Shimada
Nagoya Institute of Technology, Nagoya, Japan
"Structure, Molecular Motion, and Aggregation Process of Isolated Polymer Chains on a Solid Surface"
Friday 21 July 2000

Professor Jung Il Nam
Korea Institute of Scienece and Technology
"Organosilicon Chemistry Researches at KIST"
Saturday 22 July 2000

Professor François Mathey
Ecole Polytechnique, Palaiseau, France
"Phosphinines and Phosphametallocenes: the Coordination Chemistry of 6?-Aromatic Ligands"
Friday 28 July 2000

Associate Professor Jun-ichiro Ishibashi
Department of Earth & Planetary Sciences
Faculty of Science, Kyushu University
"Hydrothermal Geochemistry of Trace Elements"
Wednesday 9 August 2000

Professor Albert Fert
Unité Mixte de Physique CNRS-Thomson and Université Paris-Sud, France
" CPP GMR in Nanowires"
Thursday 31 August 2000

Dr Junichiro Mizuki
Synchrotron Radiation Research Center, Japan Atomic Energy Research Institute
"Interface Structure Study with Anomalous X-ray Scattering Effect"
Tuesday 5 September 2000

Professor Seizo Miyata
Tokyo University of Agriculture & Technology, Tokyo, Japan
"Organic Electroluminescence Devices"
Saturday 9 September 2000

Professor Junji Watanabe
Tokyo Institute of Technology, Tokyo, Japan
"Main-Chain Type of Polymer Liquid Crystals"
Saturday 9 September 2000

Professor Xiaojiang Hao
Kunming Institute of Botany, China
"Studies on Natural Nitrogen Containing Compounds"
Monday 11 September 2000

Dr. Shigenobu Toki
University of Akron, Akron, U.S.A.
"Elongation Crystallization of Natural Rubber"
Monday 11 September 2000

Professor Ashok. Date
National Chemical Laboratory, India
"Low Temperature Synthesis and Characterization of Ni-Zn Ferrites"
Tuesday 26 September 2000

Prof. Sang-Soo Kwak
Plant Cell Biotechnology Laboratory,
Korea Research Institute of Bioscience and Biotechnology (KRIBB), Korea
Metabolic Engineering of Antioxidative Mechanism in Transgenic Plants
Tuesday 3 October 2000

Professor Yoshinori Tokura
University of Tokyo
"Photo Spectroscopy of Strongly Correlated Materials"
Thursday 12 October 2000

Professor Werner Keune
Gerhard-Mercator-Universität Duisburg, Germany
"Observation of the BCC-to-FCC Bain Transformation in Epitaxial Fe Ultrathin Films on Cu_3Au (001)"
Friday 13 October 2000

Professor Motonari Uesugi
Department of Biochemistry and Molecular Biology, Baylor College of Medicine, Texas, USA
"Transcriptional Activation and Drug Discovery"
Saturday 14 October 2000

Dr. Kiyozo Asada
Takara Shuzo Co. Ltd.
"An *in vitro* new procedure for gene amplification"
Wednesday 25 October 2000

Professor Dietmar Seyferth
Massachusetts Institute of Technology
"The Organometallic Chemistry of Ambident Dianions. Reactions of Group 4 Metallocene Dichlorides and Organosilicon Dihalides with Acetone Dianions. A New Synthesis of Polylithioallenes"
Tuesday 31 October 2000

Dr. Nita Dragoe
Graduate School of Engineering, The University of Tokyo, Japan
"The Synthesis of an Unsymmetrical Bisfullerene. Evidence for the Presence of Both Fulleroid and Methanofullerene Bonding Patterns in the Same Molecule"
Wednesday 1 November 2000

Doctor Peter Fischer
"Imaging of Magnetic Domains with High Resolution Soft X-Ray Microscopy"
Universität Würzburg, Germany
Wednesday 1 November 2000

Doctor Thibaut Devolder
Université Paris-Sud, France
"Irradiation-Induced Magnetic Patterning: Basic Phenomena, Nanostructure Fabrication and Potential Applications"
Tuesday 7 November 2000

Dr. Michael Beutelspacher
Max-Planck-Institut for Kernphysik Heidelberg, Germany
"Results on Electron Cooling at the TSR"
Tuesday 7 November 2000

Dr. Jean Claude Wittmann
Institut Charles Sadron, Strasbourg, France
"Nucleation of Poly(vinylidene fluoride) and its Blends by Poly(tetrafluoroethylene)"
Friday 10 November 2000

Professor Marie-Claire Bellissent-Funel
Laboratoire Leon Brillouin, CEA, France
"Neutron Scattering Studies of Supercritical Water"
Tuesday 14 November 2000

Professor Russel, Christian
Otto-Schott-Institute, Friedrich Schiiler University, Jena,

German
"Redox behaviour of glass melts"
Monday 20 November 2000

Doctor Peter D. Olmsted
Department of Physics & Astronomy, University of Leeds, Leeds, U. K.
"Spinodal-Assisted Crystallization in Polymer Melts"
Friday 24 November 2000

Dr. Anil G. Gaonkar
Kraft Co. Chicago, USA
"Developments and Applications of Microemulsions in Food Industry"
Sunday 26 November 2000

Dr. Le Xuan Hien
Institute for Tropical Technology, Vietnam National Center for Natural Science & Technology, Hanoi, Vietnam
"Design of Speciality Polymers by the Use of Chemical Modification of Natural Products"
Tuesday 28 November 2000

Professor Peter Kundig
University of Geneva, Switzerland
"Transition Metal and Lewis Acids in Asymmetric Synthesis and Catalysis
Saturday 2 December 2000

Professor Toru Masuko
Faculty of Engineering, Yamagata University, Yonezawa, Japan
"Rheology of Smectite/Water Suspensions"
Monday 4 December 2000

Professor Semion Kuchanov
Moscow State University
"Theory of Living Radical Copolymerization"
Monday 11 December 2000

Dr. Tomonori Uesugi
National Institute of Radiological Sciences, Japan
"Experimental study of a half integer resonance with space charge effects in a synchrotron"
Thursday 14 December 2000

Professor Parthasarathy Ganguly
National Chemical Laboratory, Pune, India
On the Systematics of Insulator-Metal Transition: (La,Sr) CoO_3 system
Thursday 21 December 2000

MEETINGS AND SYMPOSIUMS

Workshop: "Genome Projects"

21 January 2000

1. DNA Chip and Application
   Professor Satoru Kuhara
   Graduate School of Bioresource and Bioenvironmental Sciences
   Kyushu University, Japan

2. Complete Sequence Analysis of 1,500 Human cDNA Clones Harboring Long and Nearly Full-Length Inserts
   Dr. Nobuo Nomura
   KAZUSA DNA Research Institute, Japan

3. Systematic Function Analysis of Bacillus subtilis Genome
   Professor Naotake Ogasawara
   Graduate School of Biological Sciences
   Nara Institute of Science and Technology, Japan

4. Feature of Thermophilic Archaea Extracted from Genomic Sequence
   Dr. Yutaka Kawarabayashi
   National Institute of Bioscience and Human-Technology
   Agency of Industrial Science and Technology
   Ministry of International Trade and Industry

5. Systematic Functional Analysis of Novel Yeast's Genes
   Dr. Toshihiko Eki
   Cellular Physiology Laboratory
   Institute of Physical and Chemical Research, Japan

Workshop: The Forefront in Plant Research

Tuesday 12 December 2000

1. "Right and left in plants"
   Professor Takashi Hashimoto
   Nara Institute of Science and Technology, Ikoma, Japan

2. "Polarity control in leaf morphogenesis"
   Dr. Gyung-Tae Kim
   Okazaki National Research Institutes, Okazaki, Japan

3. "Cell division and meristem construction in plants"
   Associate Professor Masaaki Umeda
   Institute of Molecular and Cellular Biosciences, The University of Tokyo, Tokyo, Japan

4. "Molecular mechanisms of gibberellin responses"
   Professor Makoto Matsuoka
   Bioscience Center, Nagoya University, Nagoya, Japan

5. "Plant vesicular transport and its control by GTPase"
   Dr. Akihiko Nakano
   Institute of Physical and Chemical Research, Wakou, Japan

6. "Isolation and analyses of rice phytochrome mutants with mutant panels"
   Dr. Makoto Takano
   National Institute of Agrobiological Resources, Tsukuba, Japan

7. "Plant mutations in DNA methylation"
   Associate Professor Tetsuji Kakutani
   The National Institute of Genetics, Mishima, Japan

THESIS

AKIYAMA, Seiji
D Eng, Kyoto University
"The Properties Control Based on the Coordination Number of Main Group Elements"
Supervisor: Tamao K
23 May 2000

AO, Hiroyuki
D Sc, Kyoto University
"Model Test of Biperiodic L-support Disk-and Washer Linac Structure"
Superviser: Noda A
23 March 2000

FUJIEDA, Miho
D Sc, Kyoto University
" Barrier Bucket Experiment with Magnetic-Alloy loaded RF Cavity"
Superviser: Noda A
23 March 2000

HAMADA, Sunao
D Sc, Kyoto University
"Magnetism of Co/Au Multilayers Probed by ^{57}Fe Mössbauer Spectroscopy"
Supervisor: Shinjo T
14 March 2000

ICHIYAMA, Susumu
D Agr, Kyoto University
"Mass Spectrometric Studies of the Mechanisms of Two Halo Acid Dehalogenases"
Supervisor: Professor Esaki N
23 March 2000

KAWANISHI, Hiroyuki
D Eng, Kyoto University
"Studies on Dynamics and Structure Formation of Semiflexible Polymers in Solution"
Supervisor: Horii F
23 March 2000

KULAKOVA, Ljudmila Borisovna
D Agr, Kyoto University
"Studies of Cold-active Enzymes from Cold-adapted Microoganisms"
Supervisor: Professor Esaki N
23 March 2000

KUWABARA, Kazuhiro
D Eng, Kyoto University
"Solid-State NMR Studies on Structure and Dynamics of Polyethylene and Related Alkanes in Various Crystal Forms"
Supervisor: Horii F
23 March 2000

MATSUDA, Tomoko
D Sc, Kyoto University
"Asymmetric Synthesis of Ketones by Geotrichum candidum"
Supervisor: Associate Professor Nakamura K
23 March 2000

MATSUMOTO, Tomoharu
D Sc, Kyoto University
"The Membrane Destabilizing Activity and the Critical Glycine Residue of the Influenza Virus Hemagglutinin Fusion Peptide-Based Synthetic Peptide"
Supervisor: Professor Takahashi, S
23 March 2000

MURAKAMI, Takeshi
D Eng, Kyoto University
"Physically Crosslinked Amphiphilic Elastomers: Network Characteristics and Physical Properties"
Supervisor: Kohjiya S
23 March 2000

SATO, Tomohiro
D Eng, Kyoto University
"Rheology of Triblock Copolymers in selective Solvents"
Supervisor: Osaki K
23 March 2000

SHIMIZU, Toshiki
D Eng, Kyoto University
"TEM Studies on Natural Rubber and Polychloroprene Thin Films Crystallized Under Molecular Orientation"
Supervisor: Kohjiya S
23 March 2000

SUGA, Takeo
D Sc, Kyoto University
"Crystal Structures, Orientations and UV-Vis-spetra of Non-planar Phthalocyanines Complexes Thin Films"
Supervisor: Professor Kobayashi T
23 March 2000

SUZUKI, Chikashi
D Sc, Kyoto University
"Kidorui-Kagoubutsu wo tyusin to suru Fukanzen-kakubussitsu no NaikakuKuukouDensiJoutai"
Supervisor: Mukoyama T
23 March 2000

TANAKA, Toru
D Eng, Kyoto University
"Studies on Synthesis and Properties of Novel Hydrocarbons Containing Fullerene Frameworks"
Supervisor: Professor Komatsu K
23 March 2000

TOSAKA, Masatoshi
D Eng, Kyoto University
"Structural Study on Polymer Crystals by Cryogenic High-Resolution Transmission Electron Microscopy"
Supervisor: Kohjiya S
24 January 2000

VLAICU, A. Mihai
D Sc, Kyoto University
"X-ray spectroscopic research of ^{74}W L emission spectra and satellite"
Supervisor: Mukoyama T
23 March 2000

YAMADA, Takahiro
D Sci. Kyoto University
"Synthesis and magnetic properties of cupric oxides containing Spin-1/2 quantum antiferromagnetic chains"
Supervisor: Takano M
23 March 2000

YAMAMOTO, Shinpei
D Eng, Kyoto University
"Structural Control and Physical Properties of Polymer Assemblies at Interfaces"
Supervisor: Miyamoto T.
23 March 2000

SHIMIZU, Bun-ichi
D Agr, Kyoto University
Study on Disease Resistance in Plants Induced by *Fusarium spp*.
Supervisor: Proffesor Ueno T
24 July 2000

YAMAGUCHI, Tsuyoshi
D Sci, Kyoto University
"Studies on the microscopic fluctuation and dissipation in fluids at various densities"
Supervisor: Professor Nakahara M
24 July 2000

ITOH, Fumio
D Pharm Sci, Kyoto University
"Studies on Action Mechanism of Pyrro 2,3-d Pyrimidine-Type Antifolates and Creation of Non-Glutamate-Type Antifolates"
Supervisor: Professor Sugiura Y
25 September 2000

OKUNO, Yasushi
D Pharm Sci, Kyoto University
"Studies on Apoprotein/DNA Recognition and Reaction Mechanism of Antitumor Antibiotic C-1027 Chromophore"
Supervisor: Professor Sugiura Y
25 September 2000

SHIGETO, Kunji
D Sc, Kyoto University
"Magnetization Switching Phenomena in a Single Magnetic Submicron-Wire Using Giant Magnetoresistance Effect"
Supervisor: Shinjo T
25 September 2000

INOUE, Makoto
D Agr, Kyoto University
Synthesis and Characterization of Mechanism-Based Inhibitors of γ-Glutamyl Amide Bond Formating/Cleaving Enzymes
Supervisor: Proffesor Sakata K
24 November 2000

ORGANIZATION AND STAFF

INSTITUTE FOR CHEMICAL RESEARCH
KYOTO UNIVERSITY

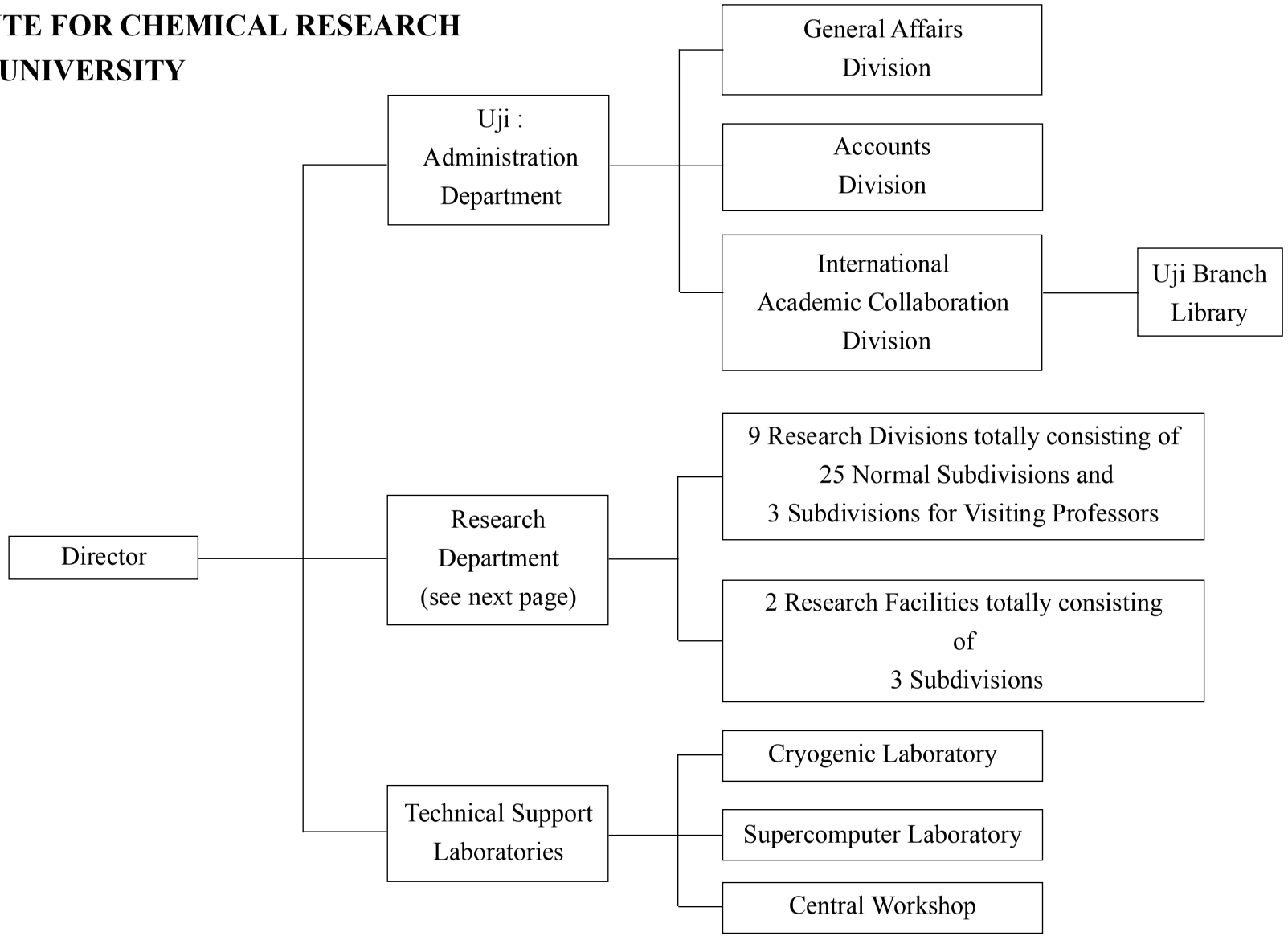

INSTITUTE FOR CHEMICAL RESEARCH, KYOTO UNIVERSITY As of 31 December 2000

RESEARCH DIVISION (G: Laboratory for Visiting Professors)

	Research Division	Subdivision (Laboratory)	Related Graduate School *Graduate School of / Division of*	Professor	Associate Professor	Instructor
Director TAMAO, Kohei	States and Structure	I. Atomic and Molecular Physics	*Science / Physics I*		ITO, Yoshiaki	KATANO, Rintarou NAKAMATSU, Hirohide
		II. Crystal Information Analysis	*Science / Chemistry*	KOBAYASHI, Takashi	ISODA, Seiji	OGAWA, Tetsuya NEMOTO, Takashi
		III. Polymer Condensed States	*Engineering / Polymer Chemistry*	KOHJIYA, Shinzo	TSUJI, Masaki	URAYAMA, Kenji TOSAKA, Masatoshi MURAKAMI, Syozo
	Interface Science	I. Solutions and Interfaces	*Science / Chemistry*	NAKAHARA, Masaru	UMEMURA, Junzo	MATSUMOTO, Mutsuo MATSUBAYASHI, Nobuyuki
		II. Molecular Aggregates	*Science / Chemistry*	SATO, Naoki	ASAMI, Koji	KITA, Yasuo YOSHIDA, Hiroyuki
		III. Separation Chemistry	*Science / Chemistry*	SOHRIN, Yoshiki	UMETANI, Shigeo	SASAKI, Yoshihiro OKAMURA, Kei
	Solid State Chemistry	I. Artificial Lattice Alloys	*Science / Chemistry*	SHINJO, Teruya	HOSOITO, Nobuyoshi	FUJITA, Masaki
		II. Quantum Spin Fluids	*Science / Chemistry*	YAMADA, Kazuyoshi	MIBU, Ko	IKEDA, Yasunori
		III. Multicomponent Materials	*Science / Chemistry*	TAKANO, Mikio	TERASHIMA, Takahito	AZUMA, Masaki
		IV. Amorphous Materials	*Engineering / Molecular Engineering*	YOKO, Toshinobu	UCHINO, Takashi	TAKAHASHI, Masahide
		G. Structure Analysis		KIKKAWA, Shinichi	YAMANAKA, Akio	
	Fundamental Material Properties	I. Molecular Rheology	*Engineering / Molecular Engineering*	OSAKI, Kunihiro	WATANABE, Hiroshi	INOUE, Tadashi
		II. Polymer Materials Science	*Engineering / Polymer Chemistry*	KAJI, Keisuke	KANAYA, Toshiji	NISHIDA, Koji
		III. Molecular Dynamic Characteristics	*Engineering / Molecular Engineering*	HORII, Fumitaka	TSUNASHIMA, Yoshisuke	KAJI, Hironori
		G. Composite Material Properties		TANAKA, Yoshinobu	YOSHINOBU, Jun	
	Organic Materials Chemistry	I. Polymeric Materials	*Engineering / Polymer Chemistry*		FUKUDA, Takeshi	TSUJII, Yoshinobu
		II. High-Pressure Organic Chemistry	*Engineering / Energy & HC Chemistry* *Engineering / Energy & HC Chemistry*	KOMATSU, Koichi		MORI, Sadayuki MURATA, Yasujiro NISHINAGA, Tohru
	Synthetic Organic Chemistry	I. Synthetic Design	*Pharmaceutical Sci. / Pharmac. Chem.*	TAMAO, Kohei	TOSHIMITSU, Akio	KAWACHI, Atsushi YAMAGUCHI, Shigehiro
		II. Fine Organic Synthesis		FUJI, Kaoru	KAWABATA, Takeo	TSUBAKI, Kazunori
		G. Synthetic Theory	*Science / Chemistry*	KIBAYASHI, Chihiro	IWABUCHI, Yoshiharu	
	Bioorganic Chemistry	I. Bioorganic Reaction Theory	*Pharmaceutical Sci. / Drug System*	TOKITOH, Norihiro	NAKAMURA, Kaoru	KAWAI, Yasushi SUGIYAMA, Takashi TAKEDA, Nobuhiro
		II. Bioactive Chemistry	*Medicine / Internal Medicine*	SUGIURA, Yukio	FUTAKI, Shiro	NAGAOKA, Makoto
		III. Molecular Clinical Chemistry	*Agriculture / Agricul. Chem.*	UEDA, Kunihiro	TANAKA, Seigo	ADACHI, Yoshifumi
	Molecular Biofunction	I. Functional Molecular Conversion	*Agriculture / Agricul. Chem*	SAKATA, Kanzo	HIRATAKE, Jun	MIZUTANI, Masaharu SHIMIZU, Bun-ichi
		II. Molecular Microbial Science	*Science / Biophysics*	ESAKI, Nobuyoshi	YOSHIMURA, Tohru	KURIHARA, Tatsuo MIHARA, Hisaaki
	Molecular Biology and Information	I. Biopolymer Structure	*Science / Biophysics*		HATA, Yasuo	HIRAGI, Yuzuru FUJII, Tomomi
		II. Molecular Biology	*Science / Biophysics*	OKA, Atsuhiro	AOYAMA, Takashi	
		III. Biological Information Science	*Science / Physics II*	KANEHISA, Minoru	GOTO, Susumu	NAKAYA, Akihiro
	Nuclear Science Research Facility	I. Particle and Photon Beams	*Science / Physics II*	NODA, Akira	IWASHITA, Yoshihisa	SHIRAI, Toshiyuki
		II. Beams and Fundamental Reaction	*Science / Biophysics*		MATSUKI, Seishi	
	Research Facility of Nucleic Acids			KANEHISA, Minoru	SUGISAKI, Hiroyuki	KAWASHIMA, Shuichi

PERSONAL

Early Retirement

Professor Sho Takahashi (Biopolymer Structure, Molecular Biology and Information)

On the 31st of March, 1999, Dr. Sho Takahashi retired from Kyoto University after 29 years of service to the University and, on the 6th of July, 1999, was honored with the title of Professor Emeritus of Kyoto University.

Dr. Takahashi was born in Hyogo on the 22nd of July, 1936. After graduation from Department of Chemistry, Faculty of Science, Nagoya University in 1958, he continued his studies as a graduate student on the structural determination of physiologically active natural products. In 1963 he finished the course and was appointed an instructor of the Department of Physics, Faculty of Science, Nagoya University. He was granted a doctoral degree from Nagoya University in 1963 for his study on the determination of the structure of tetrodotoxin. On a leave of absence in the year 1967 to 1970, he stayed at the Laboratory of Chemistry, National Institute of Arthritis and Metabolic Diseases, National Institutes of Health, and studied with Dr. Louis A. Cohen a reductive conversion of protein N-terminal pyroglutamate into prolyl residue and a correlation between stretching vibration frequencies of ester carbonyls and the component alcohol pK_a.

In 1970, he moved to the laboratory that was directed by Professor Tatsuo Ooi, Institute of Chemical Research, Kyoto University, and was promoted to Associate Professor in 1972. In 1989, he was appointed full Professor of Kyoto University and directed the Laboratory of Physical Chemistry of Enzyme (presently Biopolymer Structure, Division of Molecular Biology and Information). At the Graduate School of Science, Kyoto University, he gave lectures on biopolymers and physical chemistry of protein, and supervised the dissertation works of graduate students.

During the past three decades, although his research interest comprised a wide variety of subjects, the approach of the way was a consistent use of synthetic peptides as a tool. Secondary structures are fundamental structural units in protein structure and the stability of secondary structure mostly determines protein structure. Synthetic polypeptides had been considered a straightforward model system to the study of protein secondary structures, but the lack of adequate synthetic methods limited the use to polypeptides having random amino acid sequences. Dr. Takahashi's works on regular copolypeptides having definite amino acid sequence pioneered the way to the synthesis of the required polymers and their application to the study. Block polypeptides, which were synthesized by a sophisticated method with fragment coupling on a solid-phase support, enabled him to study the local stability resided inside an α-helix. In the last ten years his interest was focused on interaction between peptides and biomembranes and discovered peptide-induced membrane fusion. Necessary conditions of peptide to trigger the fusion have been extensively studied.

He also developed practically useful analytical methods for biochemistry: such as a ninhydrin reagent for an amino acid analyzer and fluorescent rotors, which are now commercially available.

His contribution to the Institute through both academic and administrative activities is hereby gratefully acknowledged.

Early Retirement

Professor Takeaki Miyamoto (Polymeric Materials, Organic Materials Chemistry)

On the 31st of March, 2000, Dr. Takeaki Miyamoto retired from Kyoto University, one year earlier than expected, and moved to his new assignment, the Principal of Matsue National College of Technology. He had served the University for 31 years and was honored with the title of Professor Emeritus of Kyoto University in April, 2000.

Dr. Miyamoto was born in Manchuria, China on the 3rd of April, 1937. After graduation from the Department of Fiber Chemistry, Faculty of Engineering, Kyoto University in 1962, he continued his studies on polymer chemistry as a graduate student for two years. After 4 years of service to Nittobo Co. Ltd., he returned to the University to be appointed Instructor of the Laboratory of Polymer Properties headed by Professor H. Inagaki (present Professor Emeritus), at the Institute for Chemical Research, Kyoto University in 1968, where he was promoted to Associate Professor in 1976 and to full Professor in 1988, a position he held until retirement. In the meantime, he was granted in 1967 a doctoral degree from the Faculty of Engineering, Kyoto University for his studies on "Unperturbed Dimensions, Conformations & Steric Isomerisms of Polymer Chains". On leave from the University, he made a stay in Freiburg University, (West) Germany in the years 1967 and 1968 to work on functional polymers in collaboration with Professor H.-J. Cantow. From the 1st of April, 1994 to the 31st of March, 1996, he was appointed Director of the Institute and made quite a few important contributions not only to the Institute but also to the University.

Dr. Miyamoto devoted himself to the Society of Fiber Science and Technology, Japan as President for the years 1995 and 1996, and to the Cellulose Society as President for the years 1997 and 1998. In 2000, he was awarded by each of these Societies for his distinguished services to them. He made no less contributions to the promotion of international collaboration in polymer science, in particular with Germany and China. He was chair or a member of organizing committee in a number of international scientific conferences/symposiums.

During the past 40 years, Dr. Miyamoto's research interest encompassed a wide array of the sciences of functional polymers and fiber materials. His scientific life started with the synthesis and solution-property study of block copolymers and the characterization of polymers by thin layer chromatography and various spectoroscopies. With a number of achievements in these fundamental fields of polymer science, his interest was directed to polymer materials in general, above all, to naturally occurring polymers. He established a method to characterize the second-order structure of wool keratin by circular dichroic spectroscopy, with which he succeeded in disclosing details of the $\alpha-\beta$ transition of the component protein. He was the first to perform a detailed study on the interactions between wool keratin and metal ions by means of gel chromatography. This fundamental work led him to develop waste wool-based new materials like a heavy-metal adsorbent and a cosmetic substrate. He is also known as a distinguished cellulose scientist, in particular for his studies on the characterization of the substituent distributions along the chain in cellulose derivatives, and the effects of these distributions on their physical and physicochemical properties. He also developed systematic work to elucidate the relationships between the molecular structure and liquid crystallinity in cellulose derivatives. For his brilliant achievements, he was awarded in 1983 the Prize of Fiber Science and Technology, Japan.

With his extraordinary ability of planning, vitality, and characters to attract people, he will continue to make a great job in his new position, too.

Retirement

Professor Takashi Kobayashi (Crystal Information Analysis, States and Structure)

On the 31st of March 2001, Dr. Takashi Kobayashi retired from Kyoto University after his 35 years' service at Kyoto University. The title of Emeritus Professor was granted to him by the University on the following day.

After graduating from the Faculty of Science, Kyoto University, with his major in chemistry in March 1962, he started his study on powdery organic crystals under the supervision of the late Professor Eiji Suito. He received a doctor of science degree from Kyoto University for his study on phthalocyanine complexes using infrared spectroscopy in 1970.

Dr. Kobayashi was appointed an Instructor at the Laboratory of Powder Chemistry, Institute for Chemical Research, Kyoto University in 1966 and an associate professor in 1984. In these years, he made a sabbatical at the University of Münster, Germany, as an Alexander von Humboldt Stipendiat and worked on electron radiation damage in co-operation with Professor Ludwig Reimer for two years. He was promoted to a full professor of the Institute in 1988 to direct the Laboratory of Powder Chemistry (the present name, Crystal Information Analysis). During these years, he made many distinguished studies on organic crystals, especially by the high resolution electron microscopy, the fast electron energy-loss spectroscopy and the energy filtered imaging. In particular, the lattice defects in organic crystals, polymorphic and psedomorphic structures at interfaces and the epitaxy of organic molecules were analyzed in detail by the electron microscopic methods. He established multi-beam imaging in high-resolution electron microscopy. So as to realize an 0.1 nm resolution, he has made many contributions to the foundation of the 1000kV high resolution electron spectromicroscope having a twin-tank system with the Emeritus Professor Natsu Uyeda. For his excellent achievements, the Japanese Society for Electron Microscopy awarded him twice the prizes in 1988 and in 1998 on his studies of lattice defects in organic crystals by direct molecular imaging and of electron energy-loss spectroscopy, respectively.

Dr. Kobayashi contributed toward various scientific meetings and international congresses as an executive committee member. He served as a member of the board of directors in the Japanese Society for Electron Microscopy. He also served as a member of the editorial board in some international scientific journals; Journal of Porphyrins and Phthalocyanines, Journal of Electron Microscopy, and Advances in Polymer Science.

Dr. Kobayashi has given lectures on crystal chemistry since 1984 at the Graduate School of Science, Kyoto University and was charged with supervising dissertation works of many graduate students. He has been a visiting lecturer at several universities such as Tokyo Institute of Technology and Okayama University.

Because of his sincere, thoughtful and warm personality, Dr. Kobayashi wins the respect of all who come in contact with him. His contribution to the Institute through both academic and administrative activities is gratefully acknowledged.

Award

Professor Teruya Shinjo
(Artificial Lattice Alloys, Solid State Chemistry)

Dr. Teruya Shinjo, Professor of Kyoto University, was awarded a Purple Ribbon Medal (Shijuhosho) in November 2000.

Dr. Teruya Shinjo was born in Kyoto Prefecture on August 18, 1938. He graduated from Faculty of Science, Kyoto University in 1961. He studied the magnetic properties of iron oxide particles by Mössbauer spectroscopy in the Graduate School of Science, Kyoto University under the supervision of Professor H.Takaki. He finished the Doctor Course of Chemistry and received the Doctor Degree of Science in 1966.

He started his academic carrier as an instructor of Institute for Chemical Research, Kyoto University in 1966 with the late Professor T.Takada. In 1976, he was promoted to an associate professor and since 1982, he has directed the Laboratory of Solid State Chemistry, Institute for Chemical Research as a full professor. During 1996-1998, he served as the Director of Institute for Chemical Research. At the Graduate School of Science, Kyoto University, he gave lectures on the properties of magnetic materials and supervised the dissertation works of many graduate students.

During his academic carrier, Prof. Shinjo has extensively investigated the properties of magnetic thin films. The keywords of his investigation may be “Mössbauer spectroscopy” and “giant magnetoresistance effect”. He investigated the surface/interface magnetic properties of ferromagnetic metals such as iron and cobalt with ^{57}Co and ^{57}Fe Mössbauer probes. These studies are now recognized as pioneering works in surface/interface magnetism. The studies on surface/interface magnetism were developed to the production of metallic multilayer films with artificial stacking structures of nanometer scale. The artificially structured metallic multilayers are novel alloy systems which may potentially have various useful properties. He discovered a non-coupling type giant magnetoresistance (GMR) effect in NiFe/Cu/Co/Cu multilayer systems. His discovery stimulated the development of read head devices of magnetic recordings. Nowadays the GMR heads are widely used in the hard disks of computers. Recently he started new researches of nano-scale magnetism. The GMR effect is utilized to detect the magnetization reversal of narrow magnetic wires. In the submicron-size magnetic dots, he successfully observed the turned-up magnetization spot in the center of the magnetic vortex structure by magnetic force microscope. Such a magnetic structure was theoretically predicted long time ago, but has never been observed by experiments. For his long-term studies on the properties of magnetic films including the discovery of the non-coupling type GMR effect, he was awarded the Prize of the Magnetic Society of Japan in 1991 and 1998, and the Prize of the Japan Society of the Applied Physics in 1993.

It is worth referring to his international activities in the academic society. He is one of the Japanese representatives of International Board on the Application of the Mössbauer Effect for many years, and an international committee member of the International Colloquium on Magnetic Films and Surfaces and served as the chair.

Awards

Yukio Sugiura (Professor)
Bioactive Chemistry, BioorganicChemistry

The Pharmaceutical Society of Japan Award
"Molecular Mechanism for DNA Recognition and Functional Expression of Bioactive Molecules"
28 March 2000

Tadashi Inoue (Instructor)
Molecular Rheology, Fundamental Material Properties

SRJ Research Award for 1999
"Viscoelasticity and Birefringence of Amorphous Polymers in the Glass Transition Zone"
The Society of Rheology, Japan
18, May, 2000

Ko Mibu (Associate Professor)
Solid State Chemistry, Quantum Spin Fluids

The ICR Award for Young Scientists
"Control of Magnetic Structures using Metallic Multilayers"

Shinpei Yamamoto (JSPS Research Fellow)
Polymeric Materials, Organic Materials Chemistry

The ICR Award for Young Scientists
"Structures and Properties of High-Density Polymer Brushes"

NAME INDEX

KEYWORD INDEX